Republic of Iraq

Ministry of Higher Education and Scientific Research

University of Babylon

College of Science / Department of Physics

Effect of Laser Power on Non-Linear Optical Properties for Laser Dyes in Liquid and Solid Media

A thesis

Submitted to the Council of College of Science, University of Babylon in Partial Fulfillment of the Requirements for the Degree of Master in Physics.

By

Afrah Mohammad Abd AL-Ameer Muheisen

B.Sc. in Physics /1997

Supervisor

Prof. Dr.
Ban Ali Naser Ghalib

2021 A.D. **1443 A.H.**

جمهورية العراق
وزارة التعليم العالي والبحث العلمي
جامعة بابل
كلية العلوم / قسم الفيزياء

تأثير قدرة الليزر على الخصائص البصرية اللاخطية لصبغات ليزرية في الاوساط السائلة والصلبة

رسالة مقدمة إلى

مجلس كلية العلوم في جامعة بابل وهي جزء من متطلبات

نيل درجة الماجستير في العلوم/ الفيزياء

من قبل

افراح محمد عبد الامير محيسن

بكالوريوس علوم فيزياء/ ١٩٩٧

إشراف

الأستاذ الدكتور

بان علي ناصر غالب

٢٠٢١م ١٤٤٣هـ

﴿ اللَّهُ نُورُ السَّمَاوَاتِ وَالْأَرْضِ مَثَلُ نُورِهِ كَمِشْكَاةٍ فِيهَا مِصْبَاحٌ الْمِصْبَاحُ
فِي زُجَاجَةٍ الزُّجَاجَةُ كَأَنَّهَا كَوْكَبٌ دُرِّيٌّ يُوقَدُ مِن شَجَرَةٍ مُّبَارَكَةٍ
زَيْتُونِةٍ لَّا شَرْقِيَّةٍ وَلَا غَرْبِيَّةٍ يَكَادُ زَيْتُهَا يُضِيءُ وَلَوْ لَمْ تَمْسَسْهُ نَارٌ نُّورٌ
عَلَى نُورٍ يَهْدِي اللَّهُ لِنُورِهِ مَن يَشَاءُ وَيَضْرِبُ اللَّهُ الْأَمْثَالَ لِلنَّاسِ
وَاللَّهُ بِكُلِّ شَيْءٍ عَلِيمٌ ﴾

صدق الله العلي العظيم

سورة النور: الآية (٣٥)

Supervisor Certification

I certify that this thesis is titled (**Effect of Laser Power on Non-Linear Optical Properties for Laser Dyes in Liquid and Solid Media*),*** was prepared by **(Afrah Mohammad Abd AL-Ameer)** under my supervision at Department of Physics, College of Science, University of Babylon, as a partial fulfillment of the requirements for degree of master in physics.

Signature:

Supervisor: Dr. Ban A. Naser Ghalib

Title: Professor

Address: Department of Physics-College of Science-University of Babylon

Date: / / 2021

Certification of the Head of the Department

In view of the available recommendation, I forward this thesis for debate by the examination committee.

Signature:

Name: Dr. Abdulazeez O. Mousa Al-Ogaili

Title: Professor

Address: Head of Physics Department - College of Science - University of Babylon

Date: / /2021

Dedications

WHOEVER WAS TRANSFIGURED WITH THE LIGHT OF GOD TO ILLUMINATE THE DARKNESS OF THE UNIVERSES

PROPHET OF MERCY, MUHAMMAD, MAY GOD BLESS HIM AND GRANT HIM PEACE

UNTIL THEY MAKE THEMSELVES AMONG THOSE WHO SELL THEMSELVES, THEY RANGE FROM TWELVE

-MAY GOD BLESS THEM ALL -

TO EVERYONE WHO ILLUMINATED THE PATH OF KNOWLEDGE

MY DEAR TEACHERS

Afrah

Acknowledgments

First, I would like to express my deep thanks to the Almighty ALLAH, JALA JALALAH, for what I have been, prayer and peace be upon the best of his creation Mohammed and his progeny and companions. I would like to express my deep gratitude and appreciation to my supervisor ***Prof. Dr. Ban Ali Naser*** for suggesting the topic of the thesis, continuous advice and her guidance throughout this work.

I am grateful to the department of physics for providing the necessary facilities and help. Special thanks to ***Prof. Dr. Abdulazeez O. Mousa*** for providing the necessary facilities and help.

I am grateful to ***Prof. Dr. Talib Mohsen Abbas*** for providing the necessary facilities and help.

Finally, my great thanks and respect to all who help me.

Afrah

Summary

The present research includes a study of spectral, linear and non-linear optical properties of organic laser dyes doped with polymer and nanomaterials in order to benefit from them in the field of nonlinear optics. Many properties of organic dyes can be improved and developed by doping with polymers and nanomaterials, so that they are suitable for many practical applications.

Organic laser dyes (pure and doped) are good materials in the field of nonlinear optics and their applications due to their high nonlinear response that operates at a wide spectral range.

In this work, three organic dyes (Acriflavine, Orcein and Azur-B) were used. Preparing thin films from solutions of those dyes and studying the effect of laser power on the nonlinear optical properties of all samples.

Those organic laser dyes have been characterized using Fourier Transform Infrared (FT-IR). The linear optical properties of all the prepared samples (solutions and thin films) were studied using UV-VIS spectrometer at concentration (10^{-5} M) for solutions and (10^{-3} M) for thin films of each dye in ethanol solvent. The spectral optical properties of all the prepared samples have been studied using fluorescence spectroscopy.

The nonlinear calculations included using (Z-Scan) technique for the (open-aperture) and (closed-aperture) states, to obtain a nonlinear refractive index (n_2) and a nonlinear absorption coefficient (β). The measurements were performed using a diode pumped solid state laser of (457 nm) wavelength, at different laser powers (56,70,84 and 102) mW.

The results showed an increase in the nonlinear refractive index when increasing the powers, while noticed a decrease in the nonlinear absorption coefficient when increasing the powers for all the prepared samples.

Thin films have better linear and non-linear spectral optical properties as compared to solutions. All prepared samples prepared from dyes doped with polymers and nanomaterials have better nonlinear optical properties compared to samples prepared from pure dyes.

The results showed the possibility of using all the prepared samples as potential media for various optoelectronic applications including that in optical power limiting and active laser media. The results showed that all prepared samples from Acriflavine dye possess high linear and non-linear spectral properties and the best behavior as a visual determinant compared with (Orcein and Azure-B) dyes.

الخلاصة

يتضمن البحث الحالي دراسة الخصائص البصرية الطيفية الخطية واللاخطية لصبغات ليزرية عضوية مطعمة ببوليمر ومواد نانوية وذلك للإفادة منها في مجال البصريات اللاخطية. ان العديد من خصائص الصبغات العضوية يمكن تحسينها وتطويرها بالتطعيم ببوليمرات ومواد نانوية، بحيث تكون مناسبة للعديد من التطبيقات العملية. اذ تعد الصبغات الليزرية العضوية (النقية والمطعمة) من المواد الجيدة في مجال البصريات اللاخطية وتطبيقاتها وذلك لاستجابتها اللاخطية العالية التي تعمل عند مدى طيفي واسع.

في هذا العمل، تم استخدام ثلاث صبغات عضوية (الاكريفلافلين والاورسين وصبغة أزورB)، وتحضير اغشية رقيقة من محاليل هذه الصبغات. تم دراسة تأثير قدرة الليزر على الخصائص البصرية اللاخطية لجميع النماذج المحضرة من هذه الصبغات. تم تشخيص هذه الصبغات العضوية باستخدام مطياف الاشعة تحت الحمراء (FT-IR).

تم دراسة الخصائص البصرية الخطية لجميع النماذج المحضرة (المحاليل والأغشية الرقيقة) ، باستخدام مطياف الأشعة المرئية وفوق البنفسجية عند تركيز (10^{-5} M) للمحاليل و (10^{-3} M) للأغشية الرقيقة لكل صبغة في مذيب الايثانول. تم دراسة الخصائص البصرية الطيفية لجميع النماذج المحضرة باستخدام مطياف الفلورة.

تضمنت الحسابات اللاخطية استخدام تقنية (Z-Scan) لحالتي الفتح (Open-aperture) والغلق (Closed-aperture)، للحصول على معامل انكسار لاخطي (n_2) ومعامل امتصاص لاخطي (β)، انجزت القياسات باستخدام ليزر الحالة الصلبة ذو الطول الموجي (457 nm) عند قدرات ليزرية مختلفة (56,70,84,102) mW .

أظهرت النتائج زيادة في معامل الانكسار اللاخطي عند زيادة القدرات بينما نلاحظ انخفاض معامل الامتصاص اللاخطي عند زيادة القدرات لجميع النماذج المحضرة.

تمتلك الاغشية الرقيقة خصائص بصرية طيفية خطية ولا خطية أفضل بالمقارنة مع المحاليل. وان النماذج المحضرة من الصبغات المطعمة ببوليمرات ومواد نانوية تمتلك خصائص بصرية لا خطية أفضل مقارنة مع النماذج المحضرة من الصبغات النقية.

بينت النتائج امكانية استخدام جميع النماذج المحضرة كأوساط جهد لمختلف التطبيقات الكهرو بصرية كمحددات للقدرة البصرية واوساط ليزرية فعالة. حيث اظهرت النتائج ان جميع النماذج المحضرة من صبغة الاكريفلافين تمتلك خصائص طيفية خطية ولاخطية عالية وأفضل سلوك كمحدد بصري مقارنة مع صبغتي (الاورسين والازور- B).

Contents

List of Symbols

Symbol	Description
A	*The absorption*
a	*The lattice constant*
B	*Magnetic field*
C_1	*Primary concentration*
C_2	*New concentration*
c	*Light velocity*
D	*(FWHM) in radians*
d	*The distance from focal plane to the aperture plane.*
E_g	*Energy gap*
E	*Electric field*
h	*Plank's constant*
hυ	*The photon energy*
KET	*The energy transfer rate constant*
k	*wave number*
L_{eff}	*The effective length of the sample*
I_o	*The intensity at the focal spot*
I_T	*Intensity of the transmitted beam*
I_A	*Intensity of the absorbed beam*

Symbol	Description
I_R	*Intensity of the reflected beam*
M wt	*Molecular weight*
n_o	*Linear refractive index*
n_c	*Refractive index*
n_2	*The nonlinear refractive coefficient*
P_{peak}	*The peak power of the laser pulse*
R	*The reflectance*
S_{00}	*The ground state*
S_{1n}	*Higher vibrational level*
S_{2n}	*The second excited singlet state*
t	*thickness*
T	*The transmittance*
T(z)	*The minimum value of normalized transmittance*
V	*Volume of the solvent*
V_1	*The volume before dilution*
V_2	*The volume after dilution*
Z	*The distance between the focal planes in free space*
λ	*Wavelength*
α	*The absorption coefficient*
υ	*Frequency*
λ_c	*The maximum wavelength of the incident photon*
α_o	*Linear absorption coefficient*
ε_r	*Real part of dielectric constant*
ε_i	*Imaginary part of dielectric constant*
ϑ	*The velocity of propagation*
χ	*The electric susceptibility*

Symbol	Description
$\chi^{(1)}$	***The linear susceptibility***
$\chi^{(2}$	***The second order nonlinear susceptibility***
$\chi^{(3)}$	***the third order nonlinear susceptibility***
β	***Nonlinear absorption coefficient***
$\Delta\Phi_o$	***The nonlinear phase shift***
ε_s	***Two-photon absorption (TPA)***

List of Abbreviations

Abbreviation	Full Name
Ag NP_S	***Silver nanoparticles***
C.B	***Conduction band***
CW	***Continuous wave***
FWHM	***Full width at half maximum***
M.Wt	***Molecular weight***
NLO	***Nonlinear optical***
NLA	***Nonlinear absorption***
NLR	***Nonlinear refraction***
FT-IR	***Fourier transforms infrared spectrometer***
PVA	***Polyvinyl alcohol***
PL	***Photoluminescence***
PD	***Photo Detector***
UV	***Ultra violet***
V.B	***Valence band***
XRD	***X-Ray diffraction***

List of figures

List of Tables

1.1 Introduction

Nonlinear optical properties have been the subject of numerous investigations theoretically and experimentally during recent years due to their applications to many branches. The nonlinear optical properties are important parameters in characterizing and determining the applicability of any material to nonlinear optical device. There are several techniques for measuring these parameters like degenerate four waves mixing, third harmonic generation and Z-scan technique[1]. In a solid-state dye laser the organic dye molecules are uniformly distributed in a highly homogenous polymer matrix. An example of such polymer is a highly pure form of (Polyvinyl alcohol) (PVA).

Solid state dye lasers extent from the ultraviolet to the near infrared regions. An important feature of the dye laser is easily tunable over a wide range of wavelengths [2]. The use of solutions in dye lasers entails a number of liquid inconveniences, mainly related to the need of employing large volumes of organic solutions of dyes that are both toxic and expensive. So that the dye has to be changed for different wavelength regions, so attempts were made to overcome the problems posed by dye solutions by incorporating dye molecules into solid matrices .This has resulted in significant advances towards the development of practical tunable solid-state lasers[3].

The use of a synthetic polymer host presents advantages as these materials show much better compatibility with organic laser dyes ,are amenable to inexpensive fabrication techniques[4]. PVA (Polyvinyl alcohol) is the most frequently used host for laser dye due to its excellent optical transparency and its relatively high laser damage resistances [2].

Dye doped polymers have applications in similar fields of modern photonic technology,optical amplifiers, fiber optics, and optical limiting which is used for protecting the human eye and the sensors by handling the laser output [5]. Nanotechnology represents one of the major breakthroughs of modern science, enabling materials of distinctive size, structure and composition to be formed. For the smaller particles the percentage of surface atoms increases, leading to changes in physical and chemical properties of the materials[6]. The field of nanotechnology is one of the most popular areas for polymer science and technology. This area can generate a new material behavior [7]. Nanoparticles embedded in polymer matrix have attracted increasing interest because of the unique mechanical, optical, electrical and magnetic properties displayed by nanocomposites at low nano-filler concentrations (1-10%) [8].

This importance is due to the effect of the unique nature of the nanosized filler on the bulk properties of polymer-based nanocomposites[9]. The addition of spherical nanoparticles to polymers allows the modification of the polymers physical properties as well as the implementation of new features in the polymer matrix[10]. PVA composite films are modulated and improved by addition of Ag nanoparticals and those properties can be applied in the fields of optics and electroincs [11]. The nonlinear properties of dyes solutions, dyes doped with PVA polymer thinfilm and Ag nanoparticles can be studied by using a simple technique called Z - scan. It is a sensitive and popular experimental method to measure intensity dependent of nonlinear optical (NLO) properties of materials which can rapidly measure both nonlinear absorption (NLA) and nonlinear refraction (NLR) in solids, liquids and then studying the optical limiting behavior [12].

1.2 Literature Survey

Several researches used Z-Scan for studying nonlinear properties of organic dyes.

In 2000, O.Shaker *et al*. [13] studied nonlinear optical properties of polymer [PMMA] thin films doped with dye lasing compounds, Rhodamine 6G and acriflavine in chloroform solvent by using dip coating method. The fluorescence emission of Rhodamine 6G (R6G) and acriflavine dyes in PMMA polymer have been studied by changing the irradiation and exposure time of laser light to know the effect of these parameters. It was found that the fluorescence intensity decreases in the polymer samples doped dyes as the exposure time increases and then reaches stabilization at long times, this behavior called photobleaching, which have been shown in liquid phase less than solid phase.

In 2001, Furlani *et al*.[14] used symmetric and asymmetrical Pt (II) and Pd (II) bis-acetylides complexes and dispersed in PMMA. The nonlinear optical properties of them were measured by z-scan technique with mode locked Ti-sapphire delivering 150 fs and 770 nm. All complexes showed high value of nonlinear absorption coefficient and the Pd complexes here investigated show third-order properties less than in pt complexes .

In(2002) S. Venugopal *et al*.[15] studied the nonlinear absorption and excited state dynamics in Rhodamine B solutions at (532 nm), the absorption band's resonance wavelength, and (600 nm), the absorption edge wavelength determined using standard Z-Scan technique. According to the results of concentration-dependent experiments, reverse saturable absorption exhibits a complex behavior within the context of saturable absorption.

In (2003) R.Ganeev *et al*. [16] studied the Z-scan technique at wavelength (1064 nm), the nonlinear refraction, nonlinear absorption, and saturable absorption

of polymethine dyes. The coexistence of several nonlinear optical processes in dye solutions driven by picosecond pulses was explored, which found to be quite interesting. A number of different models were used to compute the saturable absorption. On a variety of polymethine dyes, Nonlinear refractive indices, nonlinear absorption coefficients, and saturation intensities were determined utilizing nonlinear refractive indices, nonlinear absorption coefficients, and saturation intensities.

In (2004) V.Rosso *et al*. [17] studied the optical Kerr effect, a third-order nonlinear optical phenomenon, was investigated in DR1-doped sol–gel using the Z-scan approach, which enables the examination of nonlinear absorption and refraction processes simultaneously. In this experiment, we used amorphous silica glasses doped with the azo dye Disperse Red 1 as substrates. By adjusting the parameters of the sol–gel synthesis, specifically the pH of the catalytic fluid, we were able to change the morphology of the sol–gel substrate. We discovered nonlinear effects with a wide range of amplitudes on sol–gel substrates with a wide range of porosities by employing a variety of nonlinear mechanisms in a variety of nonlinear processes.

In 2005, S.Chen *et al*.[18] Studied the characteristics of a Z- scan for a thin nonlinear medium with a large nonlinear phase shift induced by a pulsed laser. By comparing the peak-to-valley configuration of Z-scan curves for a large nonlinear phase shift induced by a pulsed laser with that by a CW laser, they found that some peak to valley features of Z-scan curves appear as the aperture size or the light intensity increases in the case of a large nonlinear phase shift .

In 2006, D. Yan , [19] Studied the composite PMMA films containing Ag nanoparticles and rhodamine 6G. Investigate the fluorescence properties and

nonlinear optical properties of R6G/PMMA films influenced by Ag nanoparticles. The fluorescence enhancement factor is about (3.3). The corresponding nonlinear refractive index is measured to be (2.423×10^{-8}) cm^2/GW using the *Z*-scan technique, which is much enhanced compared with the R6G/PMMA film. The results indicate that these enhancements are attributed to surface plasmon resonance of Ag nanoparticles.

In 2007, D. Obied, [20] Studied Z-scan experiment was performed using a Q-switched (dye foil) and second harmonic generation of Nd:YAG laser pulses in two parts. The first part was done using a closed-aperture placed in front of the detector to measure the nonlinear refractive index at two wavelengths (1064 nm and 532 nm). At each wavelength, the experiment was performed at two cases (transmission and reflection) with four input energies. The results show that the nonlinear refractive index is directly proportional to the input energy, which caused by the self-focusing of the material.

In 2008, A. Tawil,[21] Studied the linear and non-linear optical properties for laser dye fluorescein sodium in solvent Ethanol doped with polymer polyvinyl alcohol (PVA) at different concentrations. Z-scan technique was used to determine the nonlinear optical properties like the refractive index (n_2) and the absorption coefficient (β) at wavelength (532nm) CW frequency doubling Nd-YAG laser. The results showing the nonlinear absorption coefficient (β) changes between saturated absorption and two-photon absorption of certain concentration while the refractive non-linear coefficient (n_2) of film samples changes between positive (self-focusing) and negative (selfdefocusing). The quantum efficiency has been calculated for the same above concentrations (87%, 83%, 76%, 73%, 70%, 67%) respectively.

In 2009, Q. Mohammed, [22] Studied nonlinear optical and optical limiting properties of chicago sky blue 6B doped PVA film at (633 nm) and (532 nm) studied using a continuous wave laser. The sign and magnitude of the third-order nonlinearity from the closed aperture Z-scan data while the nonlinear absorption properties were assessed using the open aperture data. The chicago sky blue 6B doped PVA film exhibited nonlinear saturated absorption and strong self-defocusing effect. The limiting effect of the sample was studied and the results indicate that the film possesses good characteristic of optical limiting.

In 2010, M. Zainab [23] Studied nonlinear optical properties of the mixed donor (C480) acceptor (Rh6G) by Z-Scan technique, using Q-switched Nd: YAG laser with (1064 nm) wavelength. The results showed that the optimum concentration of acceptor is responsible for increasing the absorption. The obtained nonlinear properties result of the mixture C480/ Rh6G showed a negative nonlinear refractive index and reverse saturation absorption. Results showed that mixture of laser dyes are effective nonlinear optical materials as compared to individual laser dyes.

In 2011, V. Sindhu and A. Ramalingam, [24] Studied the third order nonlinear optical properties and spectral characteristics of methylene blue dye in both polymer and liquid mixtures, by recording the absorption and fluorescence spectra of the dye doped in poly(methyl methacrylate) modified with additive n-butyl acetate(nBA) and the dye in PMMA and nBA (liquid mixture), the spectral results of the dye doped polymer rod were compared with dye in liquid mixture. The nonlinear measurements of the dye in liquid and polymer medium were performed using CW He-Ne laser of wavelength (632.8 nm) by employing Z-scan technique. The dye methylene blue showed a negative nonlinear refractive index.

In 2012, R.Manshad and A. Hassa, [25] Studied the single beam Z-scan technique was used to determine the nonlinear optical properties of the orcein dye in the solvent chloroform and a dye doped polymer film. The experiments were performed using CW solid state diod laser with a wavelength of (532 nm). This material exhibits negative optical nonlinearity. Optical limiting characteristics of the dye solution and polymer film were studied. The result reveals that orcein dye can be a promising material for optical limiting applications.

In (2014) L.Hassan *et al*. [26] Studied the spectral characteristics and the nonlinear optical properties of the laser acridine dye by recording their absorption and fluorescence spectra. The nonlinear optical properties were measured by Z-scan technique. The results showed that the optimum concentration is responsible for increasing the absorption and the emission bandwidth to full range by the energy transfer process, also the efficiency of the process was increased by increasing the concentration.

In (2015) F. Mata , [27] Studied the linear and nonlinear optical absorption as well as photoluminescence emission behavior of the organic dye, Rhodamine B in aqueous solution. The samples exhibited intense photoluminescence emission when excited with (580 nm) radiation. The samples exhibited Reverse Saturable absorption under the experimental conditions.

In (2017) F.Tawil, [28] Z-scan technique was used by using CW (Nd-YAG) laser at (532 nm) with a power of (21 mW) for solution and (21 and 80 mW) for film to measure nonlinear optical properties. The results show that the that the highest nonlinear refractive index was (27.6×10^{-9} cm^2/mW) at concentration (1×10^{-6} M), and the highest absorption coefficient was (13.93×10^{-3} cm/mW) at concentration (1×10^{-4} M) . Also the

optical limiting threshold was measured and for those samples, which was about (22.5 mW) at (1×10^{-6} M) in solution.

In (2018) J. Tahir *et al.* [29] Studied the optical properties of fluorescein sodium dye doped in polymer Poly Polyvinyl alcohol for different thickneses. Z-scan method was utilized at (532nm) and UV-visible and fluorescence spectrophotometer was utilized to study the spectral characteristics in order to compute the nonlinear optical properties in two cases close, open aperture. The empirical results for open-aperture showed that the film models of fluorescein sodium dye have shown the saturation absorption or the two-photon absorption, also in closed-aperture showed positive or negative effect.

In (2019) R. Manshad and M.Qusay, [30] Studied the optical limiting properties for solution of azure B in the chloroform solvent and azure B doped polymethyl methacrylate (PMMA) film. Measurements were performed using two continuous wave (CW) laser beams. The effects of both concentration of the sample and the wavelength of the laser used on the optical limiting properties have been investigated. The optical limiting properties of the dye solution and dye doped PMMA films were compared. A mechanism for the optical limiting is given.

In (2020), R. Muhammad *et al*. [31] Studied power-dependent nonlinear optical behaviors of ponceau BS chromophore at (532 nm) via Z-scan technique. Single-beam Z-scan technique was utilized for the nonlinear measurement. Dominant absorption peak was observed in the visible region due to the high conjugation of diazene functional group absorption. The real and imaginary components of third order susceptibility, (χ^3) are relatively high in the order of (10^{-8} and 10^{-5}) respectively under different laser powers (0.12, 0.14, 0.16, 0.18 and 0.20 W). In

short, PBS chromophore shows promising features and can be considered as a potential candidate for various NLO applications under low-power laser operation.

In (2021) A.Al Hussainey and Ban A. Naser,[32] Studied linear and nonlinear optical properties of (Acriflavine) organic laser dye at a concentrations (10^{-5}M),and preparing thin films of this dye doped with polymer and (Ag) nano material, for using it in field of nonlinear optics. The measurements performed using diode pumped solid state laser operating at (457nm) wavelength with different laser power (56,70,84 and 102 mW). The results showed that increasing the nonlinear refractive index when increasing powers but decreasing of nonlinear absorption coefficient, when increasing powers for all prepared samples.

In (2021) A. Ummu, *et al*. [33] Studied nonlinear optical studies of conjugated organic dyes for optical limiting applications show a wide optical transmittance window (400-600 nm) with absorption maxima in the UV region. However, shows an altered band structure with a broad absorption in the visible domain (448 nm). Density functional theory (DFT) calculations expose that the bandgap between HOMO and LUMO decreases.

1.3 Aims of the Work

The main aims of our research are:

1. Study the spectral, linear and non-linear optical properties of three organic laser dyes (Acriflavine, Orcein and Azur-B) as solutions dissolved in ethanol solvent and thin films.
2. Preparing thin films of those dyes by doping with Polyvinyl alcohol polymer (PVA) and (Ag) nanoparticles by using drop casting method.
3. Study the effect of laser powers on non-linear optical properties for all samples of three organic laser dyes (solutions and thin films).
4. Possibility of using all of organic laser dyes samples as optical limiting and active laser media.

2.1 Introduction

The theoretical consideration that is considered in this chapter, included the organic laser dyes, chemical structural of organic laser dyes, dyes classification, photo physical processes, phosphorescence, fluorescence, applications of organic laser dyes, nanoparticles, polymer, interaction of laser light with matter, laser beam characteristics, Z-Scan technique, and Gaussian beam.

2.2 Organic Laser Dyes

Organic laser dyes are fluorescent molecules with large molecular weights, characterized by containing extended systems of conjugated double bonds. In a dye laser, those molecules are dissolved in an organic solvent. They usually have strong absorption band somewhere from the ultraviolet to the near infrared [34]. Although dyes have been demonstrated to laser in the solid, liquid, or gas phase, it is in the liquid and solid phases that dyes have made a significant impact as laser media.

The spectroscopic techniques UV-Visible absorption, fluorescence, the UV-Visible absorption occurs when an atom or molecule absorbs light and uses the energy of that light to become electronically excited (to raise an electron to a higher energy level). Electrons in atoms and molecules can only exist in specific energy levels known as levels. The photons that cause these transitions generally have wavelength in the ultraviolet (UV) or visible range. Once an atom or molecule is electronically excited, it can lose this energy in several ways [35].

2.3 Chemical Structural of Organic Laser Dyes

Organic laser dyes are large and important groups of chemicals which, on binding with material, will give color to the material. Dyes are ionic, aromatic organic compounds with structures including aryl rings which have delocalized electron systems. Such complex aromatic molecular structures make dyes more stable and

more difficult to bio degrade. The color of a dye is provided by the presence of chromophore group. They are widely used to color the substrate such as textile paper, fiber, leather, hair, plastic material and a cosmetic base [36]. Dyes contain chromophore group which is delocalized electron system with conjugated double bonds, and an electron donating substituents that case or intensify the color. Figure (2.1) shows the Chemical structure for most important laser dyes [37].

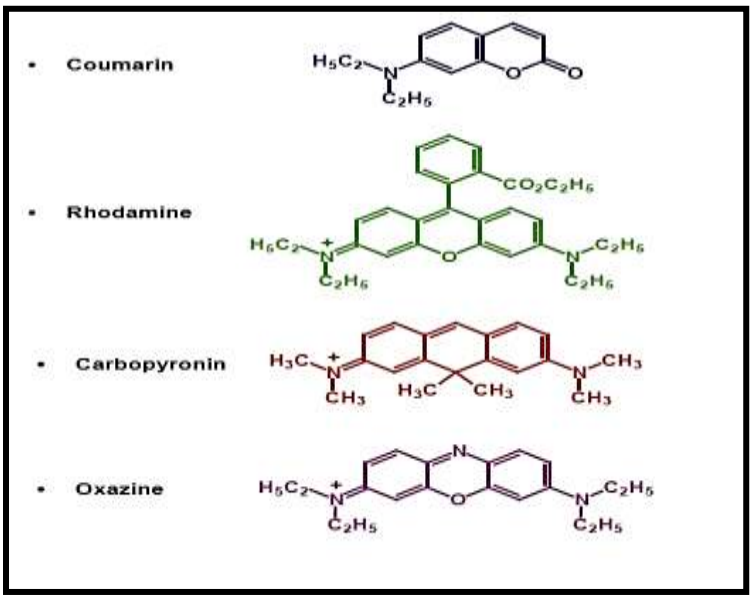

Figure (2.1): Chemical structure for most important laser dyes [37].

2.4 Dyes Classification

Normally, dyes are classified in two separate ways, either accordance to their chemical structure or according to the method of application. Around thirty different groups of dyes can be discerned based on chemical structure. Organic dyes are one of most used in dye laser and classified according to their chemical structure into:

1. Poly methane dyes: gives a laser action in near IR (0.7-1.5)μm.
2. Xanthene dyes: gives a laser action in visible region (500-700) nm.
3. Coumarin dyes: gives a laser action in blue – green region (400- 500) nm.

4. Scintillator dyes: gives a laser action in UV-region ($\lambda < 400$ nm).

The approximate working ranges of various laser dyes are shown schematically in Figure (2.2).

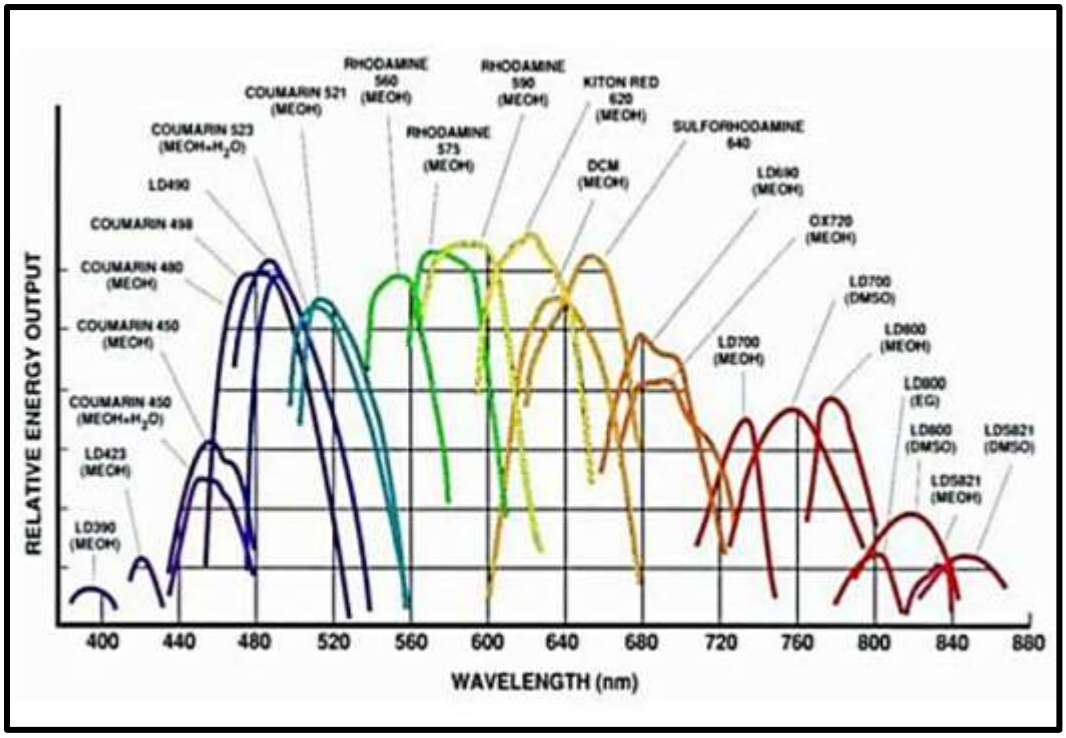

Figure (2.2): The working ranges of various Laser dyes [37].

2.5 Photophysical Processes

The photophysical process is defined as a physical process (i.e., in which it does not involve a chemical change) resulting from the electronic excitation of a molecule or system [38]. The electronic states of aromatic molecules can be grouped into two broad categories, singlet states and triplet states. A singlet state is one in which all of the electrons in the molecule have their spins paired. Triplet states are those in which one set of electron spin have become unpaired. As will be seen later, triplet states and singlet states differ significantly in their properties as well as in their

energies. A triplet state will always lie lower in energy than its corresponding singlet state [39]. The photophysical processes are divided into two types:

2.5.1 Radiative Processes

It is the process of transitions of the molecule from a higher to a lower electronic state by the emission of a photon. In the former, an electronically excited molecule loses its excitation energy by emission of radiation which is also known as (luminescence). When a radiative transition between states of same multiplicity is described as fluorescence, a radiative transition between states of different multiplicity is described phosphorescence [40].

2.5.1.1 Fluorescence

These transitions are accompanied by an energy emission during their acquisition. The molecule that is raised after reaching the lowest vibrational level (S_1) and the loss of the amount of energy in the vibration relaxation process is caused by the molecule or atom absorbing a photon and entering the irritating level. The only way to relax is by emitting the electrons, which causes an energy loss (S_o) of the fluorine process, which causes a direct radiation transmission between (10^{-8}-10^{-9}) sec. This time period differs from one sample to another and is known as the chronological age of the fluorescence sample and the wavelength longer than the wavelength that produced the excitation (energy loss), i.e., the stokes phenomenon [41]. Stokes's displacement can be defined as the difference in wavelength or frequency units in the position of the absorption and emission (fluorescence) spectra of the same electronic transitions. Stokes's displacement happens due to the vibration relaxation in excited states [42]. Figure (2.3) shows the Stokes shift between the absorption and emission (fluorescence) spectra.

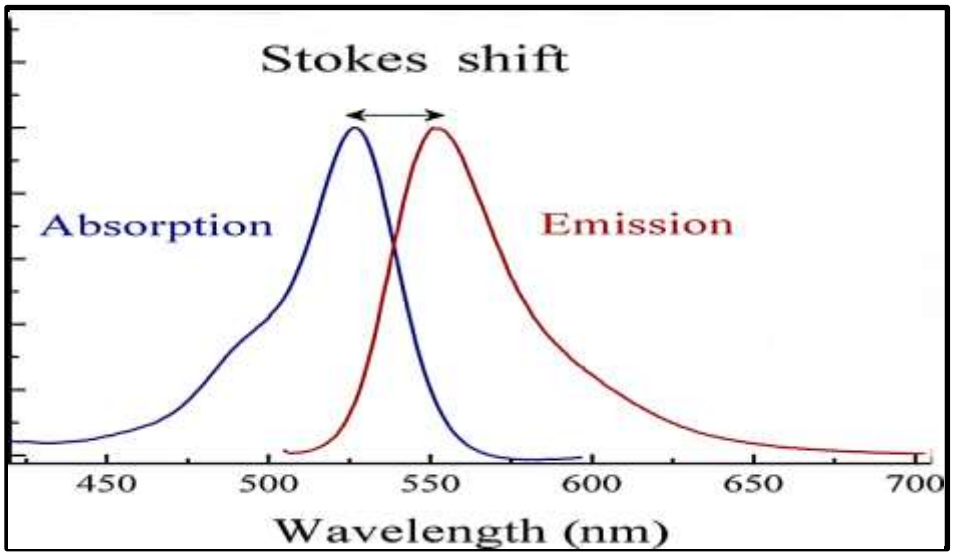

Figure (2.3): Stokes displacement between the absorption spectrum and the emission spectrum [42].

2.5.1.2 Fluorescence Quantum Efficiency

The time of the radiative transition from the lower vibrational level to the excited electronic state then to a ground vibrational level and back to its first state after this period of time is called radiative lifetime (τ_{FM}), which is defined as the inverted rate of fluorescence emission (K_{FM}) in unit (sec^{-1}) [42].

$$\tau_{FM} = \frac{1}{K_{FM}} \qquad (2.1)$$

Where: (K_{FM}) represents the probability of radiation transition.

Because of the presence of non-radiative processes competing with the possibility of radiation transition (K_{FM}), it will reduce the number of particles qualified for fluorescence emission, so the total probability of transition (K_F) will be the sum of the radiated and non-radioactive transition [42]:

$$\tau_F = \frac{1}{K_{FM} + \sum K_d} = \frac{1}{K_F} \qquad (2.2)$$

Where (ΣK_d) is the sum of constants (rate constants) for non-radioactive processes for the lowest vibratory state. The time of the fluorescence lifetime (τ_F) is the actual time of the fluorescence, which is equal to the inverted total constants of all non-radiative and radioactive processes that cause energy loss [43].

$$\tau_F = \frac{1}{K_{FM} + K_{IC} + K_{ISC}} \qquad (2.3)$$

Where K_{IC} is the rate of inter conversion (sec^{-1}) and (K_{ISC}) is the rate of intersystem crossing (sec^{-1}). The lifetime of the fluorescence (τ_F) can be the main lifetime of the excited state. There is a relation between fluorescence intensity and fluorescence lifetime (τ_F) [43].

$$I = I_\circ \exp(-t / \tau_F) \qquad (2.4)$$

Where (I) is the fluorescence intensity at time (t), ($I_\circ$) represents the highest fluorescence intensity and (t) time immediately after the cessation of excitation.

The lifetime of fluorescence (τ_F) can be calculated from a standard compound known as its chronological age, as well as the area under curve, as in the following relationship [44]:

$$\tau_F = \frac{a \times \tau_{fRB}}{a_{RB}} \qquad (2.5)$$

Where (τ_{fRB}) is the time-span of the standard compound, the Rhodamine B (3.230 ns) at concentration (10^{-4}) M and (a_{RB}) is the area under the fluorescence curve of Rhodamine B and its value (117.6 cm^{-1}), a is the area under the curve of the compound required in this research.

The quantum efficiency ($\Phi_{F)}$ represents the quantum yield of fluorescence, which is the ratio between the probability of radiation transition (K_{FM}) and the average of processes for the singles state ($K_{FM}+K_{IC}+K_{ISC}$). This value is a physical constant of each type of excited particles, or the ratio of total energy emitted to the amount of absorbed energy [44].

$$\phi_F = \frac{K_{FM}}{K_{FM} + K_{IC} + K_{ISC}} = \frac{K_{FM}}{K_{FM} + \sum K_d} \qquad (2.6)$$

$$\phi_F = K_{FM}\tau_F = \frac{\tau_F}{\tau_{FM}} \qquad (2.7)$$

It is also possible to calculate the quantum yield of fluorescence (Φ_F) by calculating the ratio between the area of the fluorescence spectrum
and the area of the absorbance spectrum, as shown in equation (2.8) [45].

$$Q_F = \frac{\int F(v')dv'}{\int \varepsilon(v')dv'} \qquad (2.8)$$

It has been observed that the quantum yield of fluorescence for several compounds depends on the wavelength used in the excitation and the temperature. So, the quantum yield of fluorescence increases when non-radiative processes decrease and when the temperature is reduced, the relation between them is reversed. The values of fluorescence production are between (0-1), therefore, the lifetime of the fluorescence is far less than the radiation lifetime due to the non-radiative processes competing for the fluorescence process. Since values of the quantum efficiency are less than or equal to one, then **($\tau_{FM} > \tau_F$)** [45].

2.5.1.3 Phosphorescence:

A radiative transition between states of different multiplicity is described as phosphorescence. It occurs when the molecules go from T_1 to various vibration

levels of the ground state (S_0) and emits photons, at lifetime is about 10^{-3} to 10^{-2} sec, and is larger than the lifetime of the fluorescence process. Since the energy of triplet state (T_{10}) is less than that of singlet state (S_{10}) (The state of fluorescence emission), thus, the energy of phosphorescence photons is less than that of fluorescence photons

2.5.2 Non – Radiative Processes

It is the transitions between vibrational levels of different electronic states. Such transitions are normally preceded by radiation less thermal activation of the initial electronic state and followed by radiation less thermal de-activation of the final electronic state. There are two types of radiation less transition [47]: -

a. non radiative transitions between state of similar multiplicity known as internal conversion, e.g. $S_2 \rightarrow S_1$, $T_2 \rightarrow T_1$.

b. non radiative transitions between states of different multiplicity, which are spin-forbidden, known as intersystem crossing, e.g. $S_1 \rightarrow T_1$, $T_1 \rightarrow S_o$. The processes that occur between the absorption and emission of light are usually illustrated by the Jablonski diagram. (Figure 2.4).

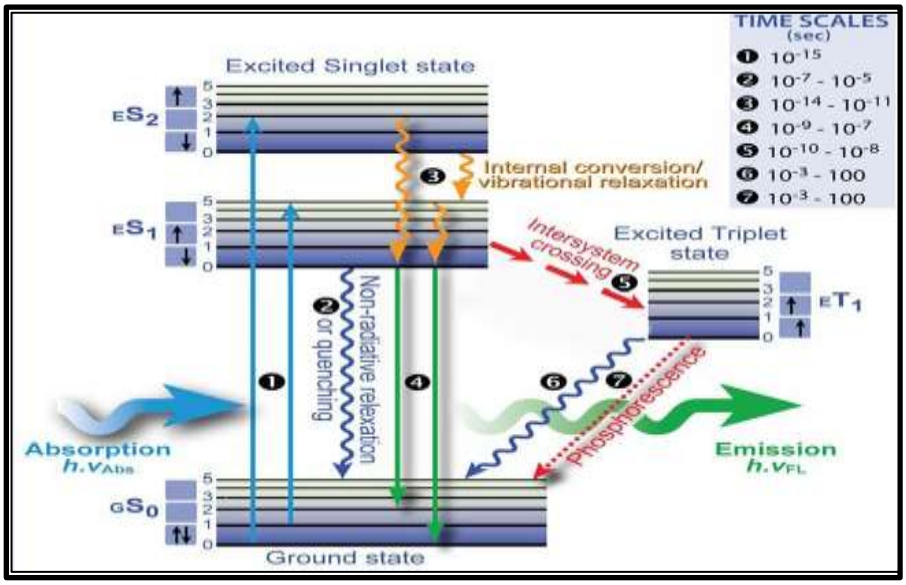

Figure (2.4): Jablonski diagram [47].

2.5.2.1 Internal Conversion

Internal conversion is a non-radiative transition between two electronic states of the same spin multiplicity. In solution, this process is followed by a vibrational relaxation towards the lowest vibrational level of the final electronic state. The excess vibrational energy can be indeed transferred to the solvent during collisions of the excited molecule with the surrounding solvent molecules [48].

The separation between excited singlet states S_2, S_3, S_4..., in an aromatic molecule is smaller than the energy separation between the lowest singlet state $S_1$and the ground state S_o. This means that the lowest vibrational level of S_2 will overlap with higher vibrational levels of the S_1state.That does not involve extremely large difference in configuration from the zero vibrational level of the S_1 state. This situation gives rise to a high degree of coupling between the vibrational levels of the $S_2$and S_1 states, which provides an extremely efficient path for crossing from the S_2 state to the S_1 state. From S_1, internal conversion to S_o is possible but is less efficient than conversion from S_2 to S_1, because of the much larger energy gap between S_1 and S_0. Therefore, internal conversion from S_1 to S_o can compete with the emission of photons(fluorescence) and intersystem crossing to the triplet state from which emission of photons (phosphorescence) can possibly be observed [49].

2.5.2.2 Intersystem-crossing

Intersystem crossing is a non-radiative transition between two isoenergetic vibrational levels belonging to electronic states of different multiplicities. For example, an excited molecule in the zero vibrational level of the S_1 state can move to the isoenergetic vibrational level of the T_n triplet state; then vibrational relaxation brings it into the lowest vibrational level of T_1. Intersystem crossing may be fast enough (10^{-7} – 10^{-9} sec) to compete with other pathways of de-excitation from S_1 (fluorescence and internal conversion $S_1 \rightarrow S_o$) [50].

Once intersystem crossing has occurred, the molecule undergoes after the usual internal conversion process and falls to the zero vibrational level of the triplet state. Since the difference in energy between the zero vibrational level of the triplet state and the zero vibrational level of the lowest excited singlet state is large compared to thermal energy, repopulation of a singlet state from a triplet state is highly improbable. There are two factors which tend to enhance a radiation-less transition between the lowest triplet state and the ground state:

1.The energy difference between the triplet state and the ground state is smaller than the difference between the lowest singlet state and the ground state. This tends to enhance vibrational coupling between these two states $T_1 \rightarrow S_o$, and therefore to enhance intersystem crossing [51].

2. The life time of a triplet state is much longer than that of an excited singlet state (about 10^{-4} to 10 sec) and therefore loss of excitation energy by collisional transfer is generally enhanced. In fact, this is so important that in solution at room temperature it is often the dominant pathway for the loss of triplet state excitation energy [52].

2.6 Applications of Organic Laser Dyes

There are too many applications of laser dyes [53]:

1- Industrial applications of laser dyes include separation of isotopes of important radioactive elements such as Uranium. Uranium is used as fuel in the nuclear power reactors to generate electricity.

2- Medical applications of laser dyes include skin treatments, including tattoo removal, diagnostic measurements, activation of photosensitive drugs for photodynamic therapy; etc. In the field of medical applications, dye lasers have potential advantages over other lasers. Dye lasers are unique sources of tunable

coherent radiation, from the ultraviolet to the near infrared. The medical applications of dye lasers are some of the most important clinical applications.

3- Optical communications
4- Image processing
5- Switching
6- 3D data storage and optical limiting.

2.7 Polymers

A polymer is a large molecule built up from numerous smaller molecules. Those large molecules may be linear, slightly branched, or highly interconnected. In the latter case the structure develops into a large three-dimensional network. The small molecules used as the basic building blocks for these large molecules are known as monomers. The process of linking monomer together to make the polymer chain is called polymerization [54]. Generally, polymerization requires a higher degree of purity and control over reaction condition such as reactant ratio, solvent, temperature and catalyst than does a normal organic reaction, the number of monomers in the polymer chain are called degree of polymerization [55].

Modification of physical properties of existing polymers could lead to enhancement of the conductivity of particular polymer by several orders of magnitude. The conductive capability of modification polymers makes possible moulded resistance heaters without the use of special heating element [56].

2.8 Polyvinyl alcohols (PVA)

Polyvinyl Alcohols (PVA) have been utilized in a variety of industrial, commercial, medical, and food applications since the early 1930s, including resins, lacquers, surgical threads, and food-contact applications. It has the ability to dissolve in water which is resistant to solvents, oils, and has

an exceptional ability to adhesive materials cellulosic so it's extensive uses included in the paper industry and in textile industries in membranes of industry resistance to oxygen in the coating photographic film as well as in high-voltage applications to possess high tensile strength in a high storage capacity, electrical and optical properties depending on the type of additives and impurities [57].

2.9 Nanotechnology

Nanotechnology or nanoscale science is concerned with the investigation of matter at the nanoscale, generally taken as the (1 to 100 nm) range. The nanotechnology deals with the production and application of physical, chemical, and biological system at scales ranging from individual atoms or molecules to submicron dimension, as well as the integration of the resulting nanostructures in to larger system nanoparticles are considered to be the building blocks for nanotechnology and referred to particles with at least one dimension less than 100nm [58].

2.9.1 Silver Nanoparticle (Ag NPs)

Silver nanoparticles are nanoparticles of silver of between (1-100) nm in size. While frequently described as being 'silver' some are composed of a large percentage of silver oxide due to their large ratio of surface-to-bulk silver atoms. Numerous shapes of nanoparticles can be constructed depending on the application of the study [59].

2.9.2 Silver Nanoparticle Applications

Silver nanoparticles are being used in numerous technologies and incorporated into a wide array of consumer products that take advantage of their desirable optical, conductive, and antibacterial properties [60].

1. Optical Applications: Silver nanoparticles are used to efficiently harvest light and for enhanced optical spectroscopies.
2. Conductive Applications: Silver nanoparticles are used in conductive inks and integrated into composites to enhance thermal and electrical conductivity.
3. Antibacterial Applications: Silver nanoparticles are incorporated in apparel, footwear, paints, wound dressings, appliances, cosmetics, and plastics for their antibacterial properties.

2.10 Interaction of Laser Light with Matter

When laser light strikes a material surface, it is absorbed in part and reflected in part. The absorbed energy begins to heat the surface. Depending on the time frame and the flounce, there are many parameter regimes that should be addressed. When a laser beam strikes a substance, the energy is absorbed first by free electrons. The absorbed energy then travels via the electron subsystem before being transmitted to the lattice, resulting in the transfer of laser energy to the material. Because materials absorb light at different wavelengths, this process has a resonant feature. The microstructure and electromagnetic properties of the material determine the absorption dependency on wavelength. Laser light has a wide spectrum of interactions due to its intensity. There are two types of matter interactions: linear and nonlinear interactions [61]. Nonlinear optics was born with the invention of the laser as a coherent light source with a high intensity. It now plays a vital function in a wide range of scientific and technological fields. The NLO effects are linked to changes in the material's optical constants, such as the absorption coefficient, refractive index, or both, caused by light. The interaction of the light beam with the atoms of the material is best described by treating it as a driving force operating on an ensemble of oscillators with natural resonance frequency [62].

2.11 Nonlinear Optical Properties

The study of events that develop as a result of changes in the optical properties of materials as a result of intense light contact is known as nonlinear optics. Nonlinear phenomena have received a lot of attention [63]. Positively charged particles travel in the direction of applied electric fields, while negatively charged particles go in the opposite direction. The displacement between positive and negative charged particles produces dipole moments, and the dipole moment per unit volume describes the induced polarization of the medium. Electric polarization is approximately linearly proportional to the applied electric field (E) when the applied electric fields are sufficiently minimal [64].

$$P = \chi.E \qquad (2.9)$$

Where (χ) is the electric susceptibility tensor. In the case of linear optics, this is the case. When the applied electric fields are high enough, however, the induced polarization has a nonlinear dependence on them and may be described as a power series with respect to them:[65]

$$P = \chi^{(1)}.E + \chi^{(2)}.EE + \chi^{(3)}.EEE + \ldots\ldots \qquad (2.10)$$

$$P = P^{(1)} + P^{(2)} + P^{(3)} + \ldots\ldots\ldots \qquad (2.11)$$

Where $\chi^{(1)}$ is the linear susceptibility, $\chi^{(2)}$ is the second order nonlinear susceptibility, and $\chi^{(3)}$ is the third order nonlinear susceptibility. The term $\chi^{(1)}$ is responsible for linear absorption and refraction, and is the only term that reflects the linearity between the induced polarization and the incident electric field. The term $\chi^{(2)}$ is present only in non-centrosymmetric materials, i.e. materials that do not have inversion symmetry. The third order nonlinear optical interactions, which are described by the term $\chi^{(3)}$[65]. The field of nonlinear optics (NLO) has been

developing for a few decades as a promising field with important applications in the domain of photo electronics and photonics. Organic materials are considered as one of the important classes of third order NLO materials because they exhibit large and fast nonlinearities [66].

To obtain materials with large third order nonlinearity, various types of organic compounds have been explored. Third order nonlinearity has been measured using a variety of approaches, including degenerate four waves mixing, third harmonic production, and the Z-Scan methodology. Among these methods, Z-Scan is the most straightforward for determining the nonlinear refractive index and nonlinear absorption coefficient. It gives not only the real and imaginary parts of the nonlinear susceptibility's magnitudes, but also the real part's sign. The Z-Scan technique, which uses self-focusing or self-defocusing events in optical nonlinear materials, may quickly quantify nonlinear refraction and nonlinear absorption in solid and liquid samples. The open-aperture and closed-aperture systems [68] are the two approaches of Z-Scan [67].

2.11.1 Z-Scan Technique and Nonlinear Optical Properties Measurements

Z-Scan technique is a simple and direct method to characterize both the nonlinear refraction and nonlinear absorption. It is based on a single beam method. It refers to the process of inserting a sample in a focused Gaussian beam and translating it along beam axis through a focal region. The wave front distortion from self-focusing or self-defocusing will cause the Kerr nonlinearity. The beam power propagating through a small aperture at far field varies with a sample position. Measuring the output power versus position sample allows to determine nonlinearity. There are two methods of Z-Scan, the closed-aperture and open-aperture system [69].

2.11.1.1 Closed-aperture Z-Scan

The change in intensity of a beam, focused by a lens (L) in Figure (2.4), as the sample passes through the focal plane is measured using a closed aperture Z-Scan. The light that travels through an axially centered aperture (A) in the far field is collected by the photo detector PD. The change in axis intensity is generated by the sample S self-focusing or self-defocusing, which results in a change in index of refraction, which forms a lens in a nonlinear sample, as shown in Figure (2.5) [70].

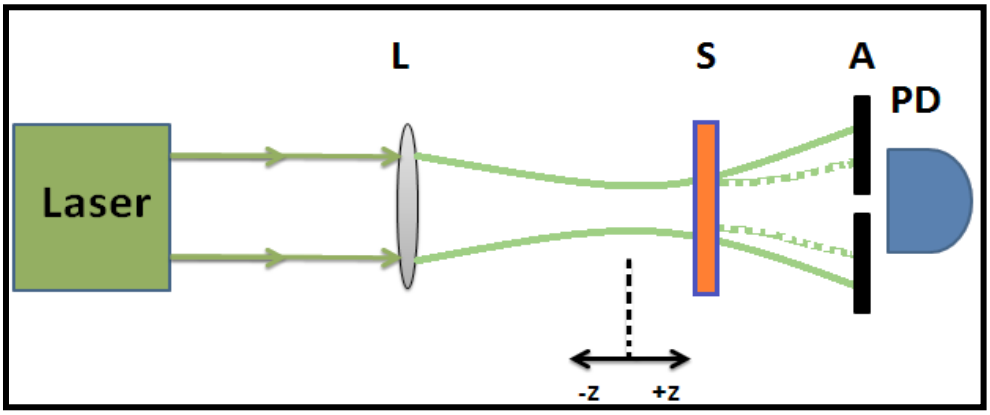

Figure (2.5): Closed aperture Z-Scan [70]

If a material with a negative nonlinear refraction index and a thickness lower than the diffraction length of the focused beam is utilized, the Z-Scan transmittance as a function of Z is related to the sample's nonlinear refraction. This can be thought of as a narrow variable focal length lens. The beam irradiance is modest and nonlinear refraction is minimal distant from the focus (Z_0). The measured transmittance remains constant in this situation (i.e., Z-independent). Irradiance increases as the sample approaches the beam focus, causing self-lensing in the sample [70].

A negative self-lens in front of the focal plane will tend to collimate the beam on the aperture in the far field, increasing the iris position transmittance. Following the focal plane, the same self-defocusing increases the beam divergence, causing the beam to diverge at the aperture and lowering the measured transmittance. Far from

focus (Z >0), nonlinear refraction is modest, resulting in a Z-independent transmittance. A negative nonlinearity's Z-Scan characteristic is a transmittance maximum (peak) followed by a transmittance minimum (valley). A positive nonlinearity is defined by an inverse Z-Scan curve (i.e., a valley followed by a peak). These two scenarios are depicted in Figure (2.6) [71].

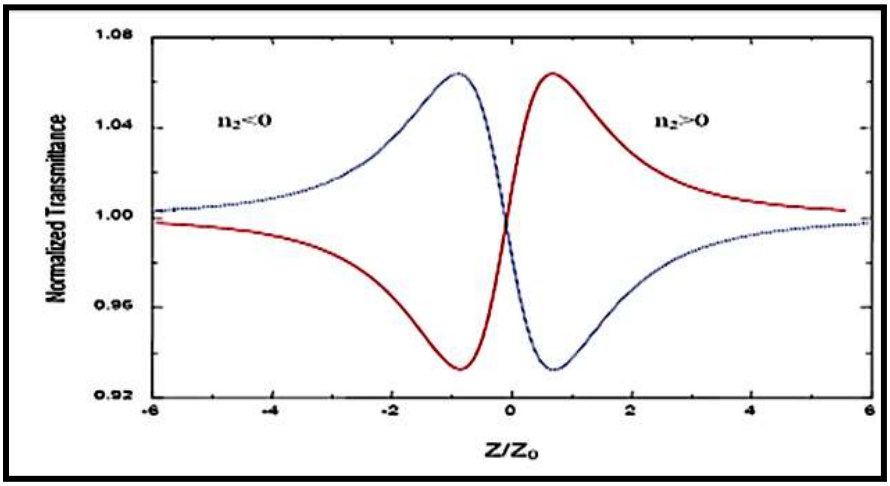

Figure (2.6): Calculated Z-Scan transmittance curves for a cubic nonlinearity [71].

The nonlinear refractive coefficient is calculated from the peak to valley difference of the normalized transmittance by the following formula [72]:

$$n_2 = \frac{\Delta\Phi_o}{I_o L_{eff} k} \qquad (2.12)$$

Where, ($k = 2\pi/\lambda$), (k) is wave number, I_o is the intensity at the focal spot and ($\Delta\Phi_o$) is the nonlinear phase shift:[72]:

$$\Delta T_{p-v} = 0.406|\Delta\Phi_o| \qquad (2.13)$$

(ΔT_{p-v})the difference between the normalized peak and valley transmittances, (L_{eff}) is the effective length of the sample, determined from [72]:

$$L_{eff} = \frac{(1-exp^{-\alpha_o L})}{\alpha_o} \qquad (2.14)$$

Where (L) is the sample length and (α_o) is linear absorption coefficient which is given as [72]:

$$\alpha_o = \frac{\ln(\frac{1}{T})}{t} \qquad (2.15)$$

Where (T) is the transmittance. The linear refractive index (n_0) obtained from equation [72]:

$$n_o = \frac{1}{T} + \left[\left(\frac{1}{T^2} - 1\right)\right]^{1/2} \qquad (2.16)$$

The intensity at the focal spot is given by [72]:

$$I_o = \frac{2P_{peak}}{\pi {\omega_o}^2} \qquad (2.17)$$

which defined as the peak intensity within the sample at the focus, where (ω_0) is the beam radius at the focal point.

2.11.1.2 Open-aperture Z-Scan

An open-aperture Z-Scan analyzes the change in intensity of a beam in the far field at photo detector PD, which captures the full beam, as focused by lens (L). Multiphoton absorption in the sample (S) as it travels through the beam waist causes the shift in intensity. Schematics of experimental setup used for the closed-and open-aperture Z-scan, is shown in Figure (2.7) [73].

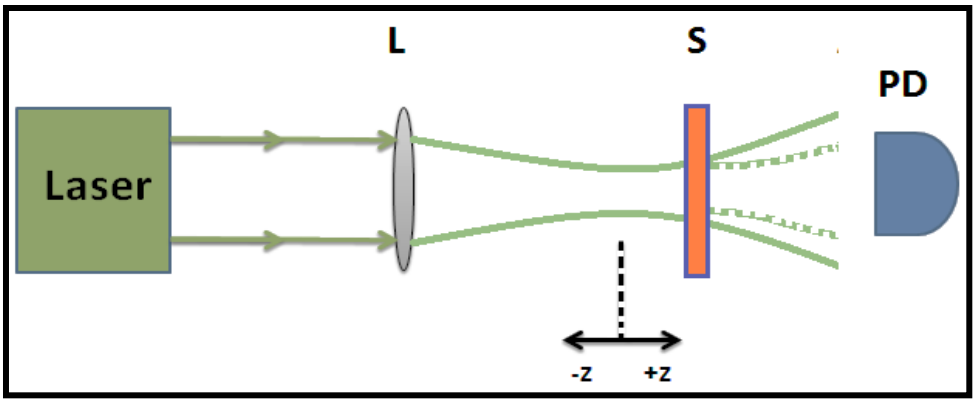

Figure (2.7): Open-aperture Z-Scan [70].

Z-Scan with a fully open aperture is clearly insensitive to nonlinear refraction, even with nonlinear absorption (thin sample approximation). With no aperture, the

Z-Scan traces should be symmetric with regard to the focus (Z = 0), where they should have the lowest transmittance (e.g., multiphoton absorption) or maximum transmittance (e.g., saturation of absorption). In fact, the coefficients of nonlinear absorption can be easily calculated from such transmittance curves. Nonlinear absorption coefficient (β), can be easily calculated by using the following equation:[74]

$$\beta = \frac{2\sqrt{2}\,\mathrm{T(z)}}{\mathrm{I}_o L_{eff}} \qquad (2.18)$$

Where T(z): the minimum value of normalized transmittance at the focal point, (Z=0). It should be clear that the transmittance versus sample position graph of such an open aperture Z-Scan should be symmetric around the focus as shown in Figure (2.8).

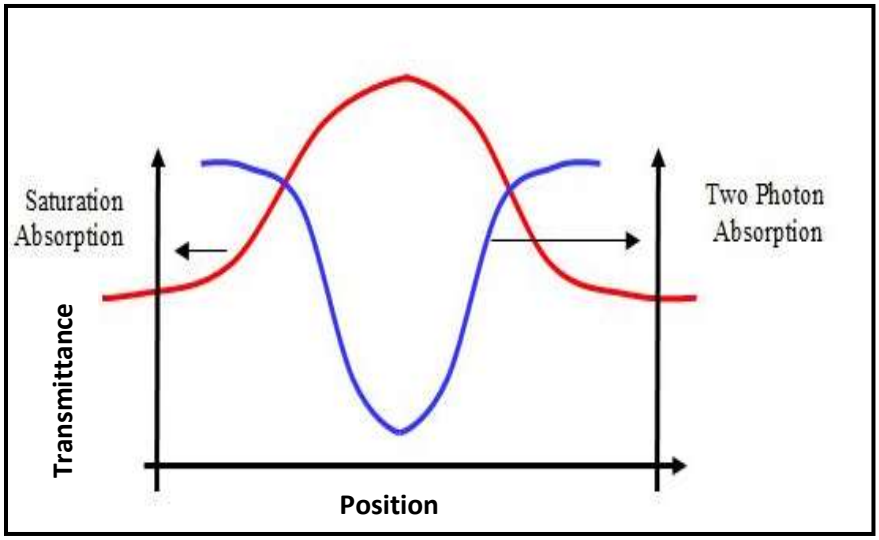

Figure (2.8): Open aperture Z-Scan curve [74].

2.12 Nonlinear Absorption and Nonlinear Refraction

Absorption, which is defined by the absorption coefficient, and refraction, which is defined by the index of refraction n, are the two primary optical qualities involved in the light matter interaction. The energy of the absorbed photons allows the

material to shift from the ground state to the excited state when it is irradiated. When a substance is exposed to a high electric field, it changes its refractive index. In reality, the intensity of the electric field influences the index of refraction, gives the refractive index at high intensity [75].

$$n = n_o + n_2 I \qquad (2.19)$$

Where (n_2) is the nonlinear refractive coefficient related to the intensity. The absorption of the material is also intensity dependent given by [76].

$$\alpha = \alpha_o + \beta I \qquad (2.20)$$

Where,(α_o) is the linear absorption coefficient and (β) is the nonlinear absorption coefficient related to the intensity. The coefficients (n), and (α) are related to the intensity of laser.

2.13 Saturable Light Absorption

A nonlinear process that can be associated with real (rather than virtual) energy levels and population changes in those levels is that of saturable absorption. This process occurred when the nonlinear absorption coefficient ($\beta < 0$), which can be appeared when a strong light absorption between two levels causes saturation (bleaching) of the corresponding electronic transition. The two levels involved surface resonance ground and excited state. On the other hand, this is a process in which a material can be highly absorbing at a specific wavelength when a low-intensity beam is incident upon the material, yet an extremely intense beam (at that same wavelength) will pass through the medium with little change in intensity [77].

2.14 Two Photon Absorption (TPA)

Two-photon absorption is defined as the simultaneous absorption of two photons of the same or different frequency in order to excite a molecule from one state (usually the ground state) to a higher energy electronic state (TPA). The process of two-photon absorption occurs when the energy difference between the implicated

lower and upper states of the molecule is equal to the total of the energies of the two photons, as in the case of a saturable absorber. This process occurred when the nonlinear absorption coefficient ($\beta > 0$). This effect is shown in Figure (2.8). The two-photon transition rate can be significantly enhanced if an intermediate level (3) is located near the virtual level shown by the dashed line in Figure (2.9) [78].

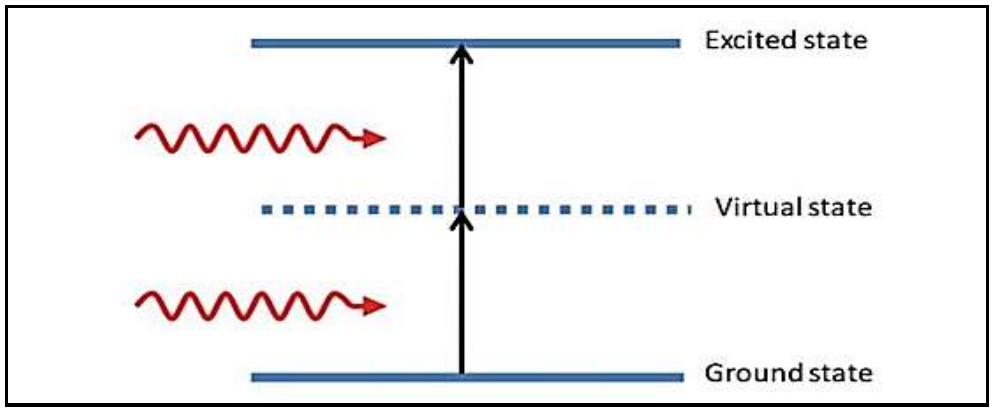

Figure (2.9): Energy levels for two-photon absorption process [78].

2.15 Kerr Effect

The nonlinear electronic polarization, which can be defined as altering the refractive index, is a nonlinear interaction of light in a material. The Kerr effect can produce a local change in the refractive index in high-intensity laser beams, causing the laser material to operate as a lens. This can cause laser beams to self-focus [79].

2.16 Self-Focusing

A powerful beam of light affects the optical properties of a material medium in such a way that the beam is made to come to a focus within the material, resulting in a nonlinear process that causes a spatial fluctuation of the laser intensity. Because the laser beam generates a refractive index variation within the material, the material behaves as a positive lens, with a higher refractive index in the center of the beam

than at its perimeter. When the nonlinear refractive index is positive in sign, self-focusing is possible [80].

2.17 Optical Limiting

In a material with a strong nonlinear effect, the absorption of light increases with intensity such that beyond a certain input intensity the output intensity approaches a constant value. Such a material can be used to limit the amount of optical power entering a system. This can be used to protect expensive or sensitive equipment such as sensors, can be used in protective goggles, or can be used to control noise in laser beams. The ideal behavior of such a device is shown in Figure (2.10) [81].

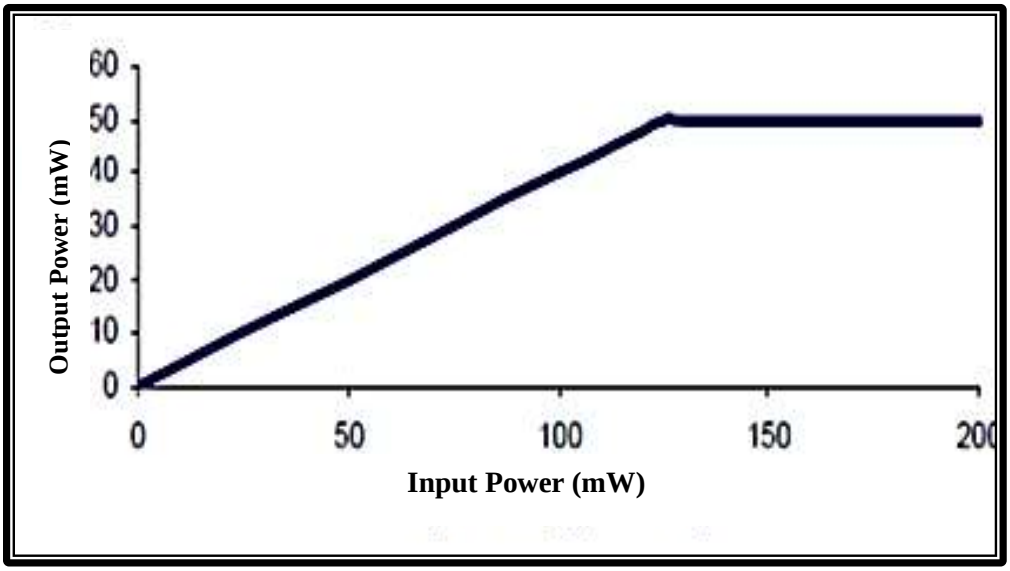

Figure (2.10): An ideal optical limiter [81].

2.18 Gaussian Beam

A Gaussian beam is a beam of electromagnetic radiation whose electric field intensity transverse is a Gaussian function. Many lasers emit beams with a Gaussian profile, in which case the laser is said to be operating on the fundamental transverse

mode or "TEM_{00}". In TEM_{00} mode, the beam emitted from a laser is a perfect plane wave with a Gaussian transverse irradiance profile as shown in Figure (2.11) [82].

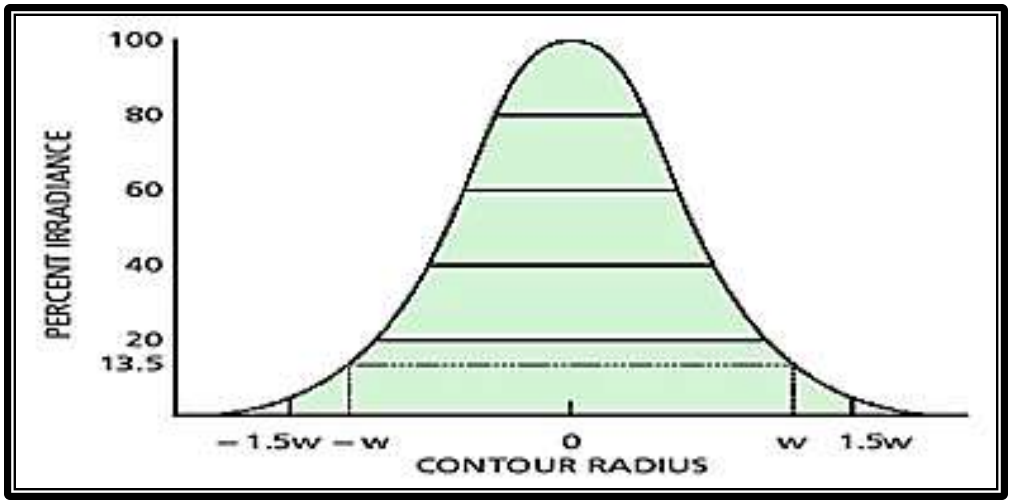

Figure (2.11): Irradiance profile of a Gaussian TEM_{00} mode [82].

2.18.1 Beam Waist and Divergence

For a Gaussian beam propagating in free space, the spot size (w) will be at minimum value (w_0) at one place along the beam, known as the beam waist. Figure (2.12) shows the Gaussian profile in free space. For a beam of wavelength (λ) at a distance (z) along the beam from the beam waist, the variation of the spot size is given by [83]:

$$w(z) = w_\circ[1 + (\frac{\lambda z}{\pi w_\circ^2})]^{1/2} \qquad (2.21)$$

R(z) is the radius of curvature of the beam; its variation is given by:[83]

$$R(z) = z[1 + (\frac{\pi w_\circ^2}{\lambda z})^2] \qquad (2.22)$$

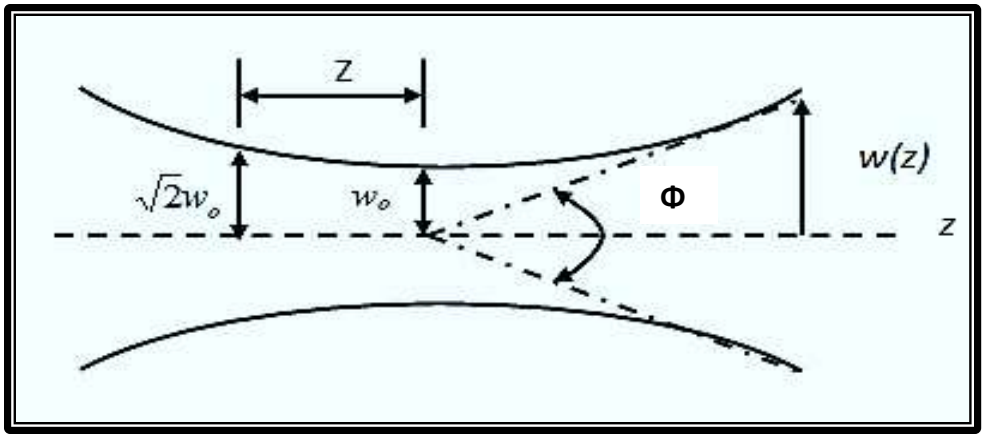

Figure (2.12): Gaussian profile in free space [83]

The divergence of a Gaussian beam, at a sufficient from the waist, tends to an angle:[83]

$$\theta_\circ \approx \tan\theta_\circ = \frac{\lambda}{\pi w_\circ} \qquad (2.23)$$

It describes the spreading of the beam when propagating towards infinity. The above quantity means that larger values of the width mean lower values of the divergence and vice versa [83].

2.18.2 Focusing Gaussian Beam with a Lens

A Gaussian beam can be imaged by lenses or mirrors. When a Gaussian beam passes through a focusing lens with focal length (f), the spot size (w_o) at the focal point is the same on both sides of the lens. The effect of focusing a Gaussian beam by a thin positive lens is shown in Figure (2.13) can be evaluated [84]:

$$w(z) = w_\circ[1 + \left(\frac{f}{z_\circ}\right)^2]^{\frac{1}{2}} \qquad (2.24)$$

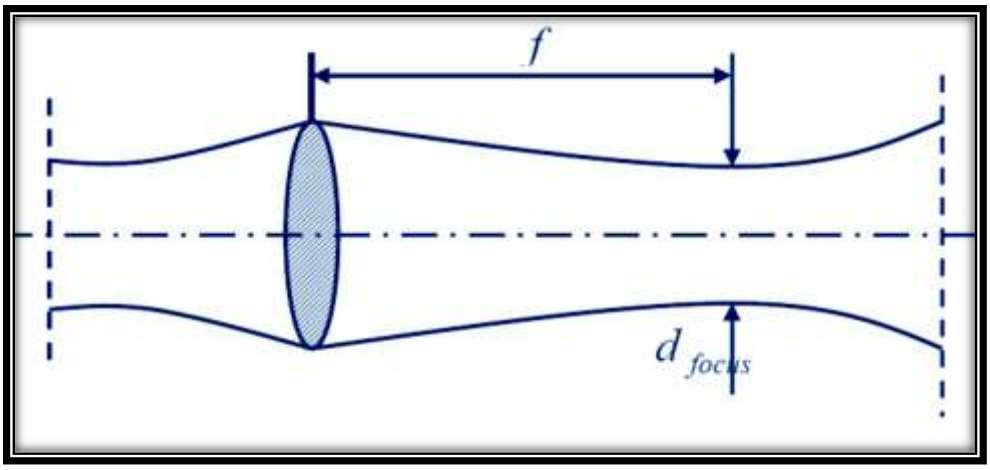

Figure (2.13): Lens focusing of a Gaussian beam [84]

In addition, the spot diameter (d_{focus}) at the focal point, at distance (f) from the lens, is now given by [84].

$$d_{focus} = f\theta_{\circ} \qquad (2.25)$$

Where, (f) is focal length of a lens, and (θ_0) is the divergence angle of the laser beam as shown in Figure (2.13).

3.1 Introduction

This chapter describes the preparation method of organic dyes, preparation solutions and thin films of organic material, and the instruments used for characterization of the material. The Z-Scan system was presented and a measurement was done at diode pumped solid state laser (DPSS) at wavelength (457nm), at different laser powers (56,70,84 and 102) mW and the procedure of these measurements with their photographic pictures.

3.2 Organic Laser Dyes

3.2.1 Acriflavine Organic laser Dye

Acriflavine is derived from (acridine family). The structural formula ($C_{14}H_{14}ClN_3$), its molecular weight is (259.737g/mol), Figure (3.1) shows the chemical structure of the Acriflavine dye.

3.2.2 Orcein Organic laser Dye

The structural formula ($C_{28}H_{24}N_2O_7$), its molecular weight is (500.51 g/mol), dissolves in water to give an acid aqueous solution, but it is rarely soluble in ethyl alcohol. Figure (3.2) shows the chemical structure of the Orcein dye.

3.2.3 Azure-B Organic laser Dye

Azure B is class of thiazine and a container of nitrogen and sulfur atoms within the middle ring. Its structural formula ($C_{15}H_{16}N_3SCl$), its molecular weight (305.8 g/mol) dissolves in water and is low in ethyl alcohol. Its peak absorption lies between the range of wavelengths (648-655nm) for this to be a blue color. The molecular structure of Azure dye is shown in Figure (3.3).

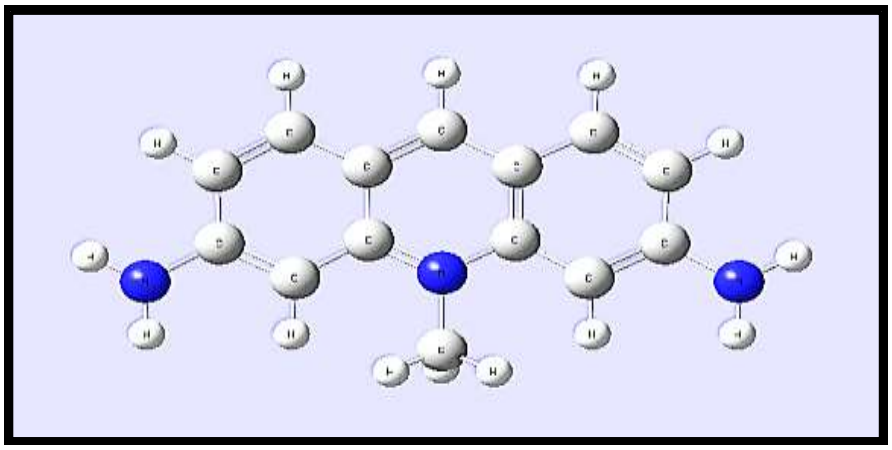

Figure (3.1): Molecular structure of Acriflavine organic dye [86].

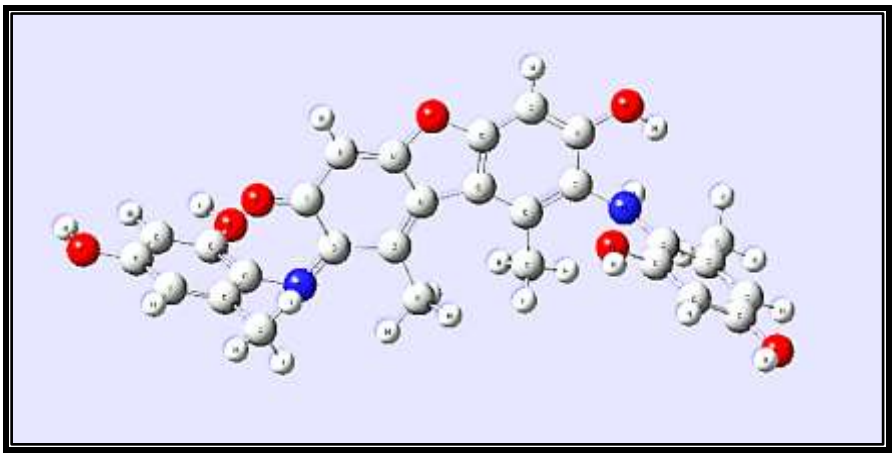

Figure (3.2): Molecular structure of Orcein organic dye [86].

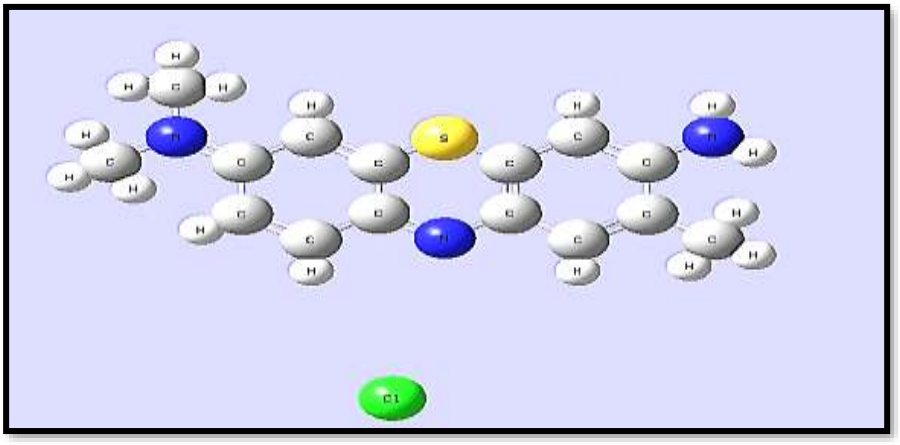

Figure (3.3): Molecular structure of Azure-B organic dye [86].

3.2.4 The solvent

Ethanol, commonly known as (ethyl alcohol), is a colorless, pure alcohol. It burns with a blue flame. The attendance of the hydroxyl collection and the shortness of the carbon chain give ethanol its physical features. Volatile colorless liquid and its density (0.789 gm / cm^3) and molecular weight (46.07 gm / mol), the ethanol molecule is showed in Figure (3.4). Table (3.1) shows the main characterstics of Ethanol solvent [87].

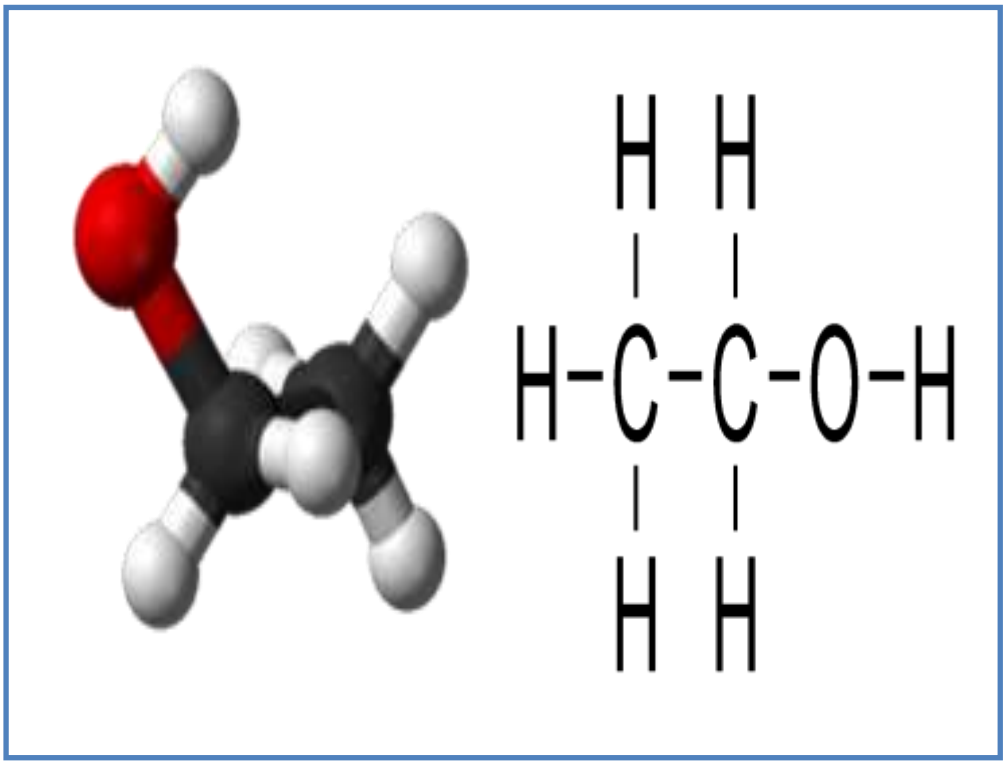

Figure (3.4): The molecular structure of ethanol molecule [87]

Table (3.1) The Main Characteristics of Ethanol Solvent [87]

Parameters	Ethanol
Chemical formula	C_2H_6O
Molar mass (g/mol)	46.07
Refractive index	1.3614
Dielectric Constant	24.195
Polarity	0.5771
Dipole Moment	1.70 D
Density	0.7936 mg/ cm^3
Freezing Point	-114 C^o
Boiling Point	78.3 C^o

3.2.5 Polyvinyl alcohol (PVA)

Polyvinyl alcohol (PVA) was utilized the present work, the properties of this polymer are listed in Table (3.2). Polyvinyl Alcohols (PVA) have been utilized in a variety of industrial, commercial, medical, and food applications since the early 1930s, including resins, lacquers, surgical threads, and food-contact applications. It has the ability to dissolve in water which is resistant to solvents, oils, and has an exceptional ability to adhesive materials cellulosic so it has extensive uses in the paper industry and textile industries in membranes of industry resistance to oxygen in the coating photographic film as well as in high-voltage applications to possess

high tensile strength in a high storage capacity, electrical and optical properties depending on the type of additives and impurities. Figure (3.5) demonstrates the Structure of polyvinyl Alcohol [88].

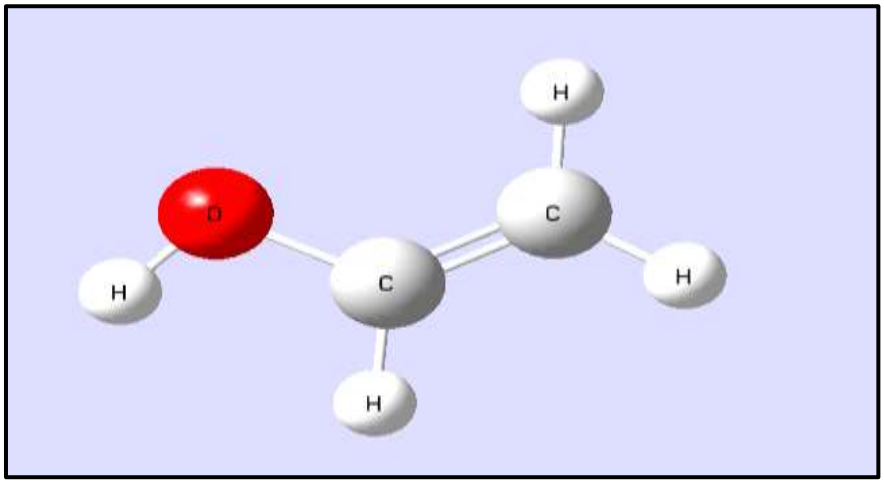

Figure (3.5): The structure of polyvinyl alcohol (PVA) [88]

Table (3.2): The principal qualities of polymer [88].

Molecular formula	C_2H_4O
Solubility	Water soluble
Physical Appearance	White, odorless

3.2.6 Silver Nanoparticles (Ag NPs)

Silver nanoparticles were supplied by laboratory Reagent LTD; the main characteristics are shown in Table (3.3). Silver nanoparticles are silver nanoparticles with a size of (1 to 100) nm. While many are referred to as "silver," some include a high percentage of silver oxide due to their high surface-to-bulk silver atom ratio. Nanoparticles can be made in a variety of shapes, depending on the study's applicability [89].

Table (3.3): The main characteristics of Ag NPs nanoparticles [89].

Description	Ag nanoparticle
Productive company	SIGMA-ALDRICH, Germany
Form	Nano powder
Surface area	> 40 m^2/g
Particle size	(1-100) nm

3.3 Work Scheme

Figure (3.6) shows the experimental procedure as a block diagram of the main steps followed in this work:

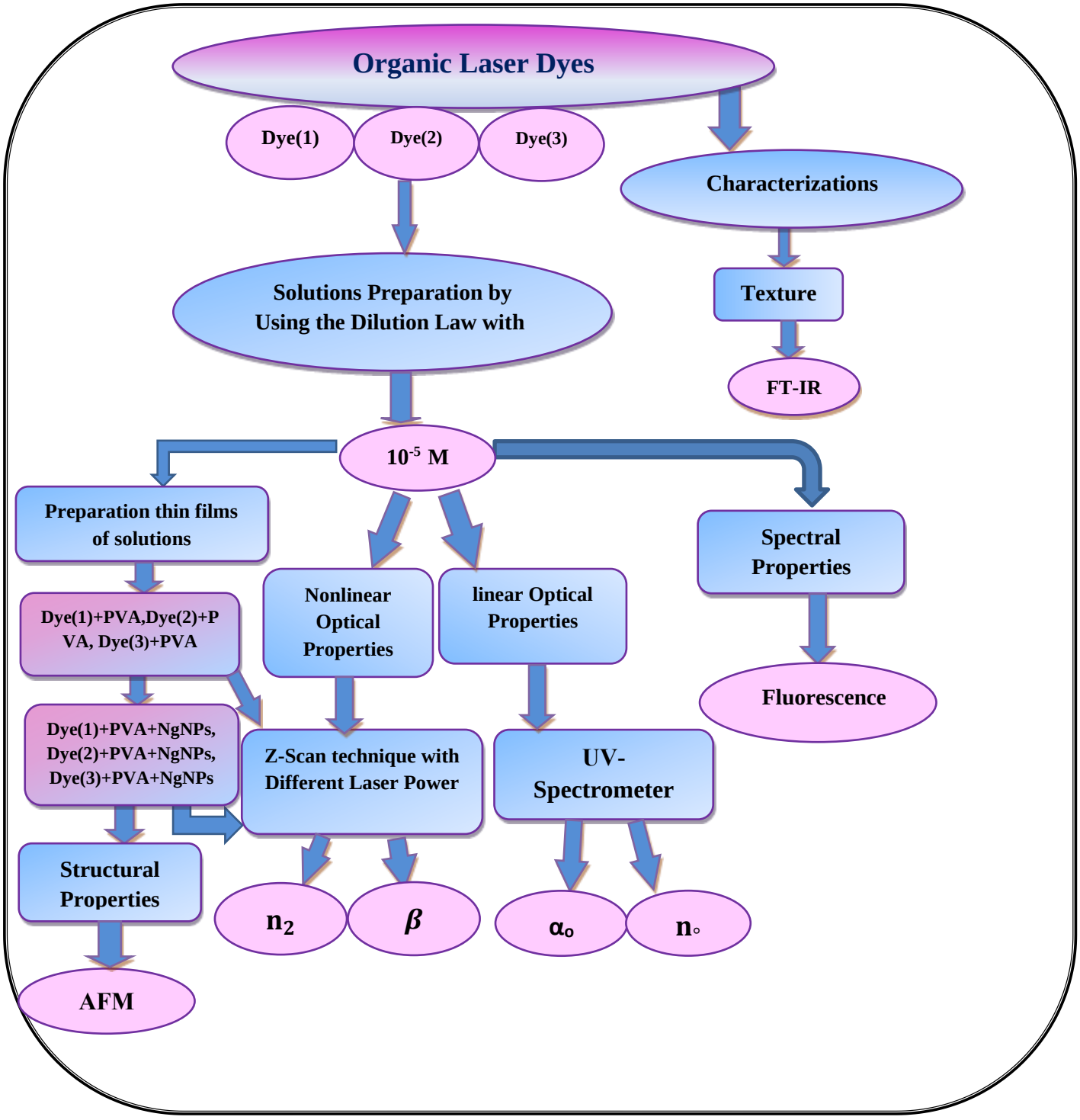

Figure (3.6): Main steps of the experimental work.

3.4 Samples Preparation

3.4.1 solutions preparation

Solutions of concentrations (10^{-3} M) of each organic dye in (ethanol) solvent were prepared. The powder was weighted by using an electronic balance type (BL 210 S), Germany, having a sensitivity of four digits.

To prepare a solution of (Acriflavine, Orcein, and Azure-B) organic laser dyes at a concentration (1×10^{-3} M), (0.02597, 0.05005, 0.03058) gm, respectively from each dye were dissolved in (1ml) of ethanol solvent according to the following equation [90]:

$$\mathrm{W} = \frac{\mathrm{M}_W \times V \times C}{1000} \qquad (3.1)$$

Where, W: Weight of the dissolved in material (g), Mw: Molecular weight of the material (g /mol), V: Volume of the solvent (mL) and C: The concentration (M). The prepared solutions were diluted according to the following equation [91].

$$\mathrm{C_1V_1} = \mathrm{C_2V_2} \qquad (3.2)$$

Where: C_1: Primary concentration, C_2: New concentration. V_1 is the volume before dilution V_2 is the volume after dilution. In this work, (10^{-4} and 10^{-5}) M concentration were prepared for each dye. Figure (3.7) shows dyes solution at concentration (10^{-3},10^{-4},10^{-5})M.

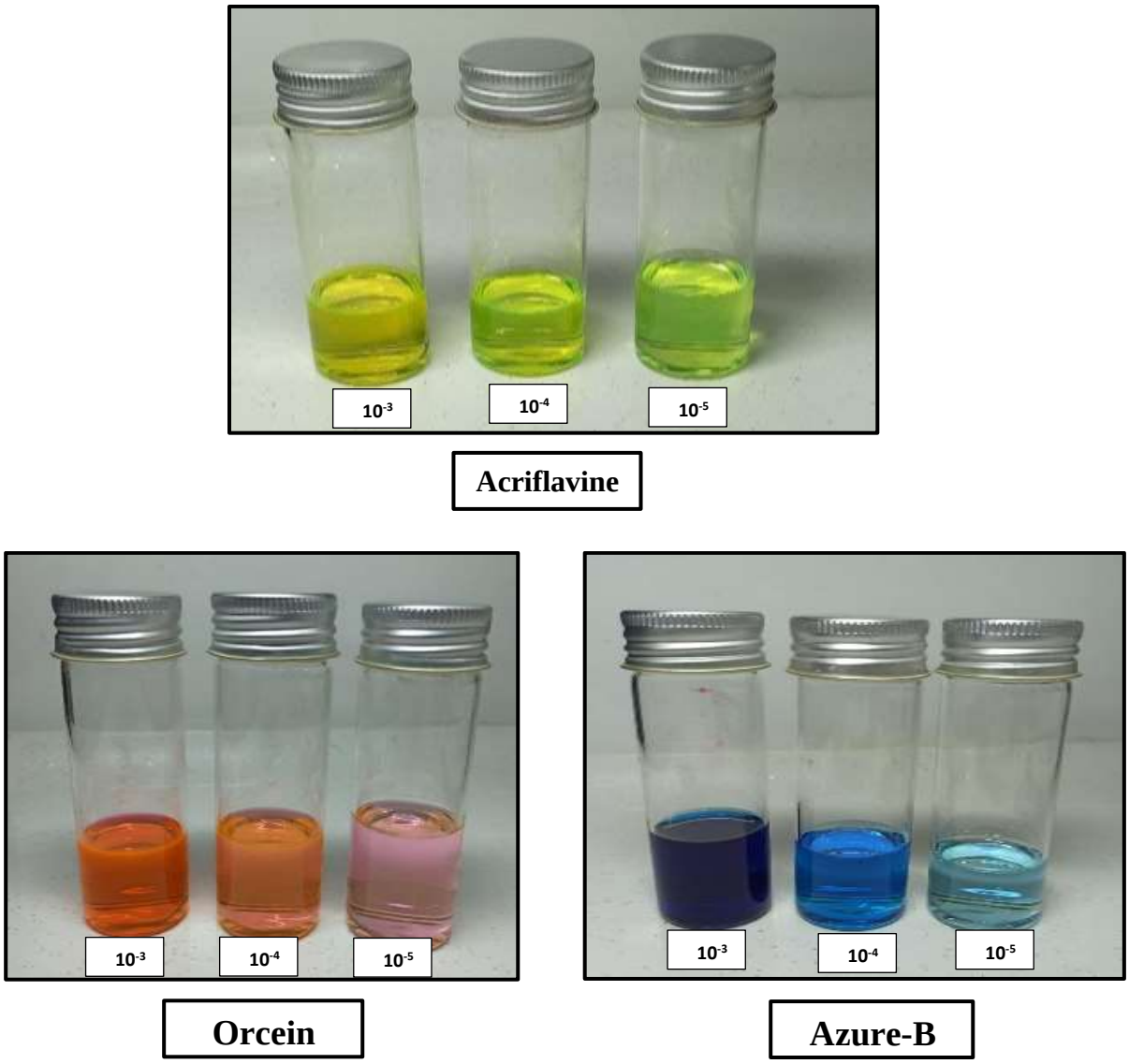

Figure (3.7): Dyes solutions at different concentrations.

3.4.2 Preparation of Solid Samples (Thin Films)

The thin films of (Acriflavine, Orcein and Azur-B) organic laser dye were prepared on a clean glass slide via drop casting method, with solution at a concentration (10^{-3}) M for each of them, and dried at room temperature for (3) days, the thickness of these thin films is about (150-200) nm, the thickness of the thin films was measured by optical method which is done by using Michelson's interferometer.

Dye doped polymer films were fabricated by drop casting method, at concentration (10^{-3}) M. The solution of the PVA polymer is prepared by dissolving the required amount of polymer (2 g in 50 ml of ethanol solvent).

A desired amount of dye solution was added to PVA polymer solution and stirred by a magnetic stirrer at room temperature to get a uniform mixture. Thin films were shaped by drying the mixed polymer dye solution on a slide at room temperature. (0.06) g of nanoparticles powder was added to polymer dye solution and stirred by magnetic stirrer at room temperature to get a uniform mixture. Thin films dye doped with PVA polymer and Ag NPs are framed by allowing the mixture to be dried on a glass block at room temperature. This process was repeated for each dye. Figure (3.8) shows thin films of Acriflavine, Orcein and Azur-B organic laser dyes doped with PVA polymer and Ag NPs nanoparticles.

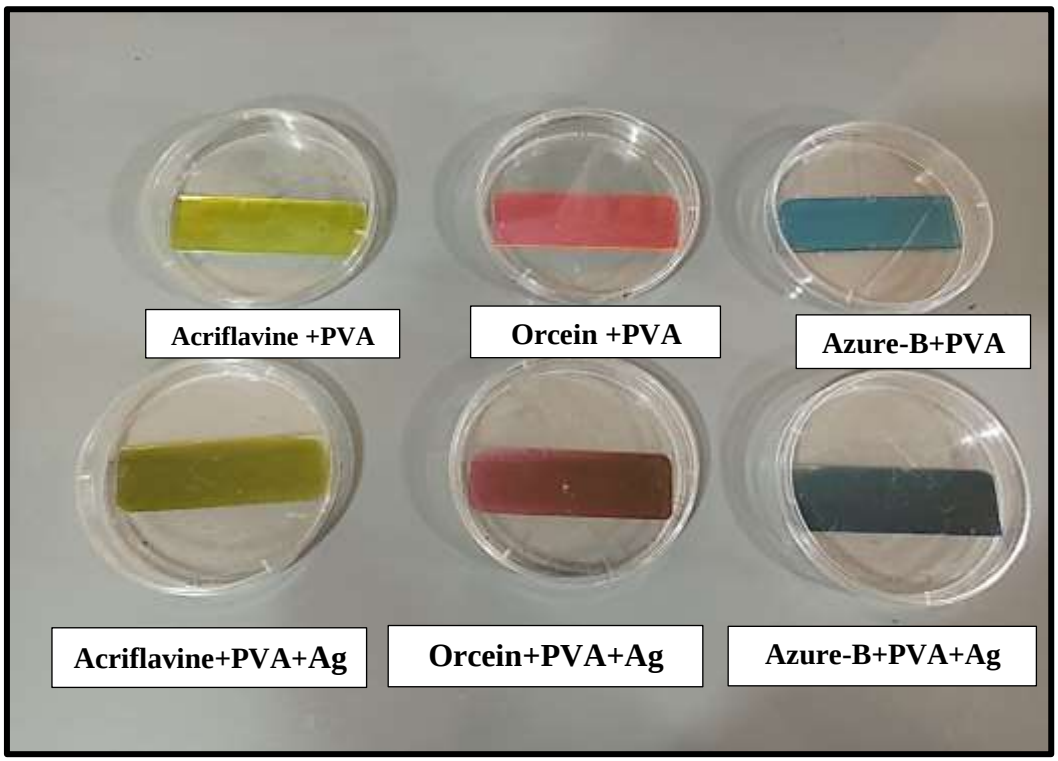

Figure (3.8) Thin films of Acriflavine, Orcein and Azur-B organic laser dyes doped with PVA polymer and Ag nanoparticles.

3.4.3 Thickness measurement

Thickness of dye doped thin film was measured using Michelson's interferometer. The collimated beam of light in the Michelson's interferometer is divided into two halves by partial reflection, which can be used to measure extremely short distances in terms of light wavelength. Figure (3.9) shows the schematic set-up of thickness measurement using Michelson interferometer. Using He-Ne laser (632.8 nm), the film thickness can be determined by the following formula:[92]

$$t = \frac{x}{\Delta x} \times \frac{\lambda}{2} \qquad (3.3)$$

Where

x : the fringe width.

Δx : the shift between the fringes in the first case and the same fringes in the second case.

λ : the laser wavelength.

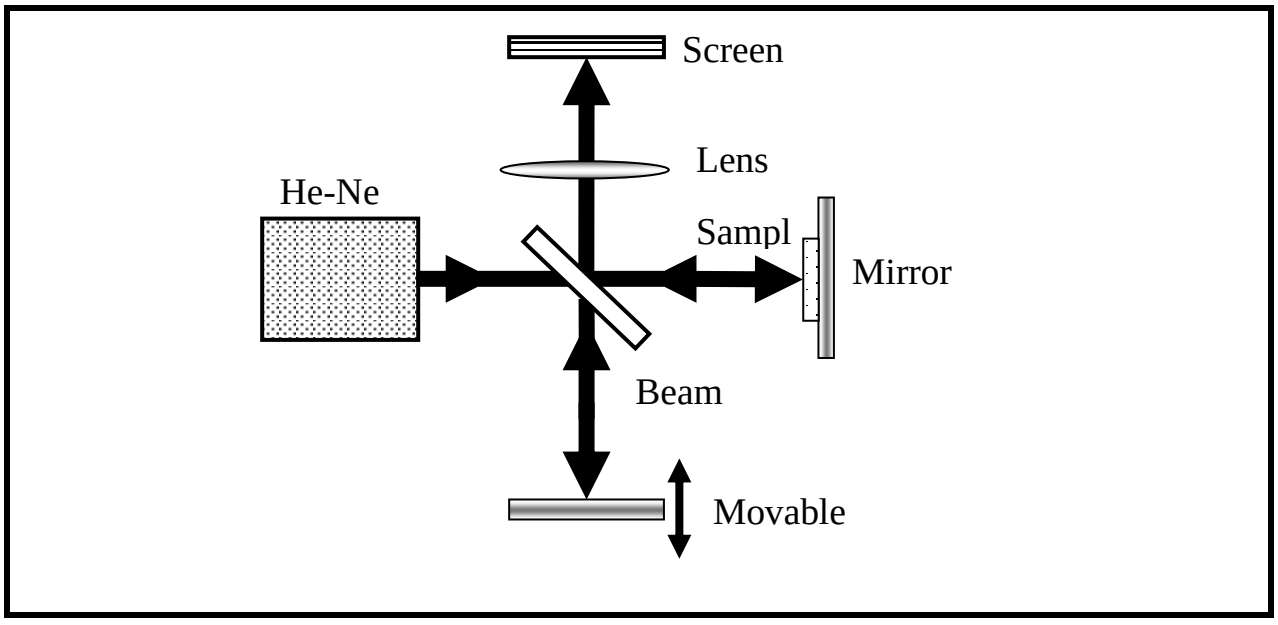

Figure (3.9): Schematic Set-up of Michelson Interferometer [92]

3.5 Structural Properties Measurements

The structural properties are examined using (FTIR) transmission.

3.5.1 Fourier Transforms Infrared Spectrometer (FTIR)

Infrared spectra of (Acriflavine, Orcein, Azure-B) organic dyes have been taken by using infrared spectrophotometer, at the laboratories of department of chemistry, college of science, university of Kufa. Figure (3.10) shows FT-IR spectrometer.

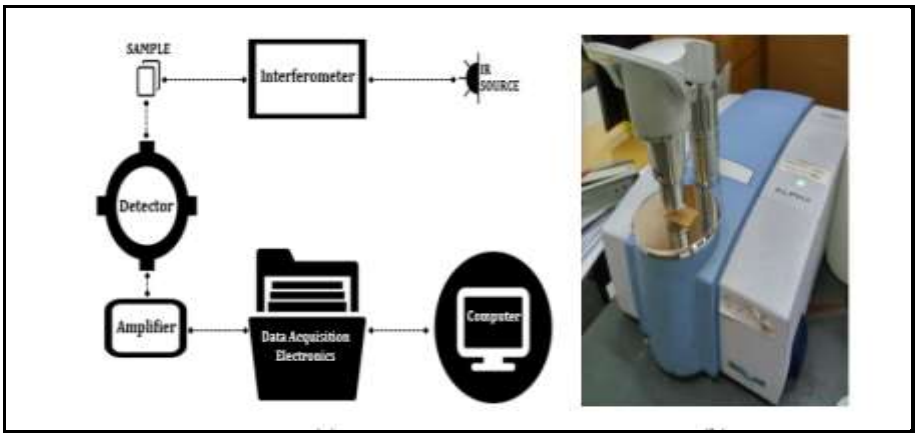

Figure (3.10): FT-IR spectrometer [93]

3.5.2 Optical Microscope

All thin films of (Acriflavine, Orcein and Azure-B) organic dyes were examined by using an optical microscope, which is supplied from Olympus name (Toupview) type (Nikon -73346) and equipped with light intensity automatic controlled camera. Under magnification (100x), this measurement was implemented in the University of Babylon, College of Education for Pure Sciences, as shown in Figure (3.11).

Figure (3.11): Optical Microscope

3.6 Linear Optical Properties

3.6.1 UV-Visible Spectrometer

The absorbance spectra were measured using a UV-Visible Spectrophotometer type (Shimadzu-1800). This device has two light sources Deuterium Lamp (190-360) nm and Tungsten Lamp (360-1100), so it covers a wide range of the electromagnetic spectrum, extending from the ultraviolet to the near infrared region. Table (3.4) shows the specifications of the device. The idea of operating the device depends on the separation of the incoming beam into two parts, one of which passes through the sample solution to be studied, while the second beam in the solvent that represents the reference beam. The device then subtracts the reference beam and registers the absorption spectrum of the sample alone. All samples were examined in the laboratory of thin films (University of Babylon / College of Education for Pure Sciences / Department of Physics), as shown in Figure (3.12).

Figure (3.12): UV – Visible spectrometer

Table (3.4): Specifications of UV-Visible spectrometer.

Wavelength range	(190-1100) nm
Wavelength scan rate	Maximum 1000 nm / min
Light source	Deuterium and Tungsten Lamps
Detector	Silicon photodiode
Power requirements	(220-240) V (AC)

3.6.2 Fluorescence Measurements

Fluorescence spectra were measured for all prepared samples using Spectrophotometer type (FluoroMate FS-2). The samples were mounted cubic cell of quartz dimensions (1×1×5) cm^3 perpendicularly with incident beam. Table (3.5) shows the specifications of the device. All samples were examined in the laboratory of thin film (University of Babylon / College of Education for Pure Sciences / Department of Physics), as shown in Figure (3.13).

Figure (3.13): The Fluorescence Spectrometer

Table (3.5): Specifications of Spectrometer.

Wavelength range	(200 - 900) nm
Wavelength scan rate	200/400/600 nm / min
Light source	150 W (Xenon arc lamp)
Power requirements	(220-240) V (AC)
Resolution	0.5 nm
Wavelength Accuracy	∓1.0 nm

3.7 Nonlinear Optical Properties

Nonlinear optical properties of all samples will be explained in details in the following paragraph:

3.7.1 Z-Scan Technique

The Z-Scan measurements were divided into two types: closed aperture and open aperture. Each part was employed by a continuous wave (CW) diode pump solid state laser with a wavelength of (457) nm and different laser power of (56,70,84 and112) mW. The nonlinear refractive index was measured using a closed-aperture Z-Scan, whereas the nonlinear absorption coefficient was measured using open-aperture Z-Scan. The beam was focused by using a convex lens (f =15 cm), and the beam waist have been measured at the focus equal to (0.025) cm. The laser intensity at the focal point is (20.408×10^{3}) mW/cm^{2}, the sample was moved along the Z-axis. The transmittance through the sample is recorded as a function of sample position. Figure (3.14)shows the open-aperture and closed-aperture Z-Scan setup.

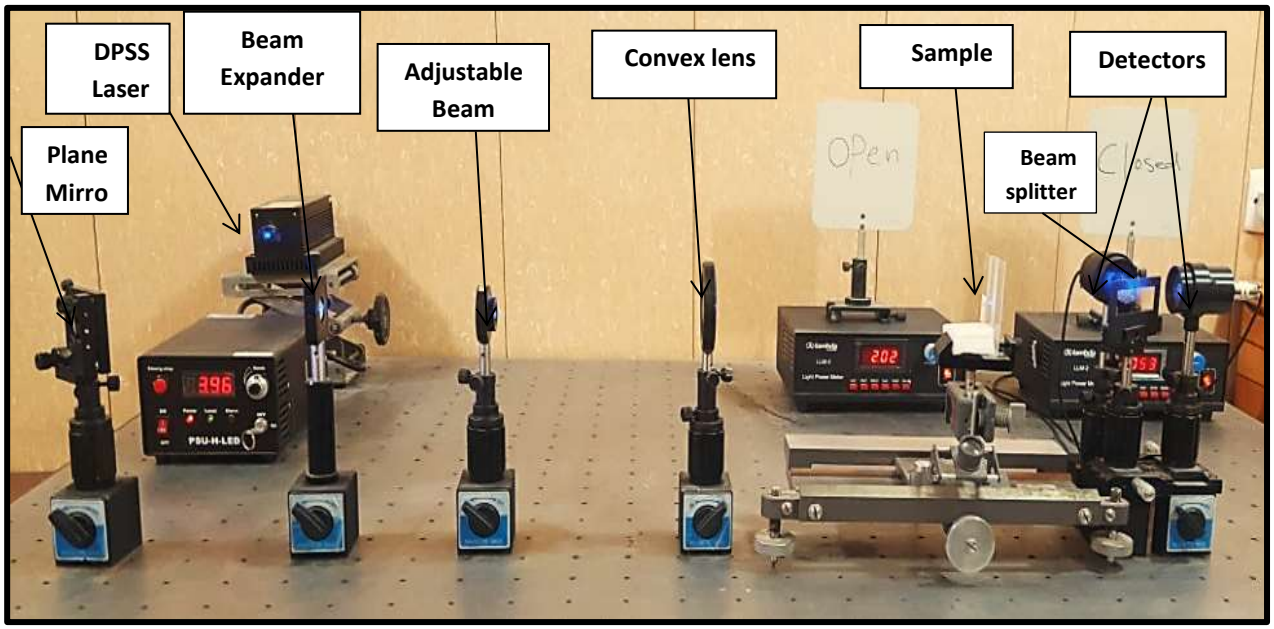

Figure (3.14): Z-Scan set-up.

3.7.2 Diode Pumped Solid-State Laser (DPSS)

CW (457) nm DPSS laser is used. Table (3.6) shows the characteristics of the laser, which used in this research.

Table (3.6): Specifications of 457 nm DPSS laser.

Wavelength (nm)	457 nm
Output power (m W) Max.	142.5 mW
Transverse mode	TEM_{00}
Operating mode	CW
Power stability	5.71%
Beam divergence, full angle (m rad)	1. 8
Beam diameter at $1/e^2$	1.883nm
Power supply	(100-240) Volt

3.7. 3 Detector

The third element in the Z-Scan is the optical power meter detector type (LLM-2), which is used to measure the output power of the laser. The detector was placed at the far field of a Gaussian laser beam.

3.7.4 Aperture

The aperture is an important parameter in Z-Scan system to measure complex refractive index (n_2) in the closed-aperture technique, and its diameter is (1mm). The aperture was aligned with the lens in the same axis.

3.7.5 The Sample

All solutions are filled into the glass cuvette (1) mm thickness. The cuvette was hand made in the laboratory, which consists of five slides of glass as shown in Figure (3.15). The geometry of a sample cuvette can be shown in Figure (3.16), which is represented engineering drawing of sample cuvette.

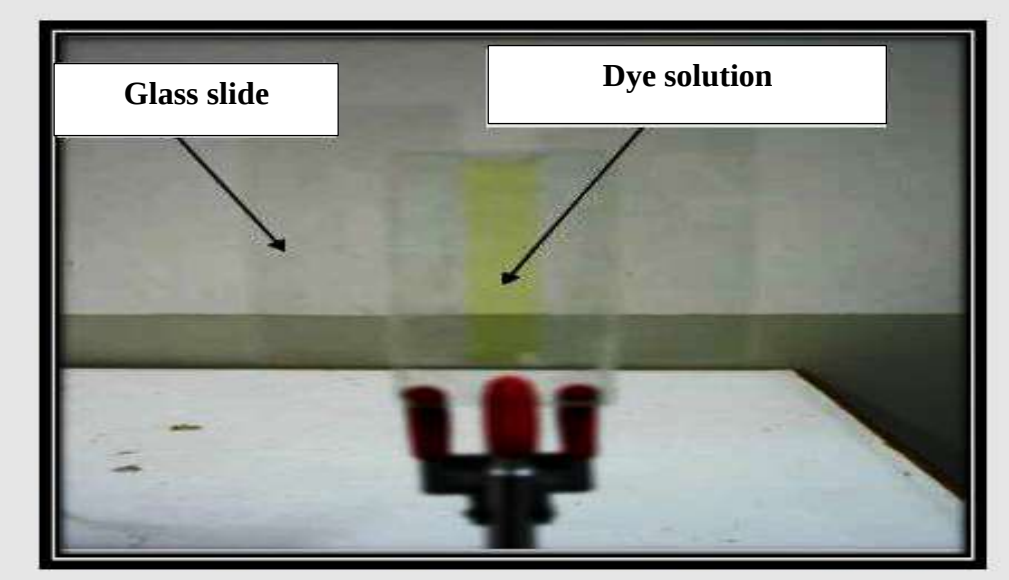

Figure (3.15): Photograph of a sample

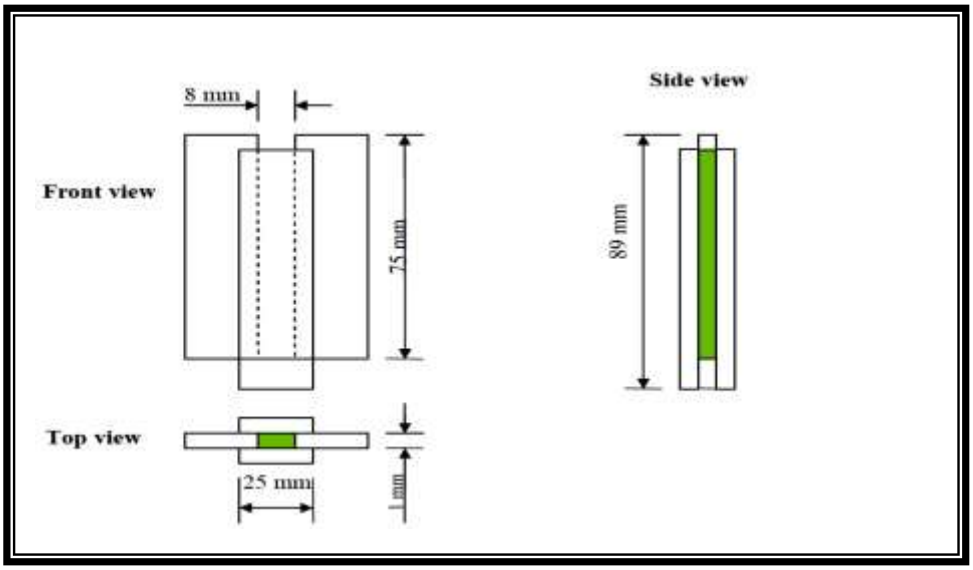

Figure (3.16): Geometry of sample cuvette

3.8 Reference Beam Measurements

In order to measure the reference power of a CW laser, the detector was placed directly in front of the (457 nm) DPSS laser. The normalized transmission as a function of sample position is given by [93]:

$$T(z) = \frac{P(I)}{P(I)_{ref}} \qquad (3.4)$$

Where, (P) is the power of the transmitted laser beam, when the cuvette is filled by dye solution, and ($P_{ref)}$ is power of the reference laser beam.

3.9 Optical Limiting Behavior

Optical limiting occurs when the optical transmission of a material saturates with increasing laser intensity, a property that is desirable for the protection of sensors and human eyes from the intense laser radiation. The optical power limiting property of pure and doped dyes with PVA polymer and their thin films, are measured with different laser powers used in Z-Scan technique.

4.1 Introduction

In this chapter,the results of all samples of (Acriflavine, Orcein and Azure-B) organic laser dyes and their thin films were presented. The structural properties which including microscopic properties using (optical microscope), Also charts of infrared (FT-IR) spectra of dyes and their thin films. The spectral, linear and non-linear optical properties of all samples are discussed. Also using Z-Scan for two cases, closed and open aperture with (457 nm) and different powers (56,70, 84, and 102) mW. The optical limiting behavior of all samples were studied.

4.2 Structural Properties

Structural properties of (Acriflavine, Orcein and Azure-B) have been determined by studying (FT-IR).

4.2.1 Fourier Transform Infrared (FTIR)

The FT-IR spectra of (Acriflavine, Orcein and Azure-B) organic laser dyes as powder is measured at room temperature as shown in Figures (4.1- 4.3). Through the practical study of the main vibration patterns of the infrared spectrum of Acriflavine dye in Figure (4.1), there are different vibration patterns appeared for most of the basic groups in its molecular structure, these vibration of the (C-H) bond is one of the basic groups in the molecular structure of Acriflavine dye, and it has been shown that one of the most important patterns of vibration for it is the stretching mode vibration, which is located at the wave number (2973 cm^{-1}), and this pattern appears with high intensity .

Other vibrational patterns appears, such as the bending of the (C-H) bond at the wave number (1590) cm^{-1}. It has been observed that these flexural vibrational patterns have low intensities relatively speaking compared to the main stretching mode vibration (C-H) bond due to the low probability of its occurrence. This behavior was in agreement with [96].

FT-IR spectrum of (Orcein) dye shows the bond stretching represented by the range (3349-2977) cm^{-1} which indicates the(OH) group. The bond absorption which indicate the bond stretching carbonyl group at the peak (1710) cm^{-1} .This indicates the presence of (C = C) bond vibration at (1448-1554) cm^{-1}, as shown in Figure (4.2). This behavior was in agreement with [97].

FT-IR spectrum of (Azure-B) dye shows the bond absorption asymmetric of N-H represented by the range (3653-3305) cm^{-1} and low value of the frequency which indicate the vibrational of the bond stretching (C = C) group represented by the range (1464-1586) cm^{-1} , as shown in Figure (4.3). This behavior is in agreement with [95].

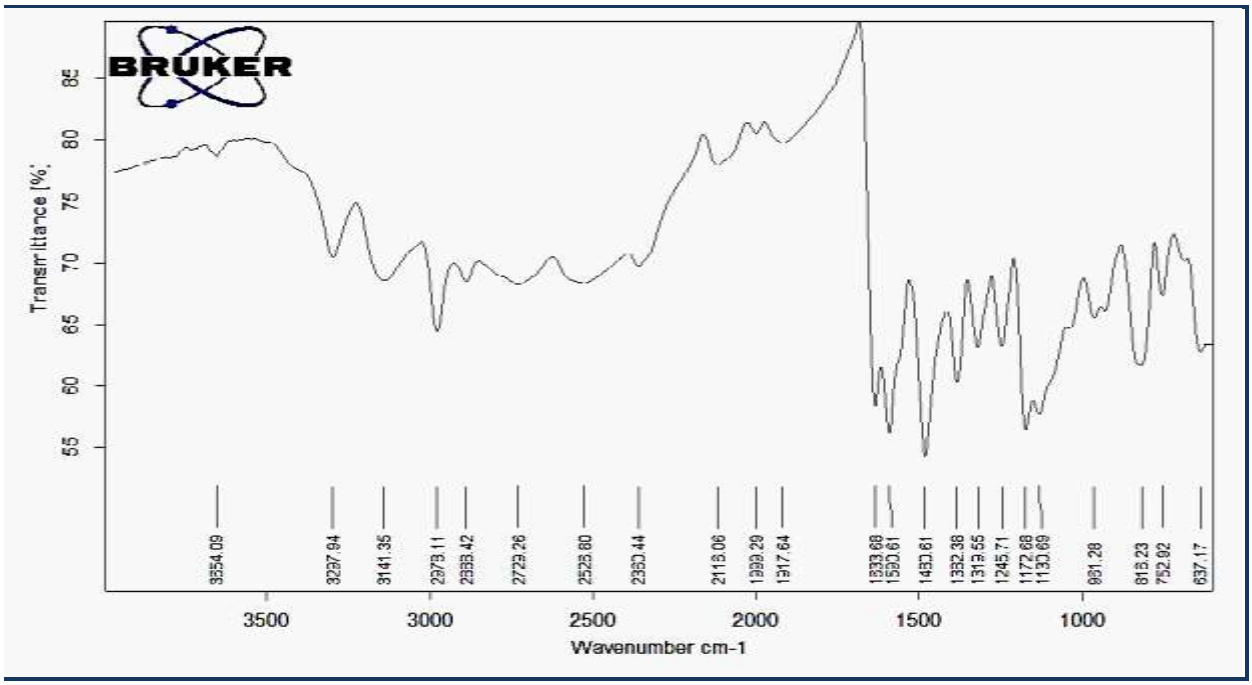

Figure (4.1): FT-IR spectrum for Acriflavine dye powder.

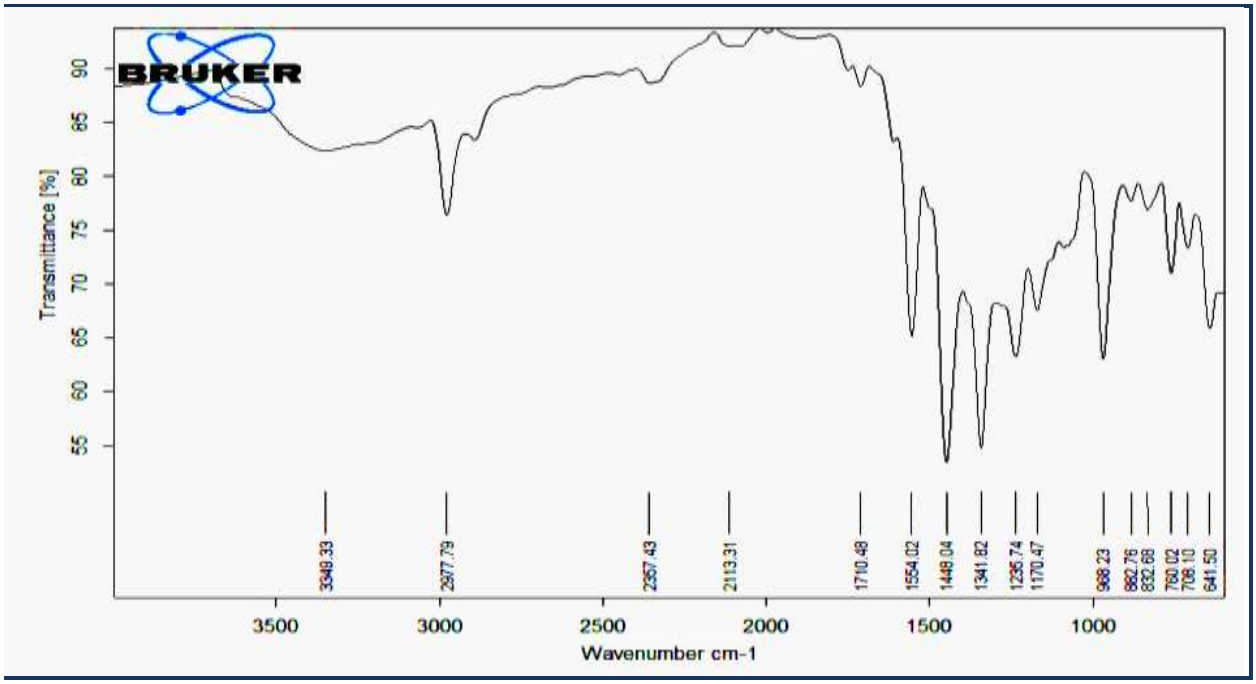

Figure (4.2): FT-IR spectrum for Orcein dye powder.

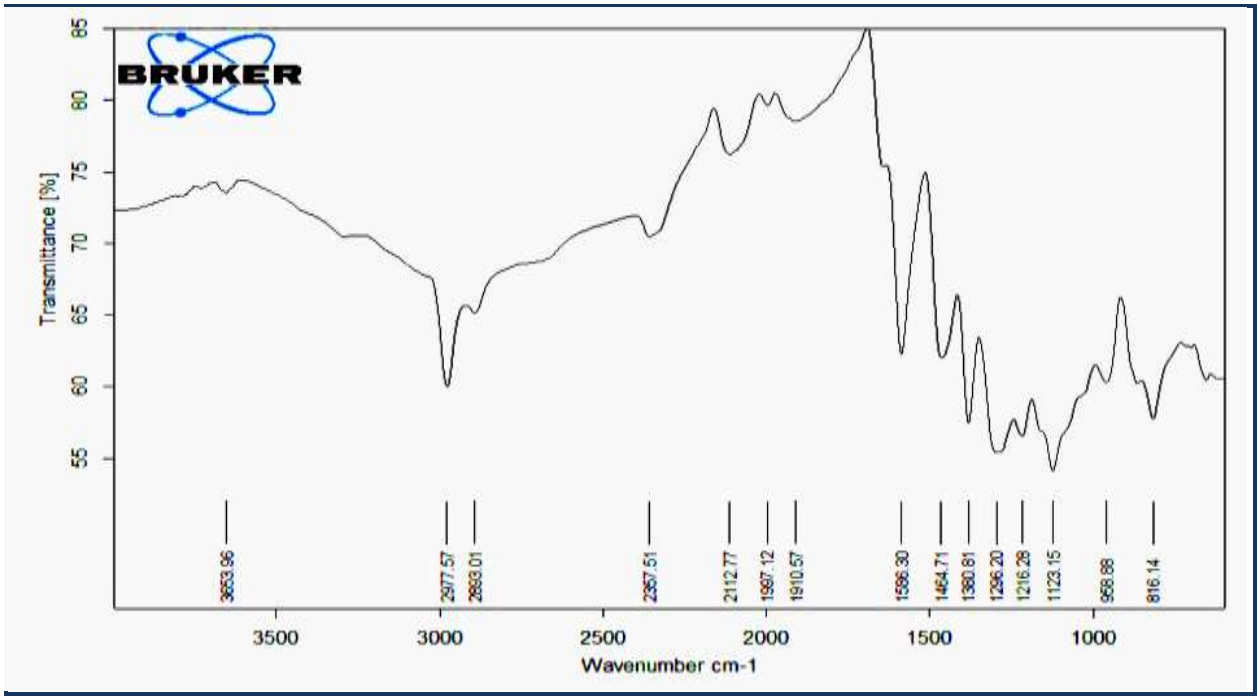

Figure (4.3): FT-IR spectrum for Azure-B dye powder.

4.2.2 Optical Microscope

Figures (4.4:A,B, 4.5:A,B and 4.6:A,B) show the optical microscope images of thin films of (Acriflavine, Orcein and Azure-B) in two case : one doping with PVA and the other case doping with (PVA) polymer and (Ag NP_S) respectively at magnification power (100 X).

Those Figures illustrate spreading dye molecules on the glass substrate with (PVA) polymer .Thin films exhibit uniform distribution of dyes at surface morphology. Thin films in Figure (4.5:A) have exhibited slightly better interference between dyes and polymer than thin films were shown in Figures (4.4: A and 4.6:A). Figures (4.4:B, 4.5 :B and 4.6 :B) shows distribution of (Ag NP_S) and form paths of network inside the (Dye-PVA) blend. Nanoparticles are aggregates as a cluster of (Dyes +PVA+ Ag NP_S) samples . This behavior was in agreement with [93].

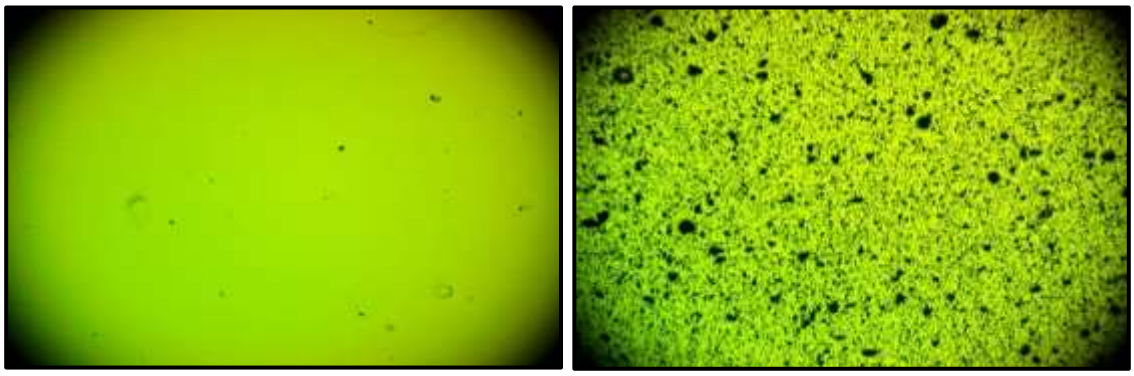

A **B**

Figure(4.4):Photomicrographs (100X) of thin films of Acriflavine dye, A: Acriflavine +PVA polymer , B: Acriflavine + PVA polymer + Ag NPs.

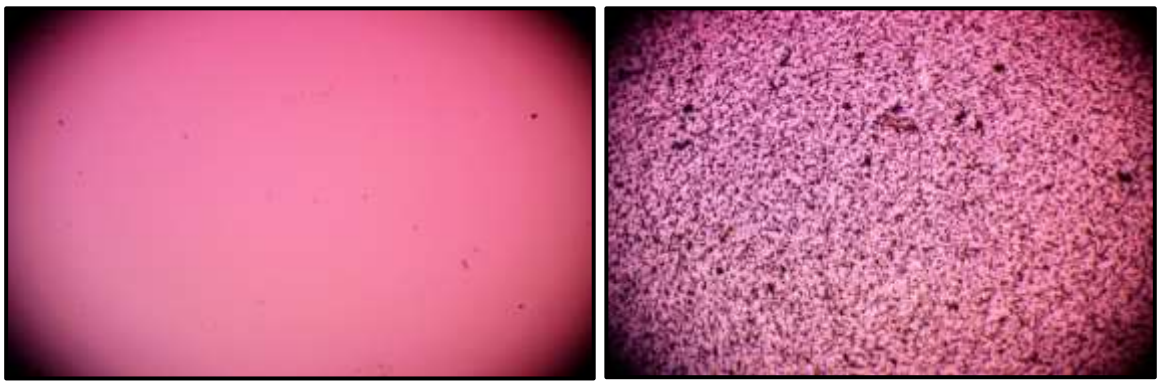

A **B**

Figure (4.5): Photomicrographs (100x) of thin films of Orcein dye, A: Orcein+PVA polymer , B: Orcein+ Ag NPs + PVA polymer.

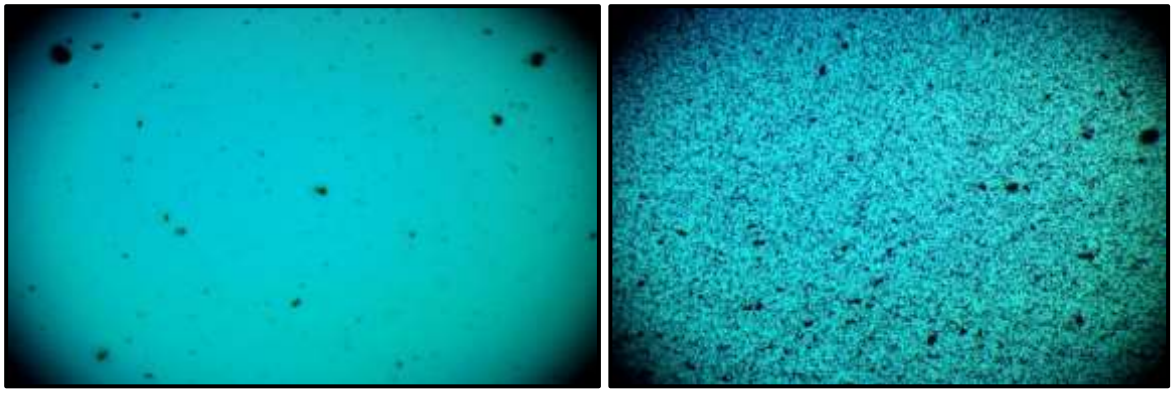

A **B**

Figure (4.6): Photomicrographs (100x) for thin films of Azure-B dye, A: Azure-B+ PVA polymer , B: Azure-B+ Ag NPs + PVA polymer.

4.3 Optical Testing Results

The optical testing included linear and nonlinear optical properties of (Acriflavine, Orcein and Azure-B) organic laser dyes is measured for solutions at concentration (10^{-5} M), and thin films at concentration (10^{-3} M),doped with (PVA) polymer and (Ag NPs) .

4.3.1 Linear Optical Properties

The linear optical properties consists of absorption and transmission spectra , as well as measurement of linear refractive index and linear absorption coefficient.

4.3.1.1 UV-Visible Absorption Spectra

Absorption spectra for (Acriflavine, Orcein and Azure-B) organic laser dyes as solutions with concentration (10^{-5}) M and thin films at concentration (10^{-3} M),doped with (PVA) polymer and (Ag NPs) were recorded in Figures (4.7 - 4.15) respectively.

4.3.1.1 Absorption Spectra of Acriflavine

The absorption spectra of Acriflavine dye as solutions at concentration (10^{-5}M) in ethanol solvent, is recorded as shown in Figure (4.7). The spectrum was characterized with very strong absorption area, in visible region, at wavelengths between (350-500) nm ($n\rightarrow\pi^*$), because they require less energy compared to the previous transitions. It is clear that transition require the presence of π-type bonds, and this group prepared for such a transition is called a chromophore. The absorption spectra of thin films of (Acriflavine) at (10^{-3} M) doping with (PVA) polymer and (Ag NPs) are prepared by drop casting method at room temperature which is shown in Figures (4.8 and 4.9). The present results show thatthe absorption peaks for (PVA and Ag NPs) at (10^{-3}) M in ethanol solvent shifted toward longer wavelengths following the addition of (PVA) polymer and nanoparticles to pure dye, and the absorption peaks were shifted toward the longer wavelengths as compared to pure dye .This behavior is in agreement with [13].

4.3.1.2 Absorption Spectra of Orcein

The behavior of Orcein dye solution at concentration (10^{-5} M) in ethanol solvent , is shown in Figure (4.10). The results show that the absorbance peak of Orcein dye solution is (525 nm).The absorbance range (420 - 570) nm. From the second case, after doped by PVA polymer, the absorption peak is (531) nm at (10^{-3}) M. The absorbance is higher than Orcein dye solution because of the thickness of thin film, also the absorbance range was wider than Orcein dye solutions. At the third case, the absorption spectra of Orcein dye solution doped PVA polymer with (0.06) wt % of Ag NP_S, as shown in Figure (4.11 and 4.12)respectively. This Figure show that absorption peaks are (535 nm) , The present results show that the absorption peaks for (PVA and Nano) at (10^{-3}) M in Ethanol solvent were moved toward longer wavelengths following the addition of (PVA) polymer and nanoparticles to pure dye,the peak shift slightly to the longer wavelengths when adding of Ag NP_S nanoparticles .This behavior was in agreement with [25].

4.3.1.3 Absorption Spectra of Azure-B

The absorption spectra of Azure-B in case of solution with concentration (10^{-5}) M in ethanol solvent, was recorded and shown in Figure (4.13). The spectrum is characterized with very strong absorption area (400-700 nm), the results show that the absorption peak of Azure-B dye solution are (607 nm). For the second case, after doped by PVA polymer, the absorption peak are (615 nm) at (10^{-3}) M as shown in Figure (4.14 and 4.15) respectively. These Figures show that absorption peaks of Azure-B dye doped PVA with weight ratio of Ag NP_S are (615 nm) at (0.06) wt %, the present results show that the absorption peaks for (PVA and Nano) at (10^{-3}) M in Ethanol solvent were moved toward longer wavelengths following the addition of (PVA) polymer and nanoparticles to pure dye,the peak shift slightly to the longer wavelengths with adding of Ag NP_S .This behavior is in agreement with [30].

The present results show that the absorption peaks for all samples (Pure, PVA and Nano) at (10^{-3}) M in Ethanol solvent were shifted toward the longer wavelengths after adding (PVA) polymer and nanoparticles to pure dye. This shift is obtained due to the electronic and vibrational states of interfacial molecules, which is lead to increasing absorption for all samples of nanocomposites at UV region, this is suggested to take place because of the excitations of high occupation molecular orbital (HOMO) electrons to the lowest unoccupation molecular orbital (LUMO). The high absorption of samples for nanocomposites at UV region attributed to the energy of photon enough to interact with atoms, the electron excites from a lower to higher energy level by absorbing a photon of known energy. Fundamental absorption of absorption spectra refers to band to band or excitation transition, at visible and near infrared regions, the absorption of all samples for pure dyes has low values, this behavior attributed to the energy of incident photons have not enough energy to interact with atoms, thus the photons will be transmitted when the wavelength increases, ie, when the amount of energy required for transmission decreases.

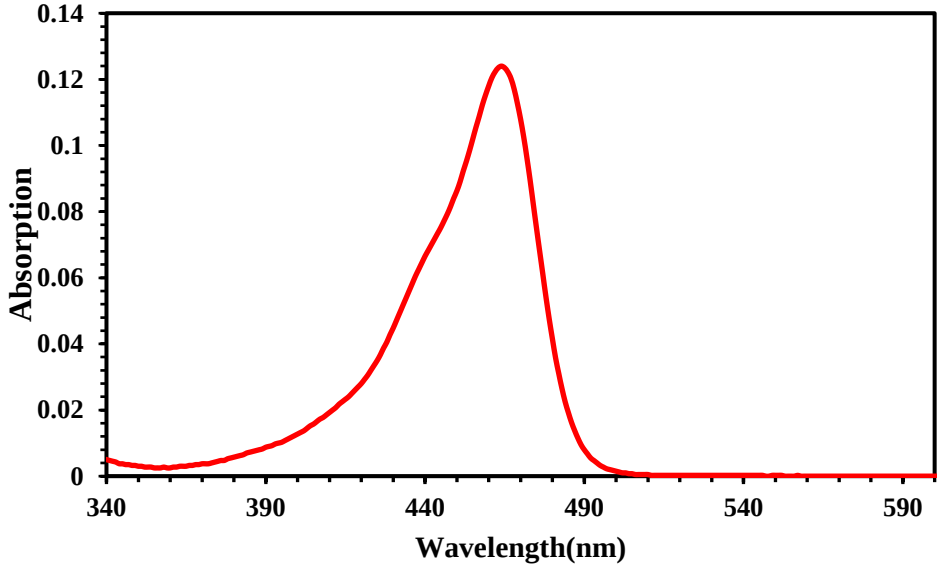

Figure (4.7): The absorption spectrum for Acriflavine dye

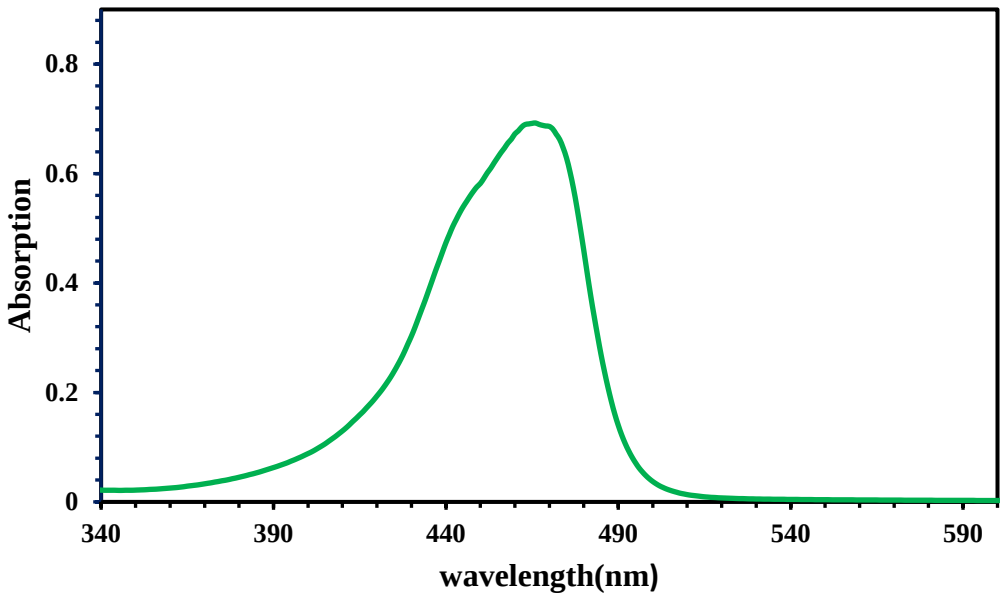

Figure (4.8): Absorption spectrum for thin film of Acriflavine at concentration (10^{-3}M) doped with PVA polymer

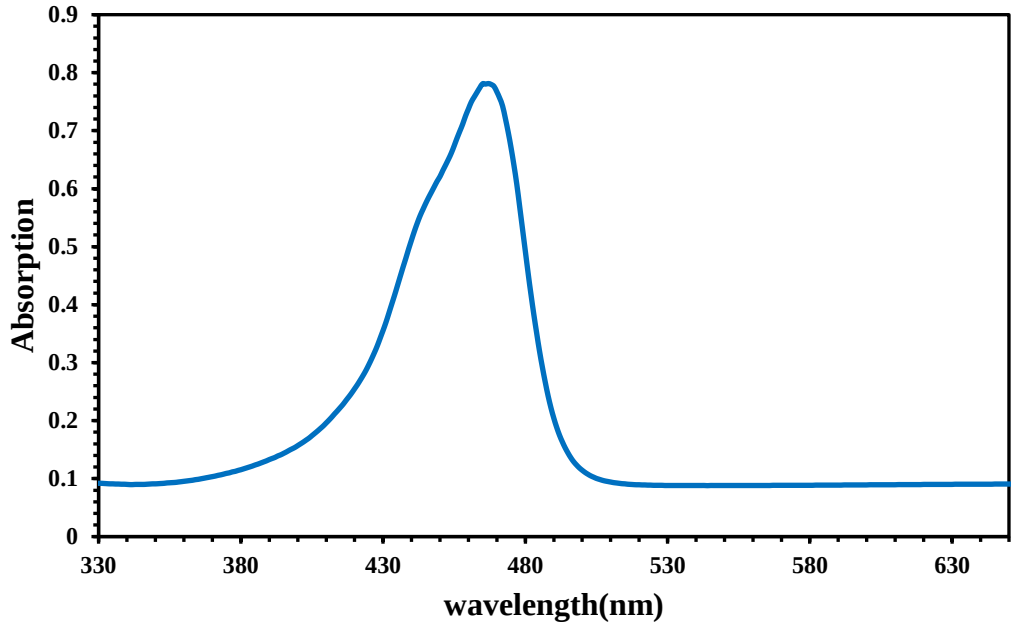

Figure (4.9): Absorption spectrum for thin film of Acriflavine at concentration (10^{-3}M) doped with PVA polymer and Ag NPs.

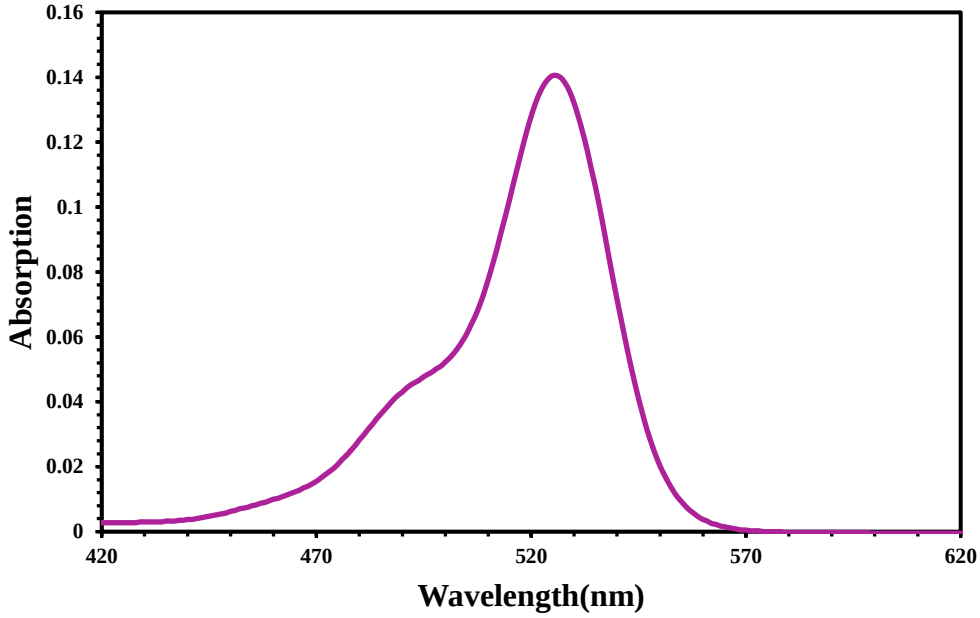

Figure (4.10): The absorption spectrum for Orcein dye at concentration (10^{-5} M).

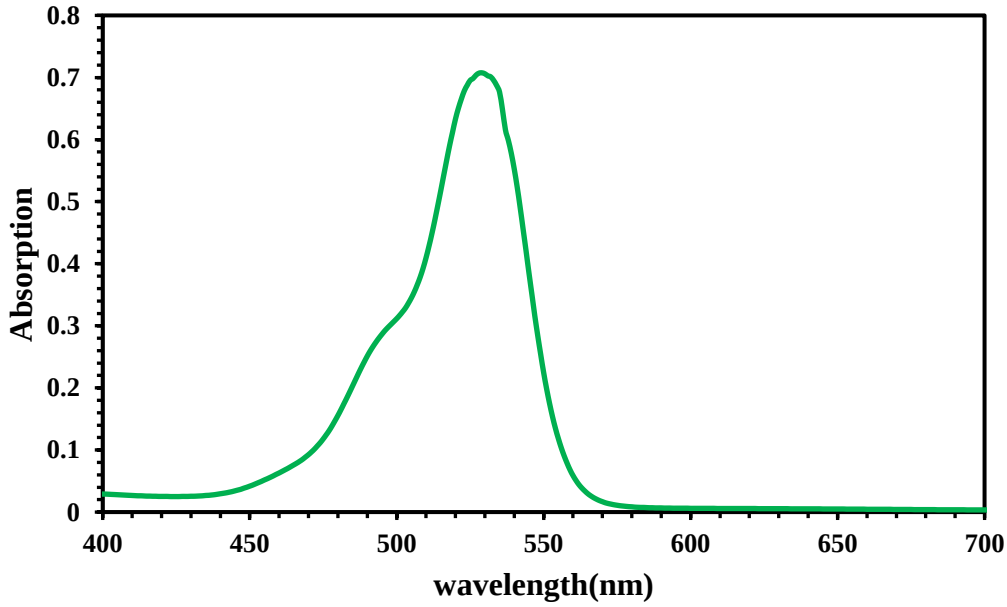

Figure (4.11): Absorption spectrum for thin film of Orcein at concentration (10^{-3}M) doped with PVA polymer

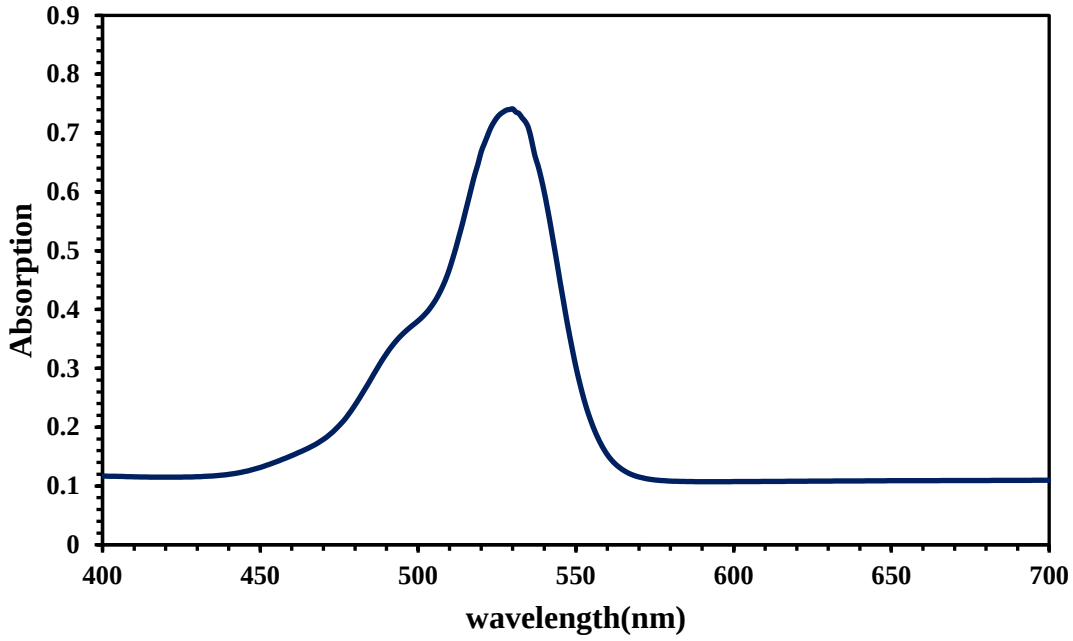

Figure (4.12): Absorption spectrum for thin film of Orcein at concentration (10^{-3}M) doped with PVA polymer and Ag NPs.

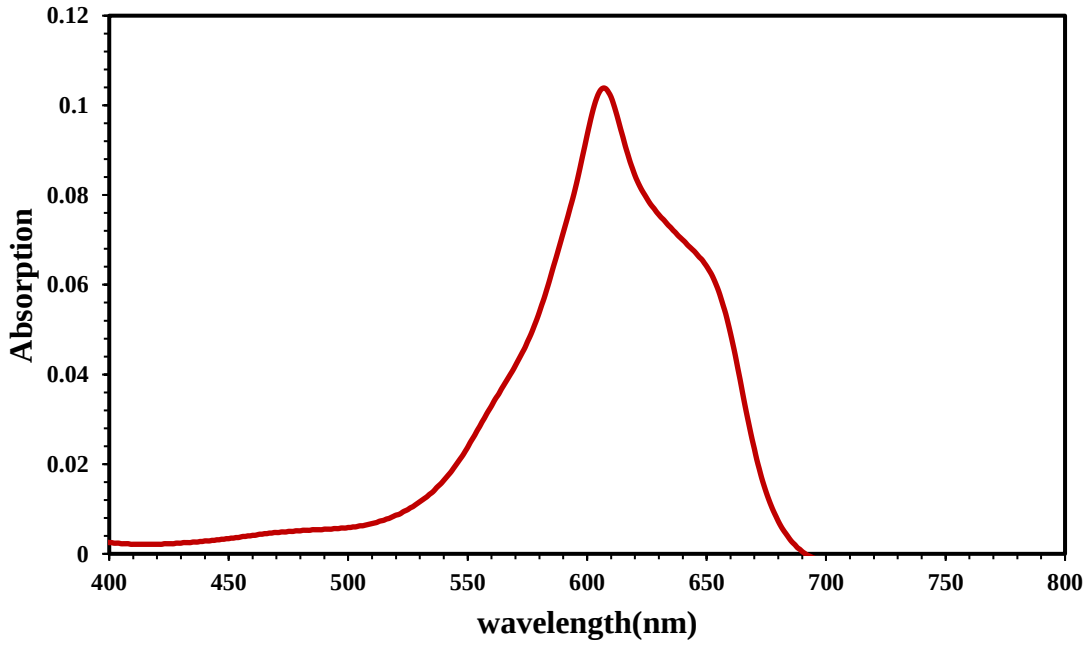

Figure (4.13): The absorption spectrum for Azure-B dye at concentration (10^{-5} M).

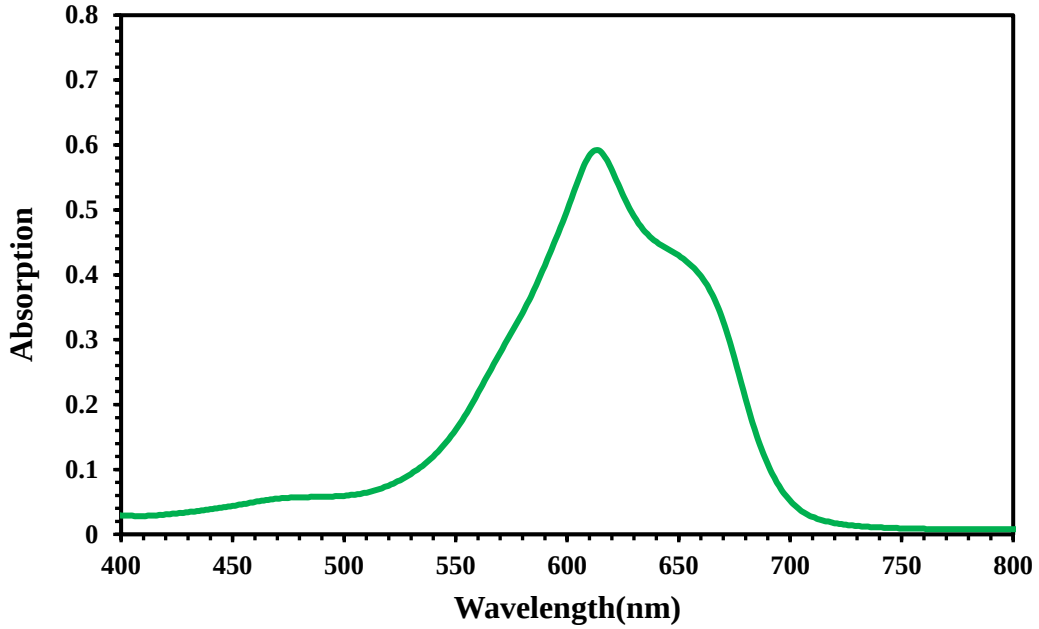

Figure (4.14): Absorption spectrum for thin film of Azure-B at concentration (10^{-3}M) doped with PVA polymer

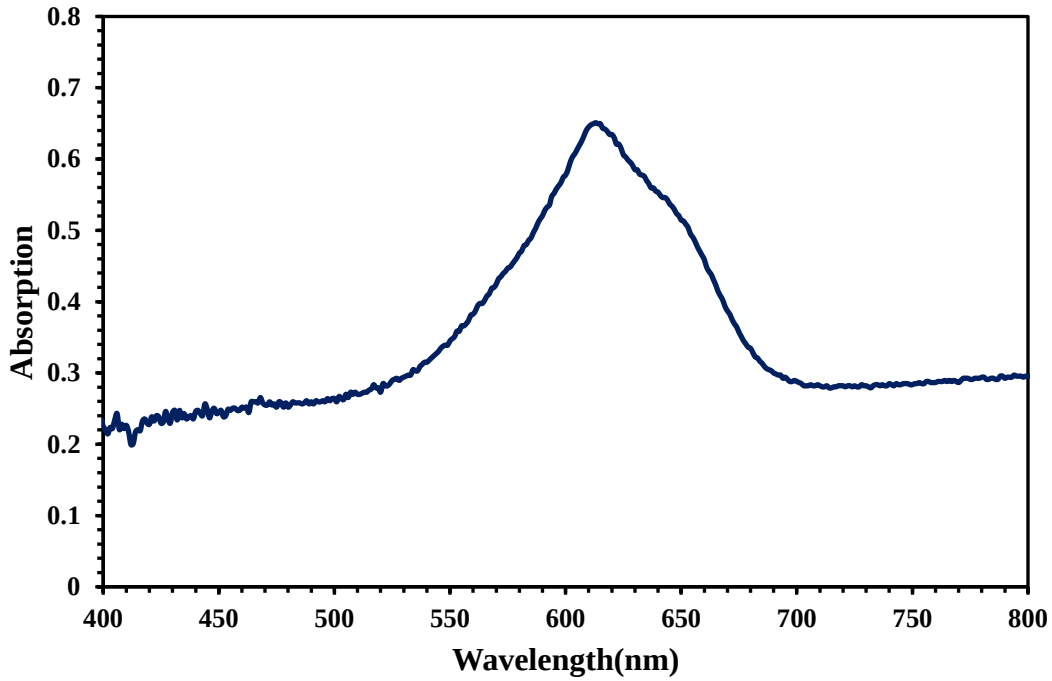

Figure (4.15): Absorption spectrum for thin film of Azure-B at concentration (10^{-3}M) doped with PVA polymer and Ag NPs.

4.3.2 Transmission Spectra

Transmission spectra for (Acriflavine, Orcein and Azure-B) organic laser dyes in case of solutions at a concentration (10^{-5} M), and thin films at concentration (10^{-3} M) doped with (PVA) polymer and (Ag NPs) is recorded as shown in Figures (4.16 - 4.24) respectively.

4.3.2.1 The Transmission Spectra of Acriflavine

Transmission spectrum of Acriflavine dye as solution, at (10^{-5} M) concentration prepared at room temperature, is shown in Figure (4.16). The Figure shows that the maximum transmittance value is at the range (400-500 nm). The transmission spectrum of thin films of (Acriflavine doped with PVA polymer and Ag NPs) at (10^{-3} M), as shown in Figures (4.17 and 4.18) respectively.

The optical transmission curve of all samples show a variable behavior of the transmission as a function of the incident wavelength. The transmittance intensity of nano composite was lower than intensity (dye without adding PVA). This behavior was in agreement with [13] .

4.3.2.2 The Transmission Spectra of Orcein

Transmittance spectra of Orcein dye as solution, at concentration (10^{-5} M) in ethanol solvent, are shown in Figure (4.19). The optical transmission curve of all samples show a variable behavior of the transmission as a function of the incident wavelength. The transmission spectra of Orcein dye at (10^{-3} M) concentration, after doping with (PVA polymer and Ag NPs) are shown in Figures (4.20 and 4.21) respectively .This behavior was in agreement with [25].

4.3.2.3 The Transmission Spectra of Azure-B

Transmission spectra of the Azure-B dye at three cases were analyzed using UV-VIS spectrophotometer. The first case transmission spectrum is obtained for Azure-B dye solution at concentration (10^{-5} M). The behavior is shown in Figure (4.22). For the second case, the transmission spectrum of PVA polymer is in the U.V region as shown in Figure (4.23). Transmission values in this case are less than Azure-B solutions. At the third case, the transmission spectrum of Azure-B dye solution doped PVA polymer with (0.06) wt % of Ag NP_S as shown in Figures (4.23 and 4.24) respectively. The behavior is in agreement with [30].

Transmittance decreases, this is suggested to take place because of Ag NP_S nanoparticle contain electrons which can be the absorption of electromagnetic energy of the incident light and travel to higher energy levels.

This process is not accompanied by emission of radiation because the hiked electron to higher levels has occupied vacant positions of energy bands, thus part of the incident light is absorbed by the substance and does not penetrate through it, on the other hand, the pure samples have more transmittance than doped samples this is suggested to take place because of no free electrons (i.e. electrons are linked to atoms by covalent bonds), this is because the breaking of electron linkage and moving it to the conduction band need photons with high energy.

The linear absorption coefficient (α_o) and linear refractive coefficient (n_o) are obtained from equations (2.15) and (2.16) respectively. The values of (α_o) for Acriflavine organic laser dyes and its thin films are higher than those of Orcein and Azure-B organic laser dyes. The values of (α_o) for thin films of (Acriflavine, Orcein and Azure-B) organic laser dyes doped with (PVA and AgNPs), are larger than those values for same dyes as pure solutions , which are listed in Table (4.1). This behavior agrees with [19].

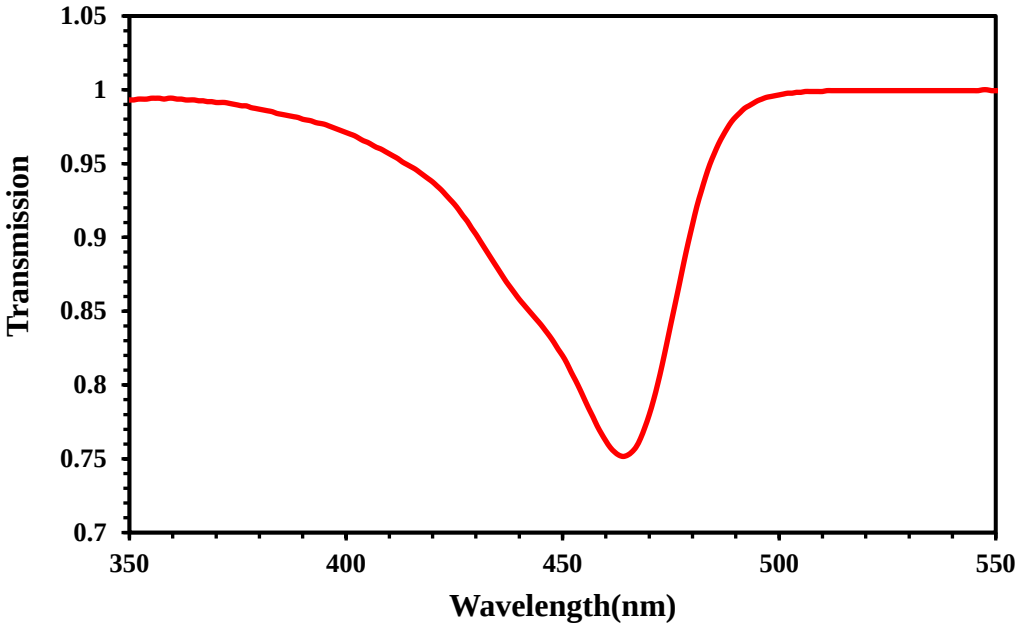

Figure (4.16): Transmission spectrum for Acriflavine organic laser dye as solution at concentration (10^{-5}) M.

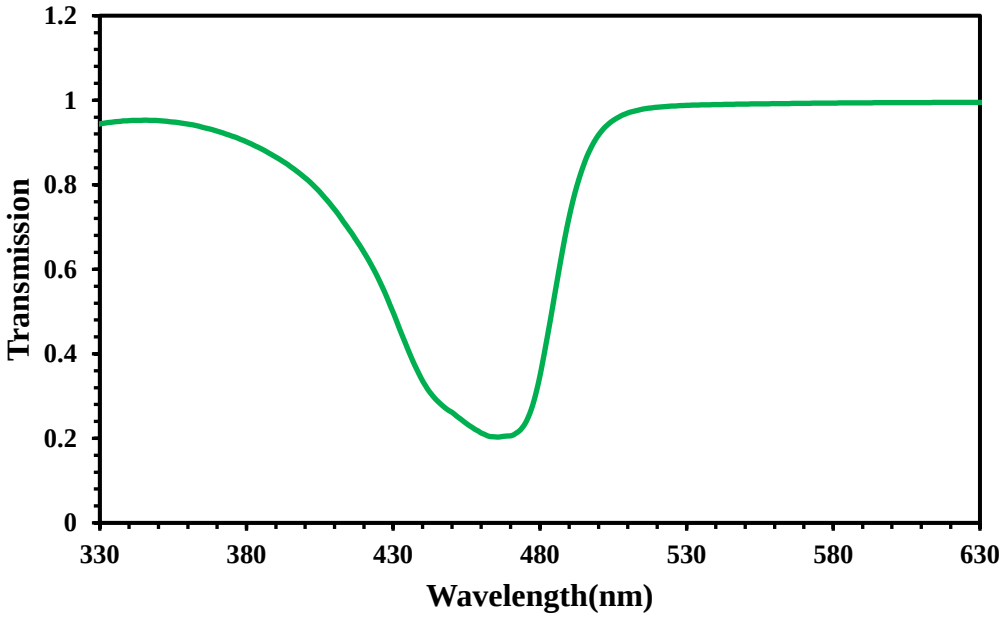

Figure (4.17): Transmission spectrum for thin film of Acriflavine at concentration (10^{-3}M) doped with PVA polymer

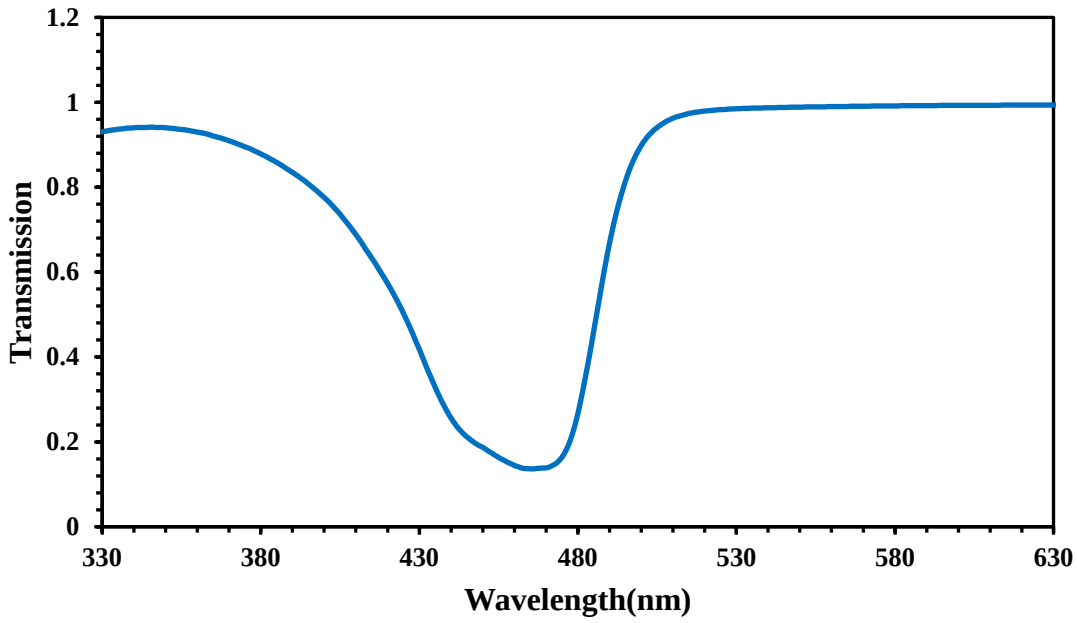

Figure (4.18): Transmission spectrum for thin film of Acriflavine at concentration (10^{-3}M) doped with PVA polymer and Ag NPs.

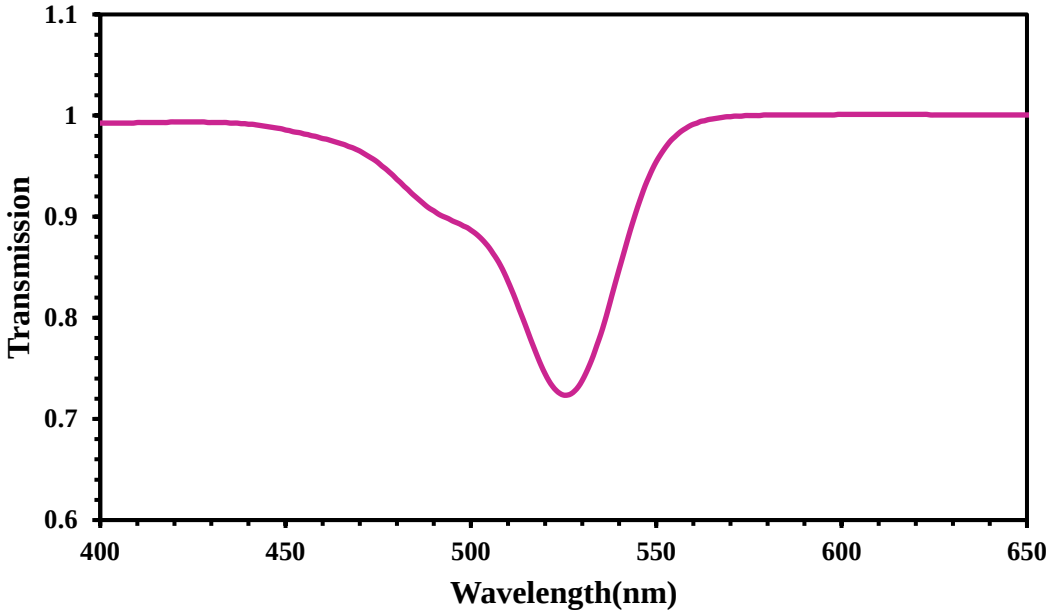

Figure (4.19): Transmission spectrum for Orcein organic laser dye as solution at concentration (10^{-5}) M.

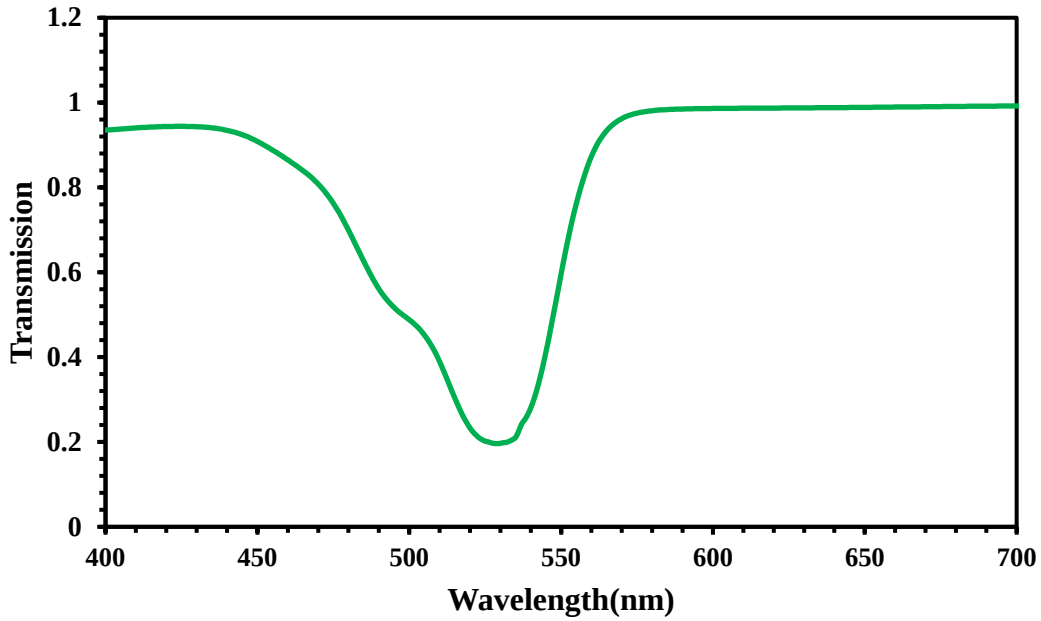

Figure (4.20): Transmission spectrum for thin film of Orcein dye at concentration (10^{-3}M) doped with PVA polymer.

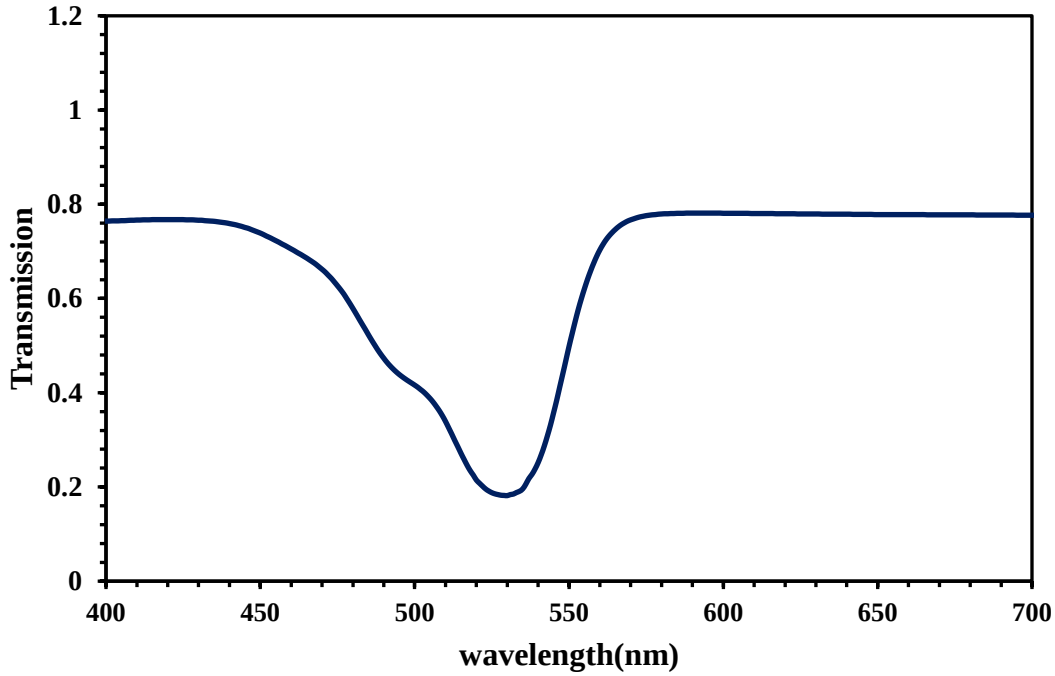

Figure (4.21): Transmission spectrum for thin films of Orcein dye at concentration (10^{-3}M) doped with PVA polymer and Ag NPs.

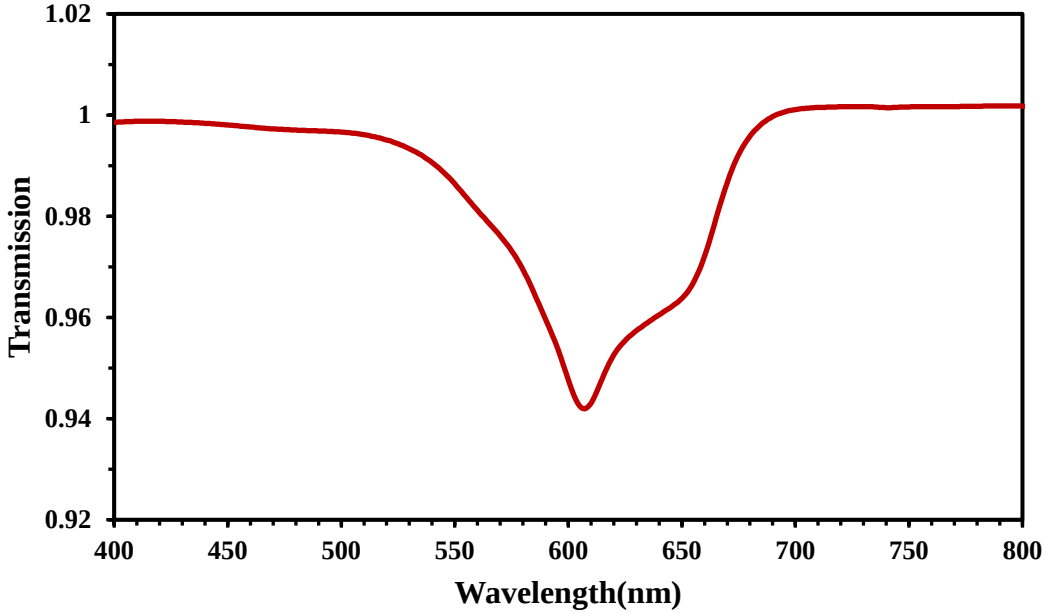

Figure (4.22) Transmission spectrum for Azure -B organic laser dye as solution at concentration (10^{-5}) M.

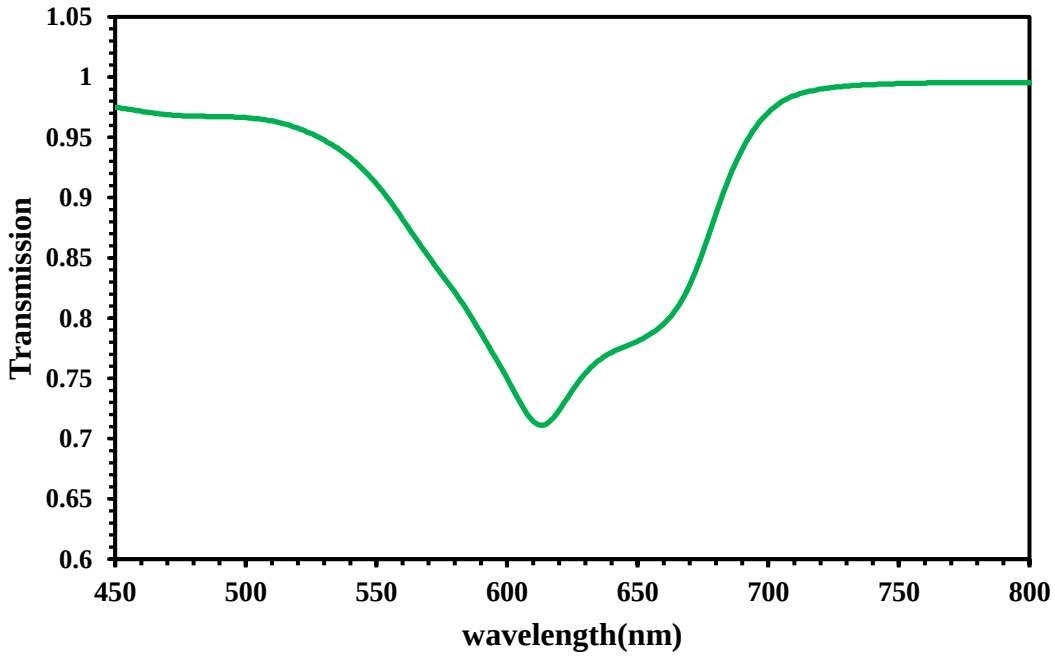

Figure (4.23): Transmission spectrum for thin films of Azur-B dye at concentration (10^{-3}) M doped with PVA polymer.

.

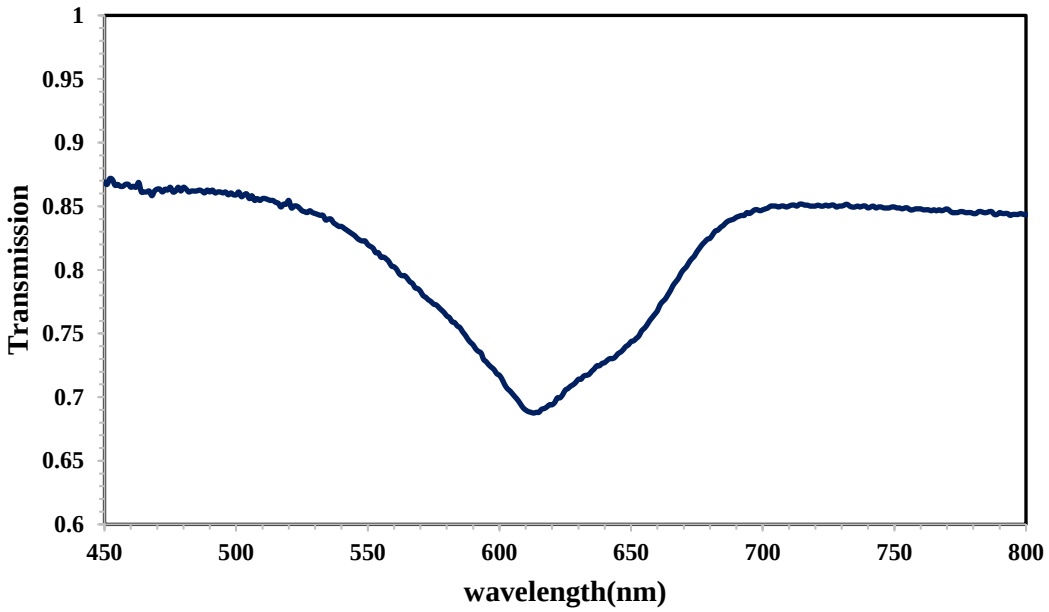

Figure (4.24): Transmission spectrum for thin film of Azur-B dye at concentration(10^{-3}) M doped with PVA polymer and Ag NPs.

Table (4.1): The linear optical parameters for (Acriflavine, Orcein and Azure-B) Organic dyes as solution and thin films doped with PVA polymer and Ag NPs.

Material	λ_{max} (nm)	A	T	$(\alpha_\circ)cm^{-1}$	$n_\circ$
Acriflavine	464	0.279	0.569	0.250	2.091
Acriflavine + PVA polymer	466	0.719	0.203	61521.426	2.502
Acriflavine+ PVA polymer + Ag NPs	469	0.781	0.182	66527.324	2.508
Orcein	525	0.244	0.523	0.020	1.223
Orcein+PVA polymer	530	0.663	0.188	43260.942	1.290
Orcein+PVA polymer + Ag NPs	533	0.731	0.138	48160.756	1.733
Azure-B	607	0.207	0.887	0.018	1.208
Azure-B+PVA polymer	615	0.619	0.713	40512.488	1.266
Azure-B +PVA polymer + Ag NPs	620	0.649	0.687	45570.138	1.513

4.4 Fluorescence Spectra

The fluorescence spectra is studied for (Acriflavine, Orcein and Azure-B) organic laser dyes in case of solutions at concentration (10^{-5}) M , and thin films at concentration (10^{-3} M) , doped with (PVA) polymer and (Ag NPs) was recorded ,as appeared in Figures (4.25 - 4.33) respectively.

4.4.1 Fluorescence Spectra of Acriflavine

Figure (4.25) shows fluorescence spectrum for (Acriflavine) dye at a concentrations (10^{-5} M). This Figure indicats emission peaks about (492 nm), the emission wavelength is always longer than the excitation wavelength. Figures (4.26 and 4.27) respectively show fluorescence spectra for thin films of (Acriflavine) at concentration (10^{-3} M) doped with (PVA) polymer and (Ag NPs).

The observed peaks for the thin films doped in (PVA) polymer short wavelengths. One of the most important characteristics of the dye doped in solid matrix is the stokes shift.Thin films have exhibited slightly more shifting towards shorter wavelengths (high energies) than those in the solution dye. From Figures, it was observed that they have narrower band width than acriflavine dye solution also the emission peak is (493 nm) at (10^{-5} M) This behavior is in agreement with [99].

4.4.2 Fluorescence Spectra of Orcein

Figure (4.28) shows fluorescence spectrum of Orcein dye solution at concentration (10^{-5} M), this Figure indicats emission peaks about (549 nm).

For the second case, the fluorescence spectrum of Orcein dye at concentration (10^{-3} M) after doped PVA polymer, is shown in Figure (4.29), the spectrum emission peaks shift to shorter wavelength (blue shift). From this Figure, it is observed that they have narrower band width than Orcein dye solution also the emission peak is (536 nm) and lower intensity than Orcein dye solution because

the fluorescence quenching. For the third case, of Orcein dye solution doped PVA with(0.06) wt % of Ag NP_S nanoparticles ,the fluorescence spectrum is shown in Figure (4.30). This behavior was in agreement with [100].

4.4.3 Fluorescence Spectra of Azure-B

Figure (4.31) shows fluorescence spectrum of Azure-B dye solution at concentration (10^{-5} M) , this Figure indicat emission peaks about (625 nm), the emission wavelength is always longer than the excitation wavelength. From Figure (4.32), it was observed that there has a narrower band width than Azure-B dye solution also the emission peak is (540 nm) at (10^{-3} M) and lower intensity than Azure-B dye solution because the fluorescence quenching. For thin film of Azure-B dye solution doped PVA with(0.06) wt % of Ag NP_S ,the fluorescence spectrum is shown in Figure (4.33) .This behavior was in agreement with [30].

Fluorescence phenomenon occurs when a molecule absorbs photons causing a transition to a high energy electronic state afterward it returns back to the first excited state through heat or vibrations. Finally, it emits photon when it returns to its initial state, so that the radiative emitted energy is less than the exciting energy i.e., the emission wavelength is always longer than the excitation wavelength**.** Also, the fluorescence of a molecule depends on the structure and environment of the molecule.

There are many factors that affect the fluorescence of dyes such as concentration, impurities and self-absorption, that could affect directly the fluorescence quantum yield and consequently the energy yield of the fluorescence[101] .

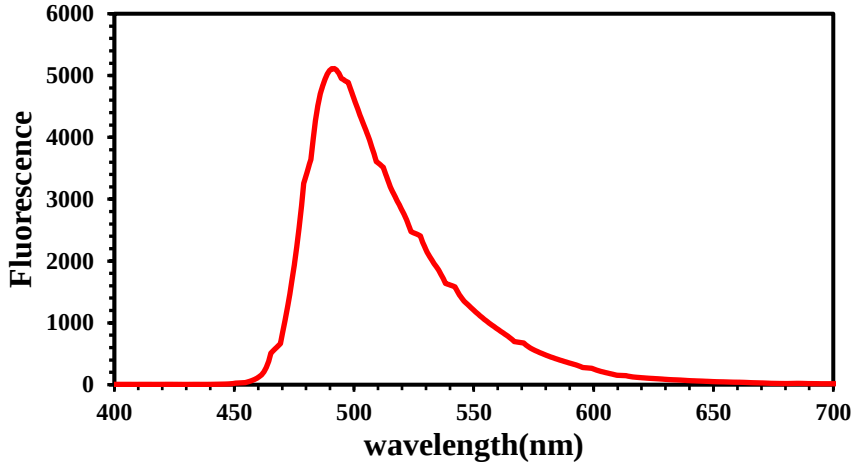

Figure (4.25): Fluorescence spectrum for Acriflavine dye as solution at concentration (10^{-5} M).

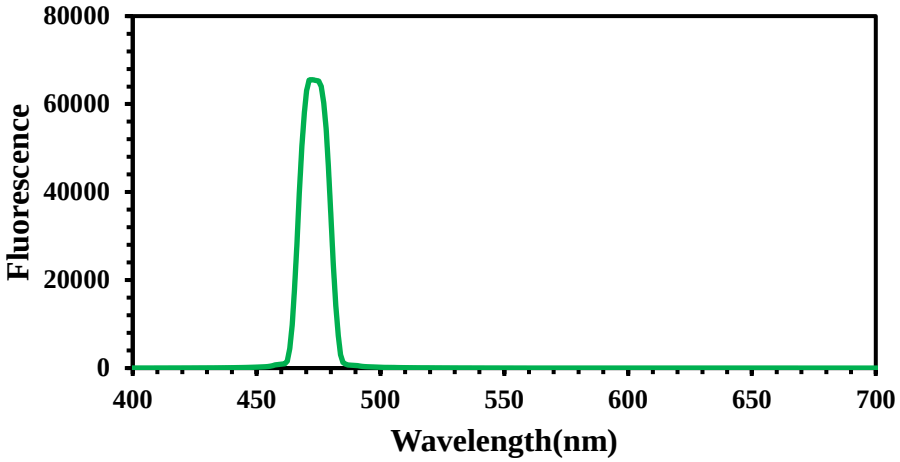

Figure (4.26): Fluorescence spectrum for thin film of Acriflavine dye doped with PVA polymer .

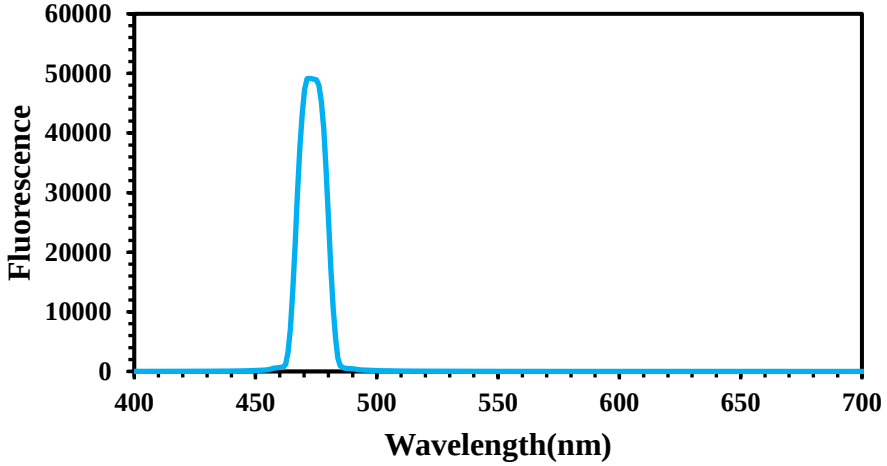

Figure (4.27): Fluorescence spectrum for thin film of Acriflavine dye doped with PVA polymer and Ag NPs.

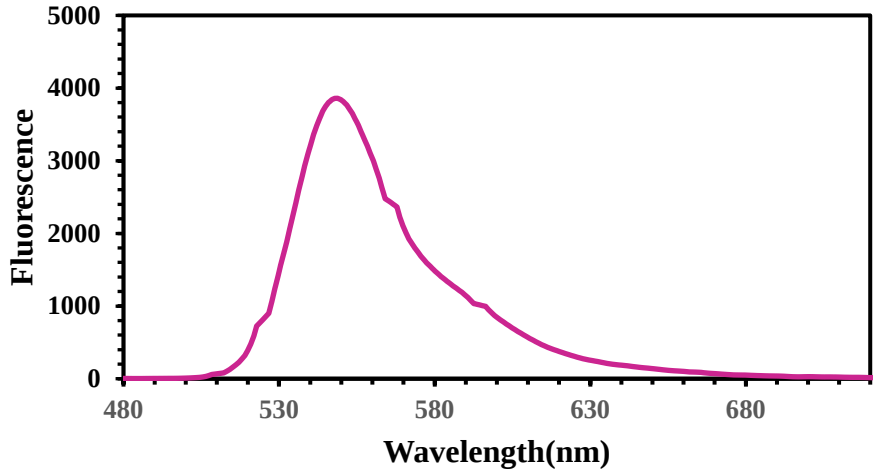

Figure (4.28): Fluorescence spectrum for Orceind dye at concentration (10^{-5} M).

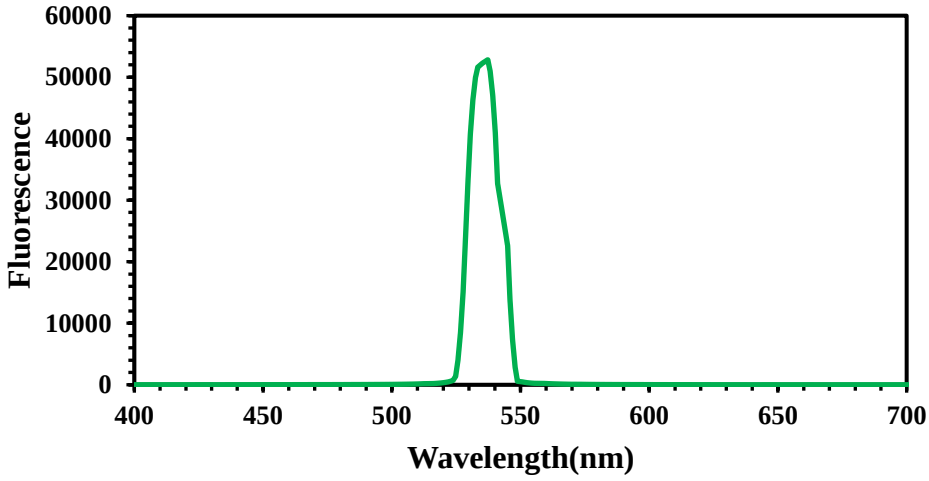

Figure (4.29): Fluorescence spectrum for thin film of Orcein dye doped with PVA polymer.

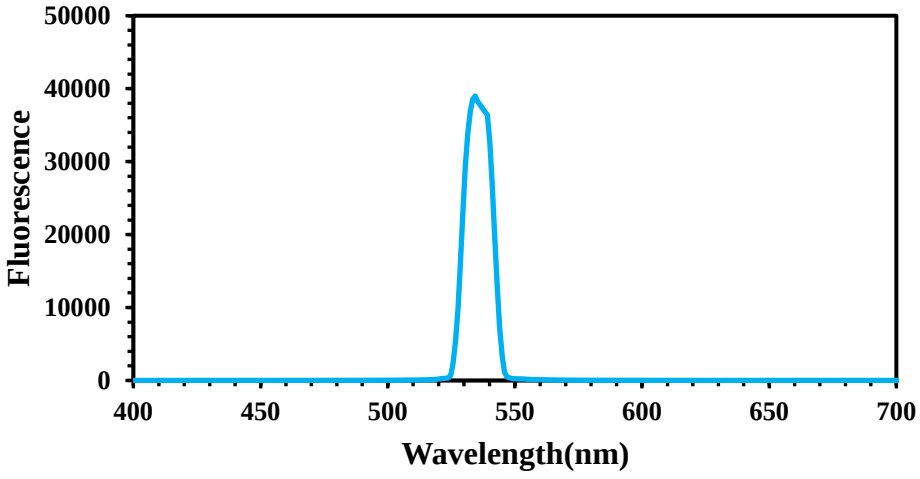

Figure (4.30): Fluorescence spectrum for thin film of Orcein dye doped with PVA polymer and Ag NPs.

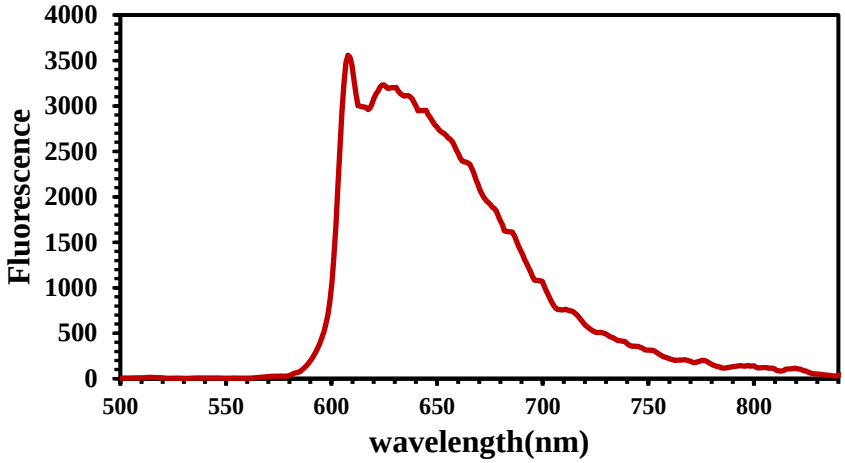

Figure (4.31): Fluorescence spectrum for Azure-B dye at concentration (10^{-5} M).

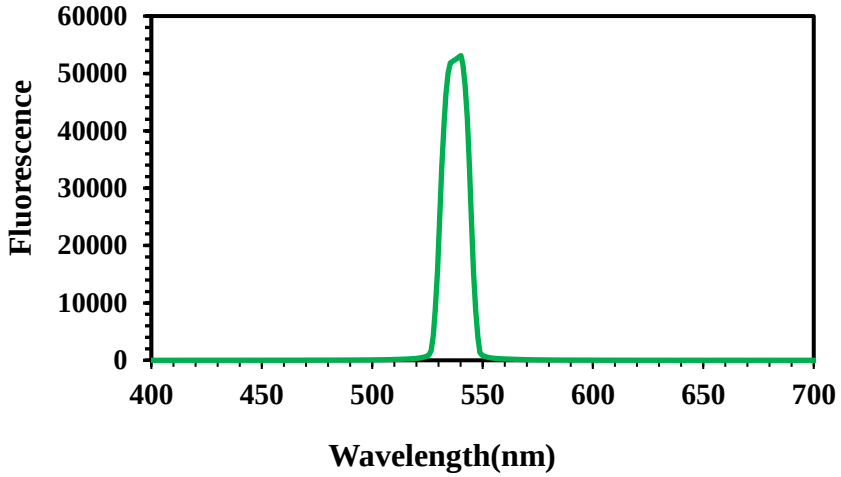

Figure (4.32): Fluorescence spectrum for thin film of Azure-B dye doped with PVA polymer.

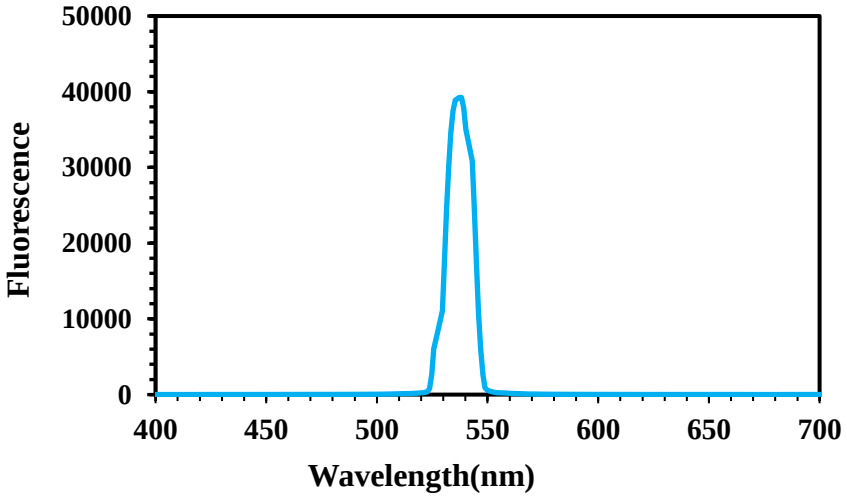

Figure (4.33): Fluorescence spectrum for thin film of Azure-B dye doped with PVA polymer and Ag NPs.

4.5 Calculation of Quantum Efficiency and Life Time

Figures (4.34 - 4.36) show the overlap between absorption and fluorescence spectra for (Acriflavine, Orcein and Azur-B) respectively at concentration (10^{-5} M). There are some important optical parameters for fluorescence spectrum, one of those is stokes shift which provides information on the excited state.

From these Figures, there is an overlapping between the absorption and fluorescence spectrum, in spite of the fluorescence shifted to longer wavelength region because of prescience of self-absorption process for the fluorescent light that leads to change the shape and width of fluorescence spectrum and quantum yield. So, it best to prepare laser dyes solution in very diluted concentration to get a smallest overlapping between the spectral band.

By observing the fluorescence spectra, the fluorescence spectra have the characteristic of mismatch of fluorescence peak with absorption peak due to the loss of the molecule part of its energy (irradiation) before it returns to stable state. Calculation of life time and quantum efficiency are obtained from equations (2.5) and (2.8) respectively, results are listed in Table (4.2).

The flourecence quantum efficiency results indicats that the best dye to use as active laser medium was Acriflavine compared with Orcein and Azure-B.

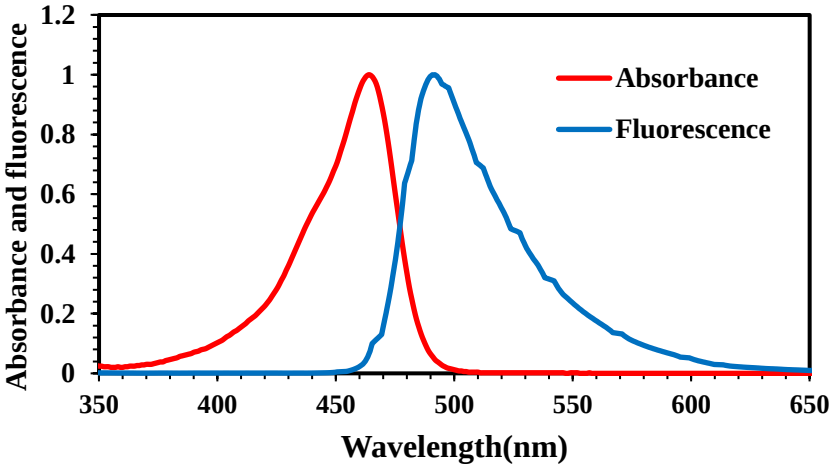

Figure (4.34): Interference between absorption and fluorescence spectra for Acriflavine dye at concentration (10^{-5} M).

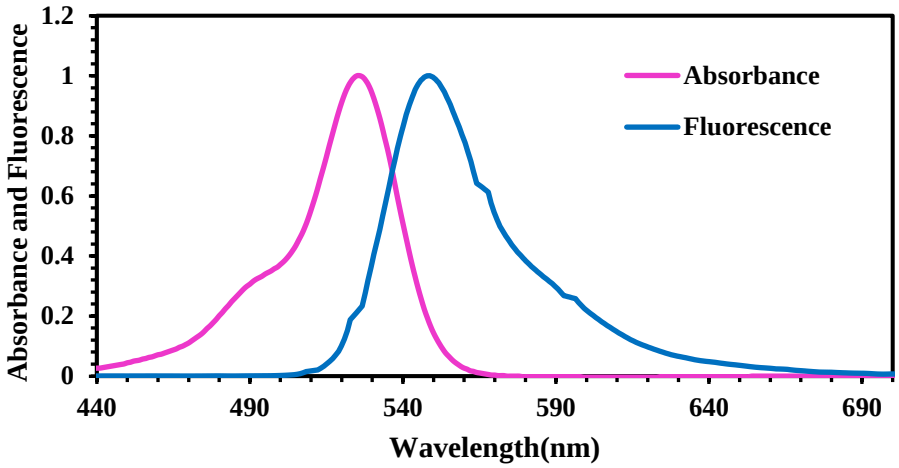

Figure (4.35): Interference between absorption and fluorescence spectra for Orcein dye at concentration (10^{-5} M).

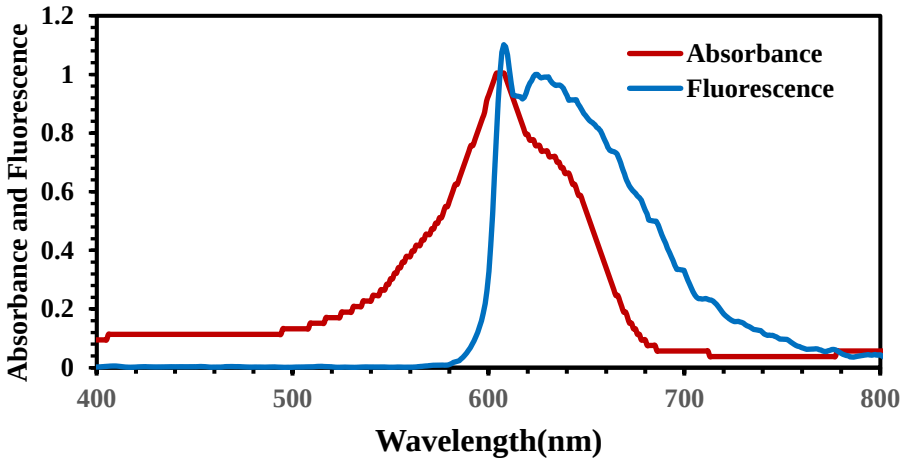

Figure (4.36): Interference between absorption and fluorescence spectra for Azure-B dye at concentration (10^{-5} M).

Table (4.2): Quantum Efficiency and life time parameters for (Acriflavine, Orcein and Azur-B) dyes laser at concentration(10^{-5}M).

Organic laser dyes	$\lambda_{abs.}$ (nm)	$\lambda_{flu.}$ (nm)	Stokes's shift (nm)	τ_F (ns)	τ_{FM} (ns)	Q_F
Acriflavine	464	492	28	0.2760	0.2816	98%
Orcein	525	549	24	0.3078	0.3206	96%
Azur-B	602	625	23	0.4505	0.5561	81%

4.6 Nonlinear Optical Properties

The nonlinear optical properties were investigated for Acriflavine, Orcein and Azure-B organic laser dyes are at concentration (10^{-5} M) , and their thin films at (10^{-3} M) , which prepared by drop coating method at room temperature , using continuous wave (CW) diode pumped solid-state laser with (457 nm) wavelength and different laser powers (56,70,84 and 102) mW. The effects of the different input powers on the nonlinear coefficients are discussed. The optical limiting behavior are also discussed. There are two parts are used to measure the nonlinear properties of the material by Z-Scan technique.The first part is open-aperture Z-Scan and the second part is the closed-aperture Z-Scan.

4.6.1 Nonlinear Absorption Coefficient of Organic Laser Dye and their Thin Films

The nonlinear absorption coefficient (β) of (Acriflavine, Orcein and Azure-B) organic dyes laser dye at concentration (10^{-5} M) in ethanol solvent, and their thin films at (10^{-3} M) doped with PVA polymer and Ag NPs, can be measured by performing the open aperture Z-Scan technique at (457 nm) wavelength and different laser powers (56,70,84 and 102) mW. The performed open aperture-Scan exhibits an increasing in the transmission about the focus of the lens, as shown in Figures (4.37,4.38 and 4.39) respectively. It is noticed (two photon absorption) phenomenon.This behavior was in agreement with [13,25,30].

The behavior of transmittance starts linearly at different distances from the far field of the sample position (-Z). At the near field, the transmittance curve begins to decrease until it reaches the minimum value (T_{min}) at the focal point, where Z=0 mm. The transmittance begins to increase towards the linear behavior at the far field of the sample position (+Z). The change of intensity, in this case, is caused by two photon absorption when the sample travels through beam waist. The open-

aperture Z-Scan defines variable transmittance values, which is used to determine absorption coefficient The behavior of z-scan curves is in good agreement with that obtained by Sheik-Bahae [98].

Saturable Absorption phenomenon was observed for open-aperture Z-Scan at (457) nm wavelength, and different laser powers (56,70,84 and 102) mW , of thin films of Acriflavine dye doped with PVA polymer and AgNPs at concentration (10^{-3} M) as shown in Figures (4.40 and 4.41) respectively This behavior is in agreement with [13]. Figures (4.42 and 4.43) show the same phenomenon for thin films of Orcen dye doped with (PVA polymer) and (AgNPs) respectively .This behavior is in agreement with [25].

Also Saturable Absorption phenomenon is observed for open-aperture Z-Scan with different laser powers (56,70,84 and 102) mW, of thin films of Azure-B dye doped with PVA polymer and AgNPs at concentration (10^{-3} M) as shown in Figures (4.44 and 4.45) respectively .This behavior is in agreement with [30].

The behavior of transmittance curves starts linearly at different distances from the far field of the sample position (-Z). At the near field the transmittance curve begins to increase until it reaches the maximum value (T_{max}) at the focal point, where Z=0 mm. Afterwards, the transmittance begins to decrease toward the linear behavior at the far field of the sample position (+Z).

The transmittance is sensitive to the nonlinear absorption as a function of input power intensity. The change in intensity is caused by saturation absorption in the sample as it travels through the beam waist [62]. In the focal plane where the intensity is the greatest, the largest nonlinear absorption is observed. At the far field of the Gaussian beam, where , the beam intensity is too weak to elicit nonlinear effects. A symmetric peak value is contributed to the negative nonlinear absorption coefficient (β), indicates that the sample shows a bleaching-like behavior (saturation of absorption). This behavior agrees with [103].

The variation of β is inversely proportional to the input power, the nonlinear absorption showed the power dependence. As the power increase there is a significant decreasing in the nonlinear absorption coefficient[20].

The nonlinearity of doped dyes is larger than those for pure dyes. As well as thin films of these dyes possess very large nonlinearity as compared with dye as solution, becauese of thin films have thickness larger than dyes as solutions, which is lead to increasing the nonlinear phase shift .This behavior agrees with [25].

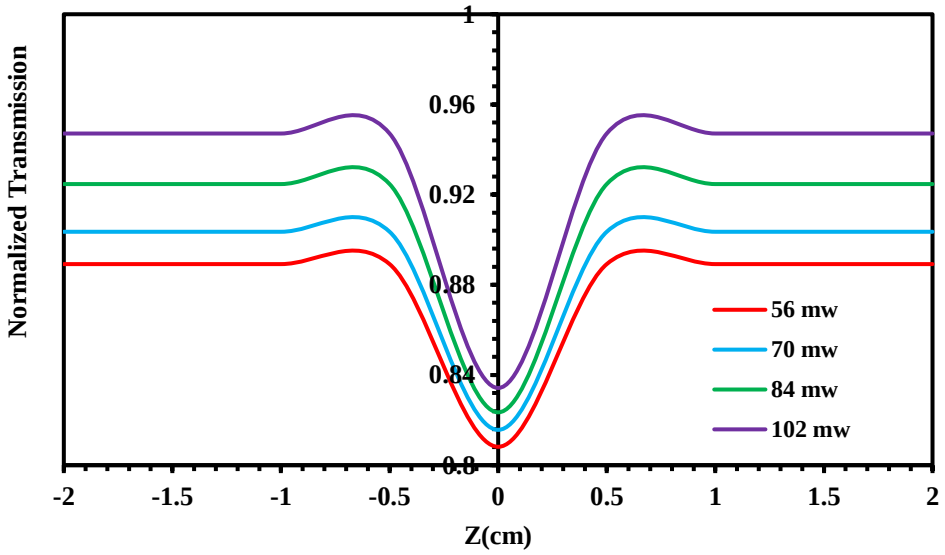

Figure (4.37): Open-aperture Z-Scan data for Acriflavine dye as solution at concentration (10^{-5} M) at different laser powers .

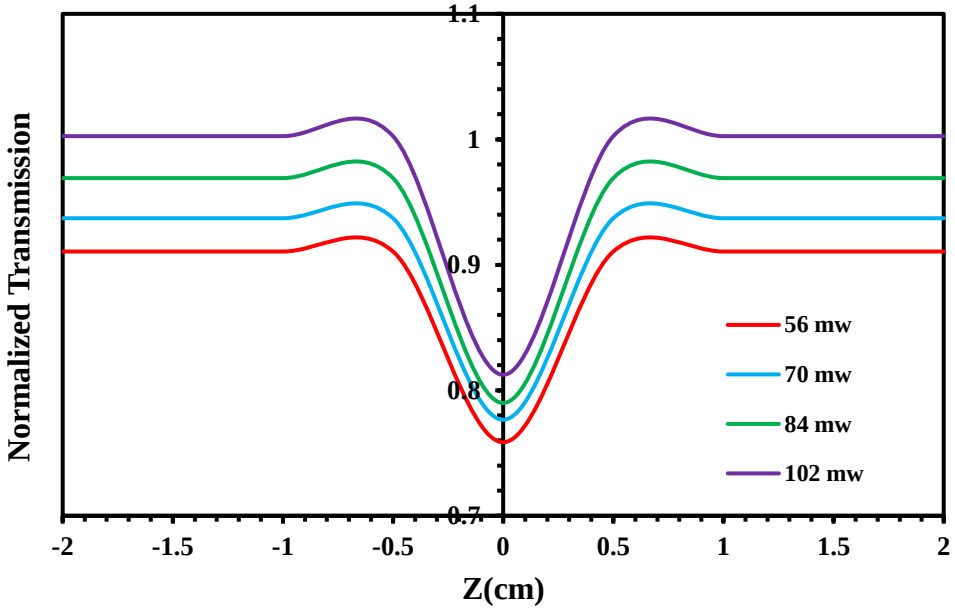

Figure (4.38): Open-aperture Z-Scan data for Orcein dye as solution at concentration (10^{-5} M) at different laser powers .

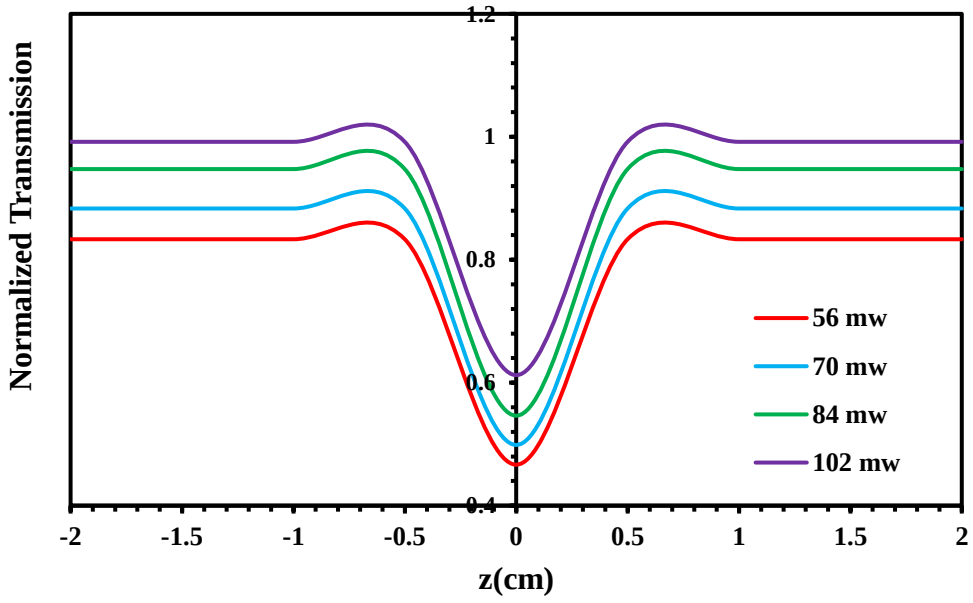

Figure (4.39): Open-aperture Z-Scan data for Azure- B as solution at concentration (10^{-5} M) at different laser powers .

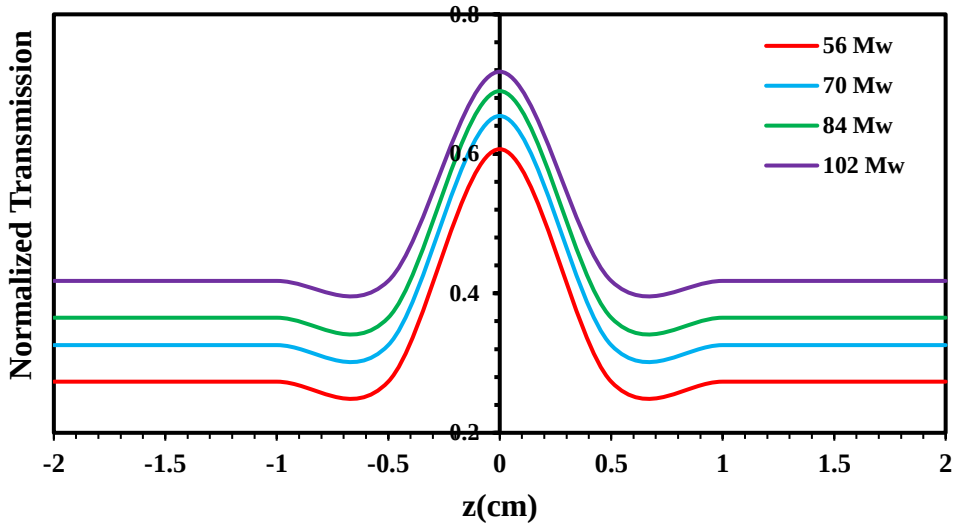

Figure (4.40): Open-aperture Z-Scan data for thin film of (Acriflavine dye+PVA polymer) at different laser powers.

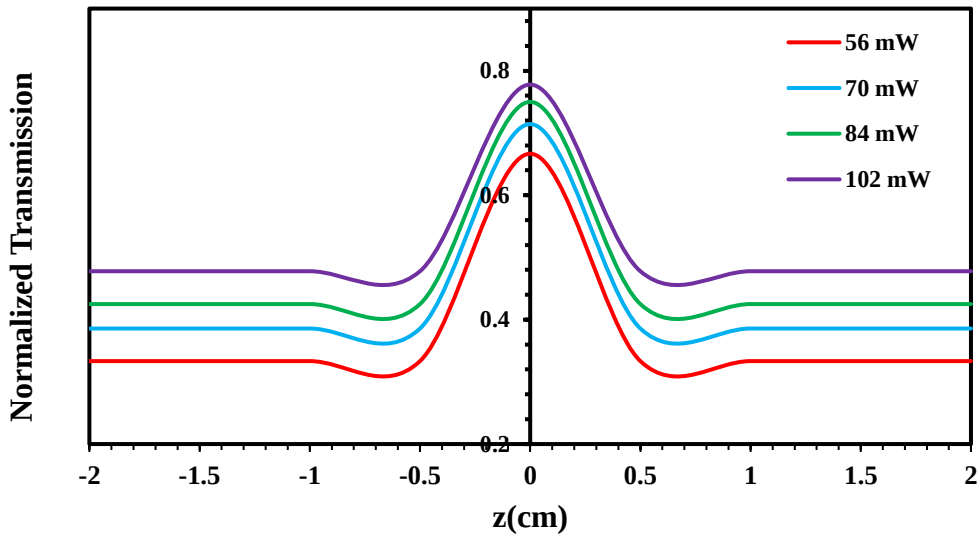

Figure (4.41): Open-aperture Z-Scan data for thin film of (Acriflavine dye +PVA polymer+Ag NPs) at different laser powers.

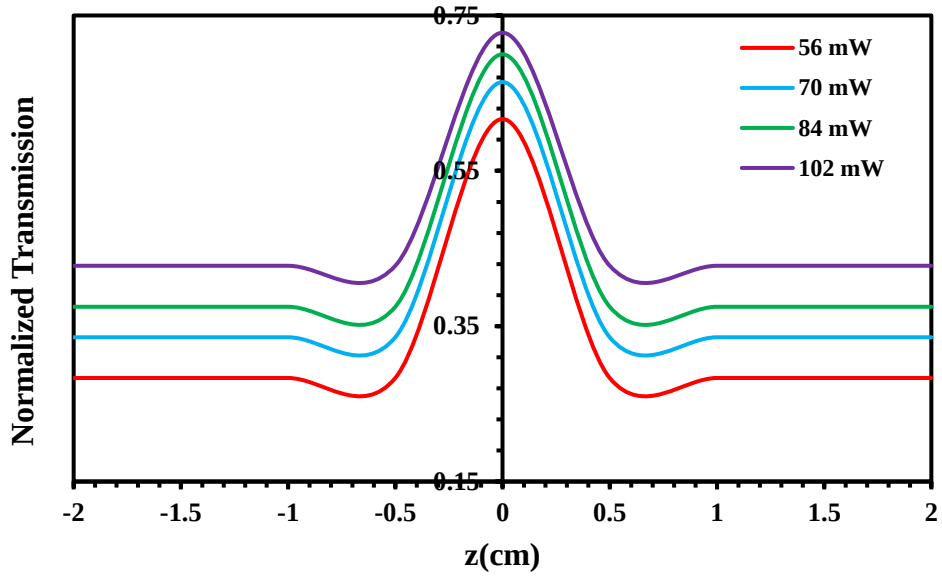

Figure (4.42): Open-aperture Z-Scan data for thin film of (Orcein dye+PVA polymer) at different laser powers.

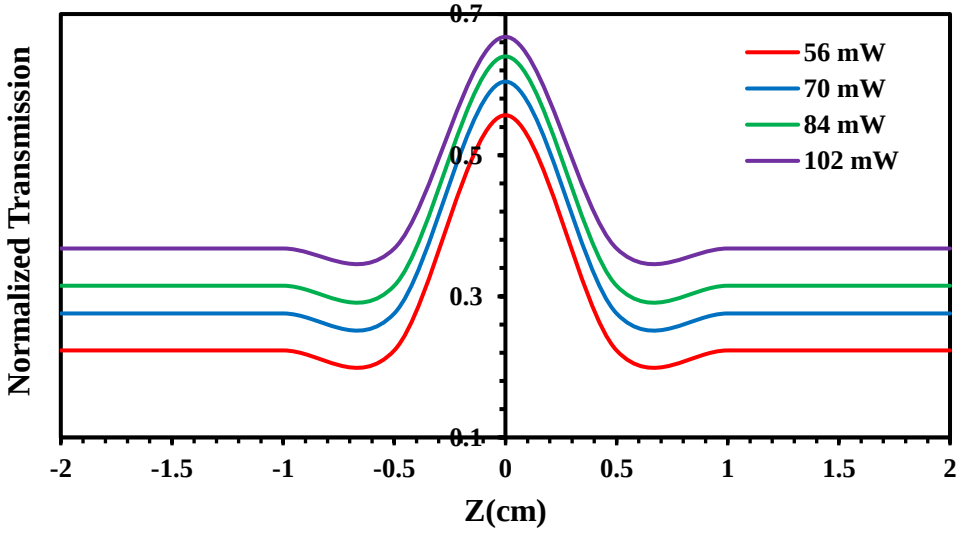

Figure (4.43): Open-aperture Z-Scan data for thin film of (Orcein dye +PVA polymer+Ag NPs) at different laser powers.

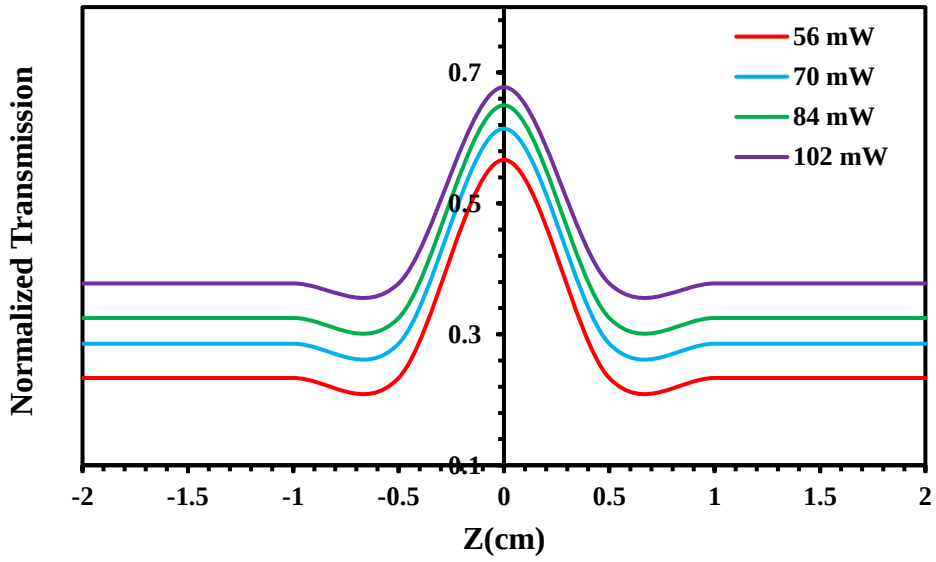

Figure (4.44): Open-aperture Z-Scan data for thin film of (Azure-B dye+PVA polymer) at different laser powers.

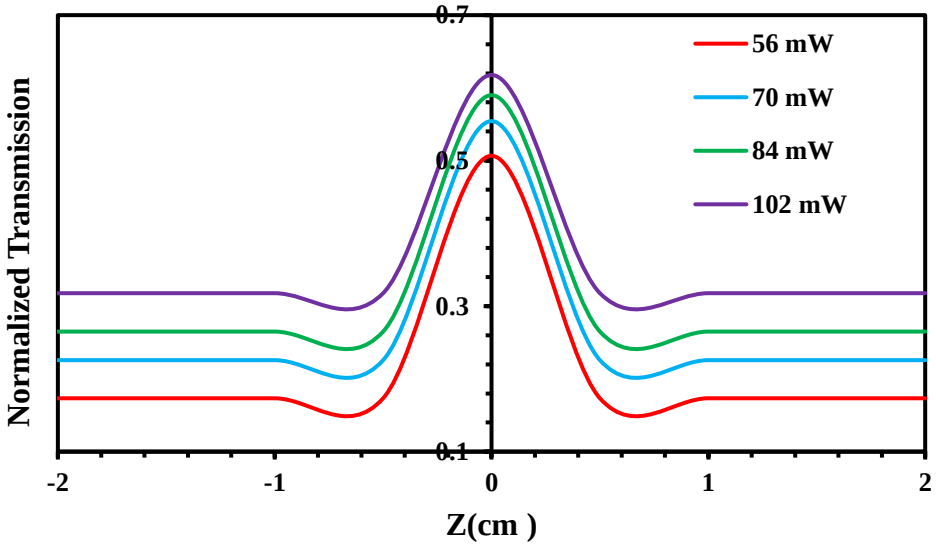

Figure (4.45): Open-aperture Z-Scan data for thin film of (Azure-B dye +PVA polymer+Ag NPs) at different laser powers.

4.6.2. Nonlinear Refractive Index of Organic Laser Dyes and their Thin Films

The nonlinear refractive index (n_2) of Acriflavine, Orcein and Azure-B organic laser dye at concentration (10^{-5} M) dissolved in ethanol solvent, and their thin films at (10^{-3} M) doped with PVA polymer and Ag NPs, which can be measured

by performing the closed aperture Z-Scan technique at (457) nm wavelength and different laser powers (56,70,84 and 102) mW .

The normalized transmittances of Z-Scan measurements as a function of distance for Acriflavine dye is shown in Figure (4.46), The valley followed by peak transmittance curve obtained from the closed aperture Z-Scan data indicates that the sign of the refraction nonlinearity is positive ($n_2 > 0$), leading to self-focusing lensing in these samples. This behavior agrees with the study in reference [13].

Figures (4.47 and 4.48) show the normalized transmittances of Z-Scan measurements as a function of distance for (Orcein and Azure-B) dyes respectively at concentration (10^{-5} M) , the nonlinear effect region is extended from (-2) cm to (2) cm. The peak followed by a valley transmittance curve obtained from the closed aperture Z-scan data indicates that the sign of the refraction nonlinearity is negative ($n_2 < 0$), leading to self-defocusing lensing in these samples. This behavior agrees with [25,30].

The nonlinear refractive index of thin films of Acriflavine dye solution at (10^{-3}M) doped with PVA polymer and AgNPs, was measured by Z-scan method at (457 nm) wavelength and different laser powers (56,70,84 and 102) mW , as show in Figures (4.49 and 4.50) respectively, these Figures show that the sign of the refraction nonlinearity is positive ($n_2 > 0$), leading to self-focusing lensing in these samples. This behavior agrees with the study in reference [13].

Figures(4.51-4.54) show the normalized transmittances of Z-Scan measurements as a function of distance for thin films of (Orcein and Azure-B) dyes respectively at concentration (10^{-3}M) doped with polymer PVA and AgNPs .

The peak followed by a valley transmittance curve obtained from the closed aperture Z-scan data indicates that the sign of the refraction nonlinearity is negative ($n_2 < 0$), leading to self-defocusing lensing in these samples. This behavior agrees with [25,30].

In order to describe the Z-Scan behavior in the previous figures, when the sample moves far from the focus, the transmitted beam intensity is low and the transmittance remains relatively constant. As the sample approaches the beam focus, intensity increases, leading to self-lensing in the sample tend to collimate the beam on the aperture in the far field, increasing the measured transmittance at the iris position.

If the beam experiences any nonlinear phase shift due to the sample as it is translated through the focal region, then the fraction of light falling on the detector will vary due to the self-lensing generated in the material by the intense laser beam. In this case, the signal measured by detector will exhibit a peak and valley as the sample is translated .

The position of the peak and valley, relative to the z-axis, depends on the sign of the nonlinear phase shift .Where the change in the normalized transmittance from the peak of the curve to the valley (ΔT_{p-v}) is directly proportional to the nonlinear phase shift imparted on the beam.

Moreover, if the beam is transmitted through the nonlinear medium the induced phase shift can also be either negative or positive accordingly when the medium is self- focusing or self-defocusing, respectively.

The magnitude of the phase shift can be determined from the change in transmittance between peak and valley. After the focal plane, the self-defocusing increases the beam divergence, leading to a widening of the beam at the focus and thus reducing the measured transmittance. Far from focus ($Z > 0$), again the nonlinear refraction is low resulting in a transmittance Z-independent[97].

The nonlinear parameters for all samples of organic dyes are calculated ,as tabulated in Tables (4.3 - 4.5) from these Tables show that the values of nonlinear refractive index (n_2) increased with increasing laser powers, but the values of nonlinear absorption coefficient (β) decreased with increasing laser powers .

The closed-aperture Z-Scan defines variable transmittance values, which used to determine the nonlinear phase shift ($\Delta\Phi$) using equation (2.13) and, the

nonlinear refractive index (n_2) using equation (2.12), nonlinear absorption coefficient (β) using equation (2.18), as listed in Tables .

The nonlinearity of thin films of doped dyes is larger than those for pure dyes as solutions due to adding PVA polymer and AgNPs, and increasing number of molecules per volume unit ,as well as thin films have thickness larger than liquid dyes which is lead to increasing the nonlinear phase shift. This behavior agrees with [22].As well as all samples of (Acriflavine) dye possess very large nonlinearity as compared with other dyes.

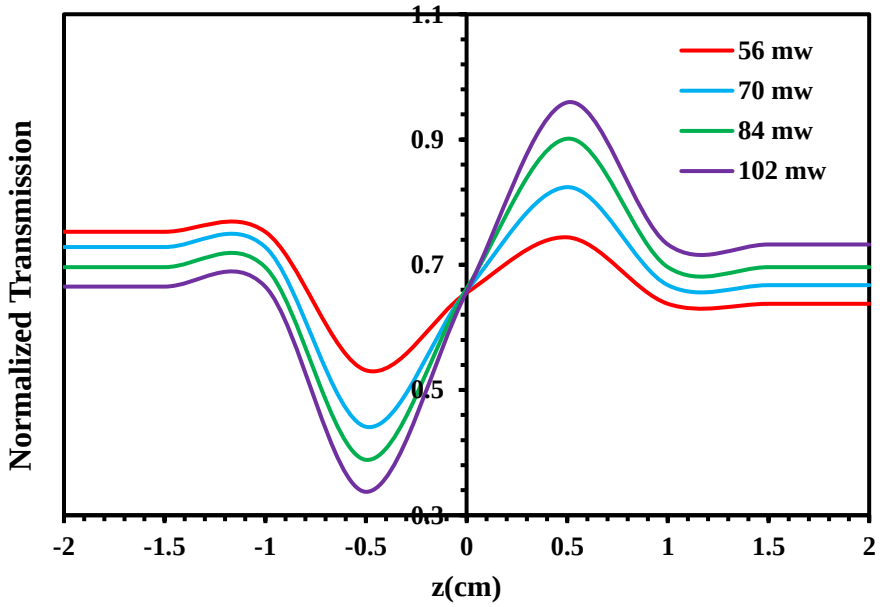

Figure (4.46): Closed-aperture Z-Scan data of Acriflavine dye as solution at different laser powers.

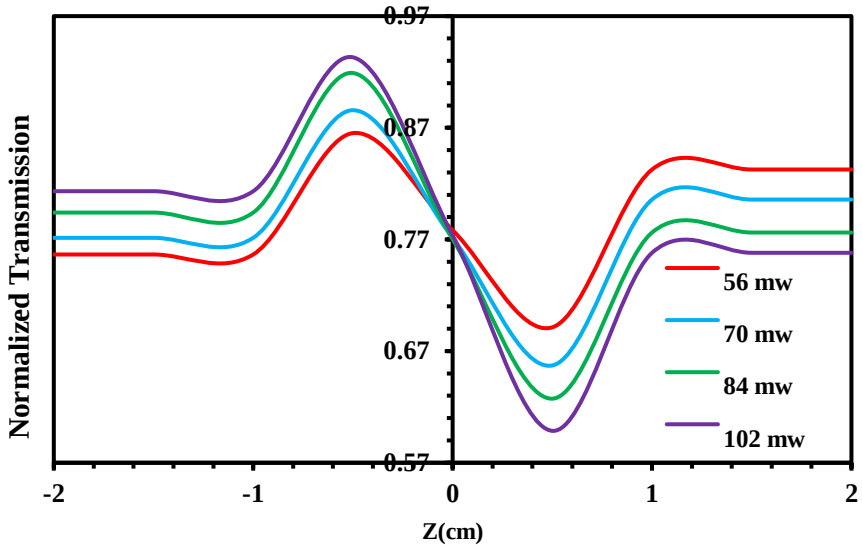

Figure (4.47): Closed-aperture Z-Scan data of Orcen dye as solution at different laser powers.

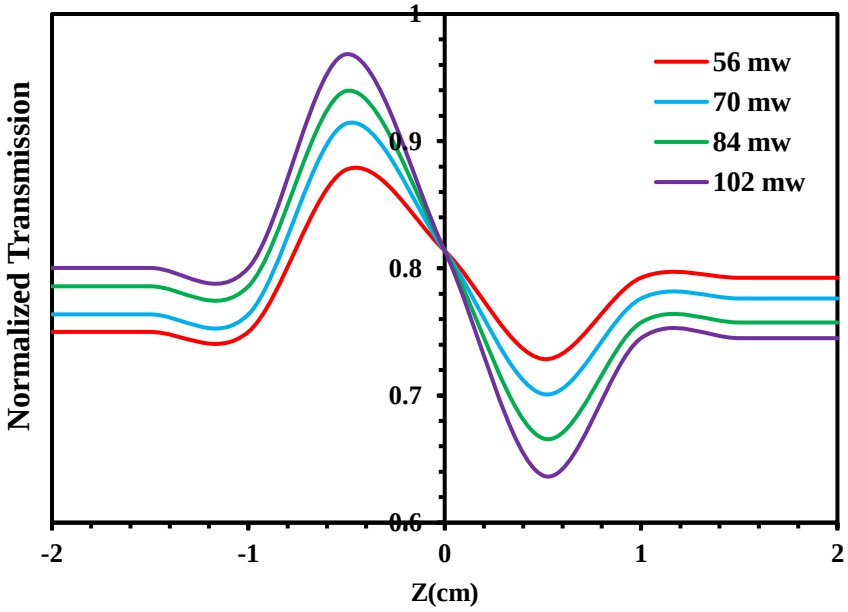

Figure (4.48): Closed-aperture Z-Scan data of Azure-B dye as solution at different laser powers.

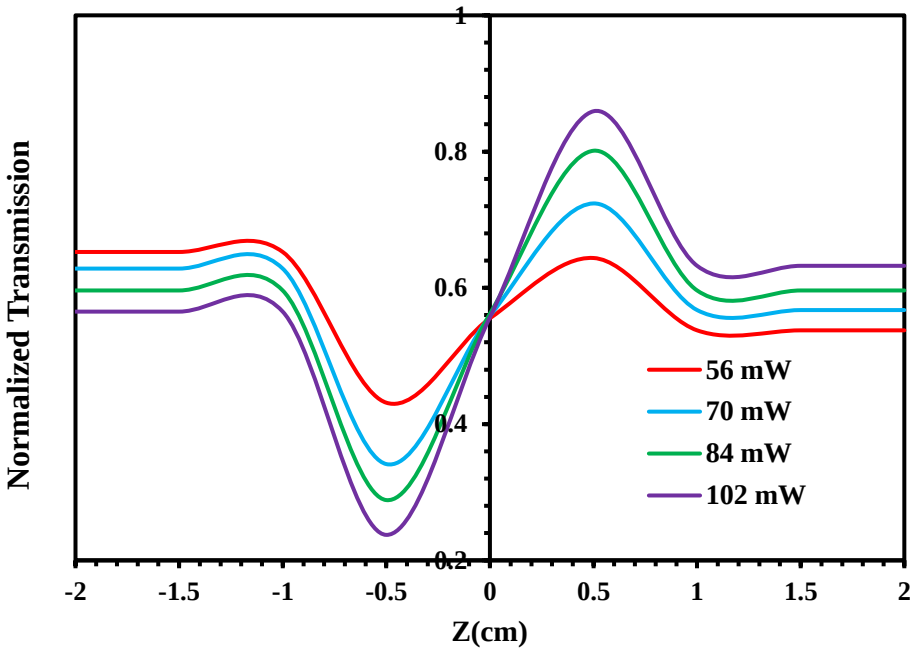

Figure (4.49): Closed-aperture Z-Scan data for thin film of Acriflavine dye Doped with PVA polymer at different laser powers.

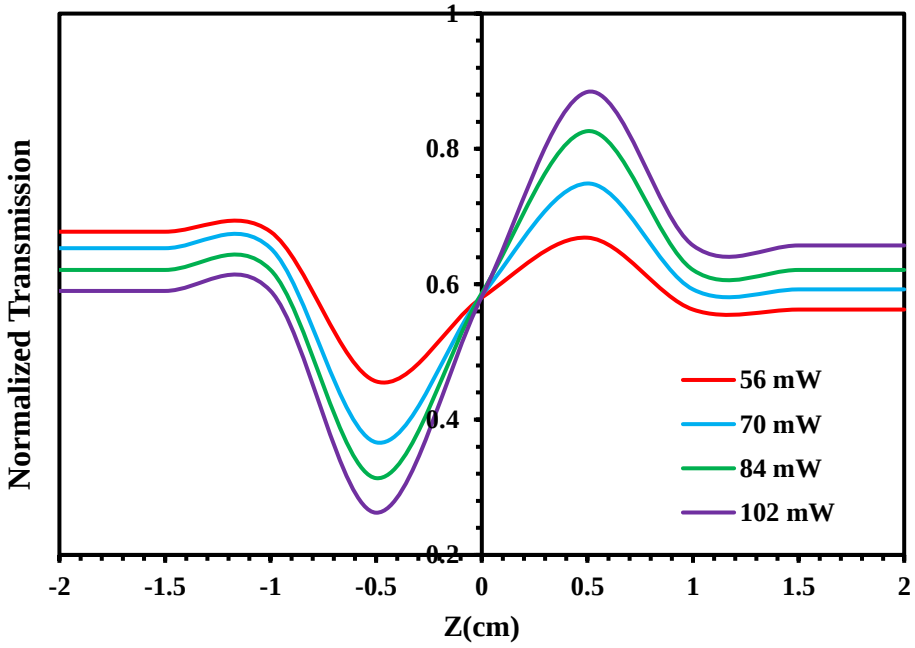

Figure (4.50): Closed-aperture Z-Scan data for thin film of Acriflavine dye doped with PVA polymer and Ag NPs at different laser powers.

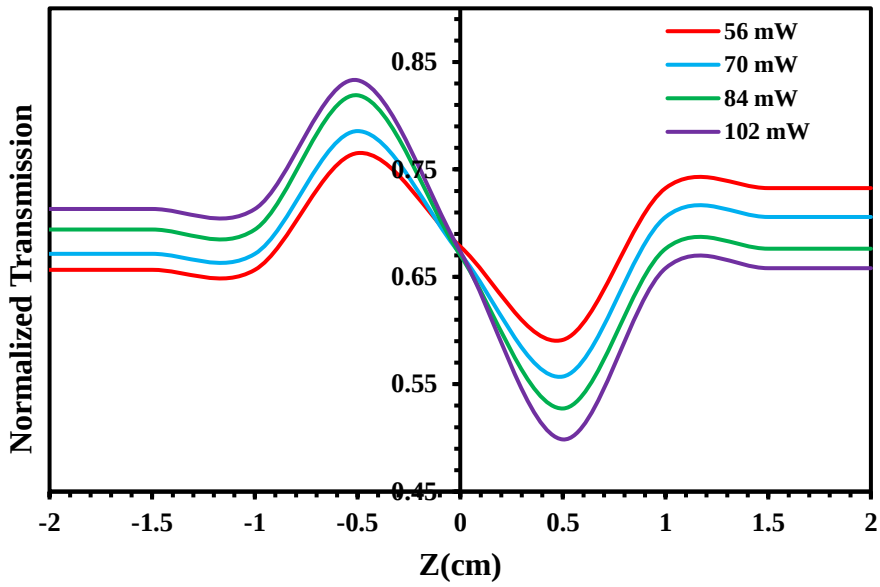

Figure (4.51): Closed-aperture Z-Scan data for thin film of Orcein dye doped with PVA polymer at different laser powers.

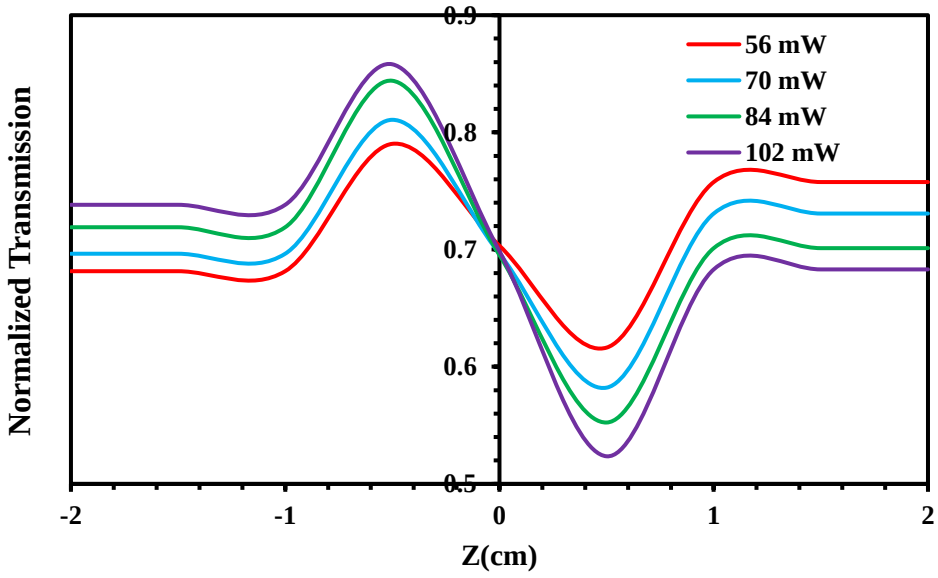

.

Figure (4.52): Closed-aperture Z-Scan data for thin film of Orcein dye doped with PVA polymer and Ag NPs at different laser powers.

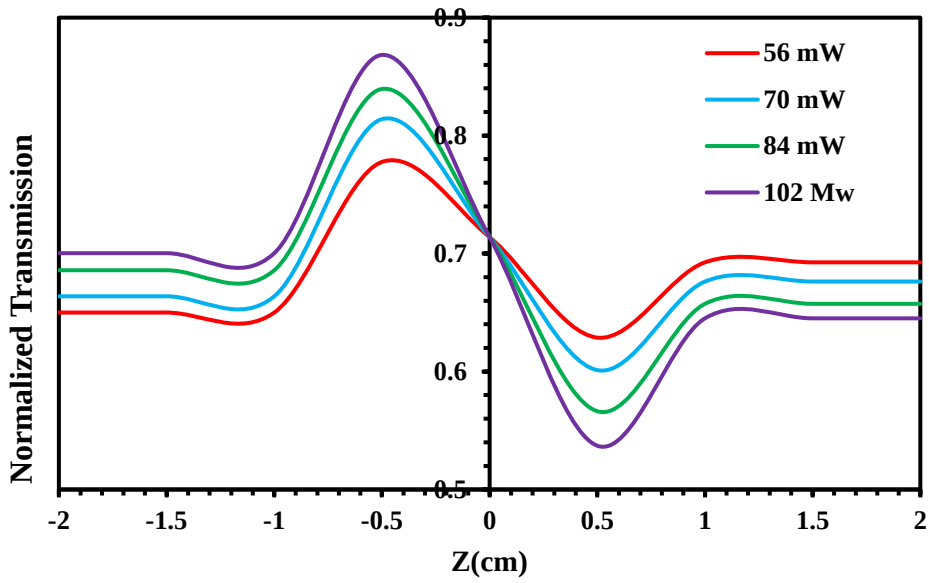

Figure (4.53): Closed-aperture Z-Scan data for thin film of Azure-B dye doped with PVA polymer at different laser powers.

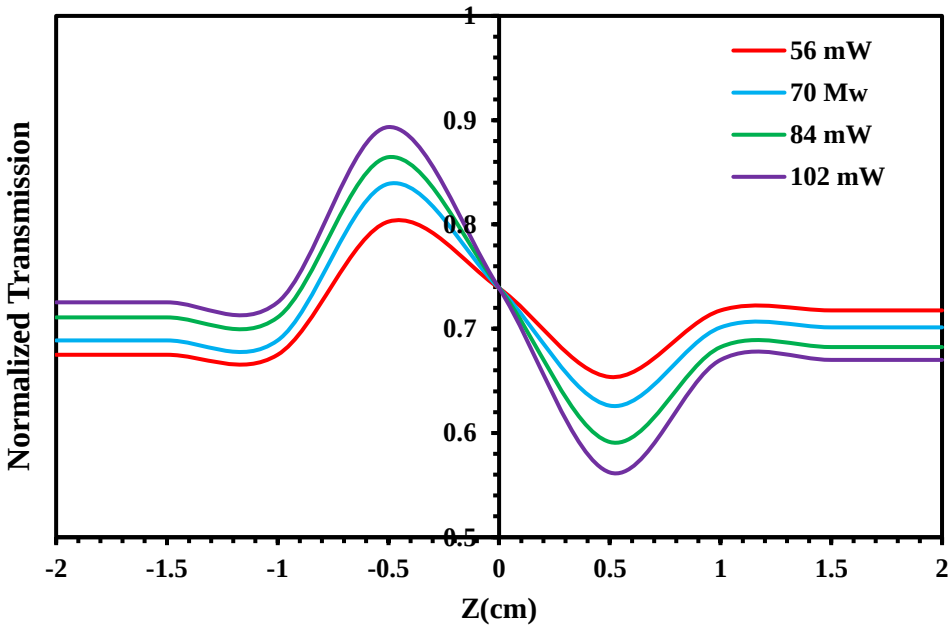

Figure (4.54): Closed-aperture Z-Scan data for thin film of Azure-B dye doped with PVA polymer and Ag NPs at different laser powers .

Table (4.3): The nonlinear optical parameters for Acriflavine dye and their thin films doped with PVA polymer and Ag NPs at λ=457nm at different laser powers.

Material	Powers (mW)	ΔT_{P-V}	$\Delta\Phi_o$	n_2 (cm^2/mW)	T (z)	β (cm/mW)
Acriflavine dye as (solution)	56	0.2123	0.5231	6.7541×10^{-10}	0.8081	0.401×10^{-3}
	70	0.3826	0.9423	9.7338×10^{-10}	0.8156	0.324×10^{-3}
	84	0.5128	1.2631	10.0872×10^{-10}	0.8234	0.272×10^{-3}
	102	0.6218	1.5316	10.1657×10^{-10}	0.8342	0.244×10^{-3}
Thinfilm of Acriflavine + PVA polymer	56	0.2623	0.6462	5.0697×10^{-3}	0.6066	2.0112
	70	0.4325	1.0655	6.6868×10^{-3}	0.6542	1.7257
	84	0.5628	1.3862	7.2498×10^{-3}	0.6900	1.5166
	102	0.6718	1.6548	7.6521×10^{-3}	0.7177	1.3950
Thinfilm of Acriflavine +PVA polymer + Ag NPs	56	0.2923	0.7201	6.1090×10^{-3}	0.6566	2.1650
	70	0.4625	1.1393	7.7323×10^{-3}	0.7042	1.8576
	84	0.5928	1.4601	8.2575×10^{-3}	0.7412	1.6292
	102	0.7018	1.7286	8.6442×10^{-3}	0.7677	1.4922

Table (4.4): The nonlinear optical parameters for Orcein dye and their thin films doped with PVA polymer and Ag NPs at λ=457nm at different laser powers.

Material	Power (mW)	ΔT_{P-V}	$\Delta\Phi_o$	n_2 (cm^2/mW)	T (z)	β (cm/mW)
Orcein dye as solution	56	0.1739	0.4284	5.4691×10^{-10}	0.7585	0.376×10^{-3}
	70	0.2285	0.5629	5.7486×10^{-10}	0.7765	0.308×10^{-3}
	84	0.2916	0.7183	6.1129×10^{-10}	0.7898	0.261×10^{-3}
	102	0.3345	0.8239	6.1995×10^{-10}	0.8123	0.238×10^{-3}
Thinfilm of Orcein + PVA polymer	56	0.2241	0.5521	4.9840×10^{-4}	0.6166	0.2163
	70	0.2785	0.6861	4.9549×10^{-4}	0.6642	0.1864
	84	0.3416	0.8415	5.0643×10^{-4}	0.7010	0.1639
	102	0.3845	0.9471	6.6397×10^{-4}	0.7277	0.1505
Thinfilm Orcein + PVA polymer + AgNPs	56	0.2439	0.6007	10.671×10^{-4}	0.59678	0.4197
	70	0.2985	0.7353	10.745×10^{-4}	0.64586	0.3633
	84	0.3616	0.8908	11.846×10^{-4}	0.6812	0.3193
	102	0.4045	0.9963	12.928×10^{-4}	0.71786	0.2976

Table (4.5): The nonlinear optical parameters for of Azure-B dye and their thin films doped with PVA polymer and Ag NPs at λ=457nm at different laser powers.

Material	Power (mW)	ΔT_{P-V}	$\Delta\Phi_o$	n_2 cm^2/mW	T (z)	β cm/mW
(Azure-B) dye as solution	56	0.1489	0.3668	4.682×10^{-10}	0.4666	0.234×10^{-3}
	70	0.2127	0.5240	5.3511×10^{-10}	0.4987	0.200×10^{-3}
	84	0.2731	0.6728	5.7251×10^{-10}	0.5463	0.183×10^{-3}
	102	0.3312	0.8159	6.1393×10^{-10}	0.6123	0.181×10^{-3}
Thinfilm of (Azure-B) + PVA polymer	56	0.1989	0.4899	2.8755×10^{-4}	0.5666	0.1292
	70	0.2627	0.6472	3.0385×10^{-4}	0.6142	0.1120
	84	0.3231	0.7960	4.1143×10^{-4}	0.6501	0.0988
	102	0.3812	0.9391	4.8487×10^{-4}	0.6777	0.0911
Thinfilm of (Azure-B) + PVA polymer + AgNPs	56	0.2189	0.5392	5.2868×10^{-4}	0.5416	0.2064
	70	0.2826	0.6962	6.4608×10^{-4}	0.5892	0.1796
	84	0.3431	0.8453	7.6252×10^{-4}	0.6251	0.1588
	102	0.4012	0.9883	8.7124×10^{-4}	0.6527	0.1466

4.7 Optical Limiting Behavior of Organic Dyes

The optical limiting behavior, was performed by closed-aperture Z-Scan with the same laser used in Z-Scan technique. Figures (4.55,4.56 and 4.57) respectively give the optical limiting characteristics at room temperature for all samples of (Acriflavine,Orcein and Azure-B) organic laser dyes as solutions and thinfilms doped with (PVA polymer and (Ag) nano-particales were dissolved in (Ethanol) solvent respectively. The samples show very good optical limiting behavior arising from nonlinear refraction.

The output power rises initially with the increasing in input power, but after a certain threshold value, the sample starts defocusing the beam resulting in a greater part of the beam cross-section being cut off by the aperture. Thus, the transmittance recorded by the photodetector remained reasonably constant showing a plateau region.

Thin films of (Acriflavine,Orcein and Azure-B) give optical power limiting threshold and limiting amplitude less as compared with the dyes as solutions, therefore, the properties of optical limiting for thin films of organic laser dyes are better than of dyes as solutions,due to increasing number of molecules per unit volume which is lead to increasing the nonlinear absorption ,as listed in Table (4.6).This behavior agree with [19,25,and 30].

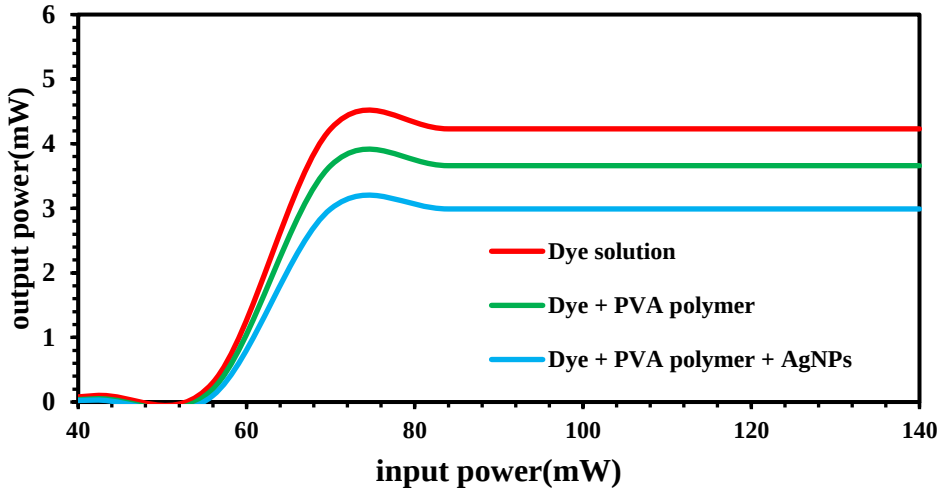

Figure(4.55) :The optical limiting response for all samples of Acriflavine dye.

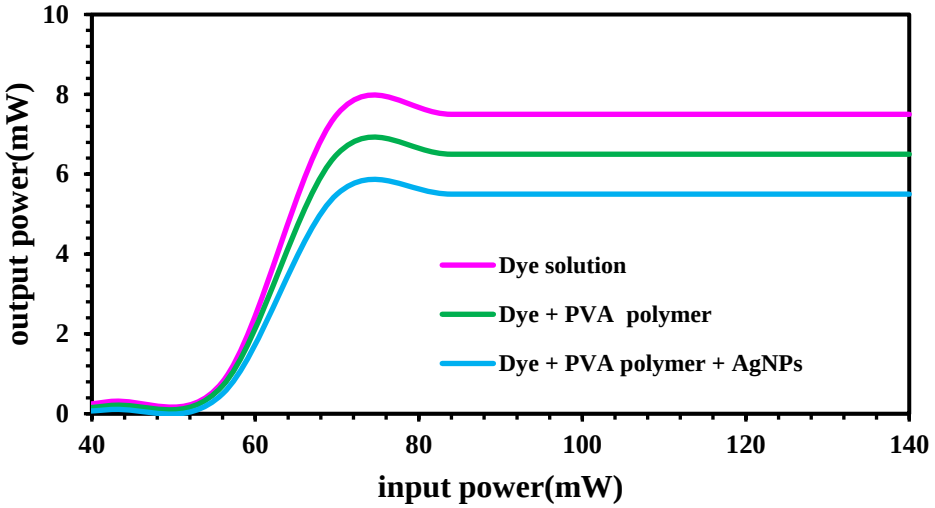

Figure(4.56) :The optical limiting response for all samples of Orcein dye.

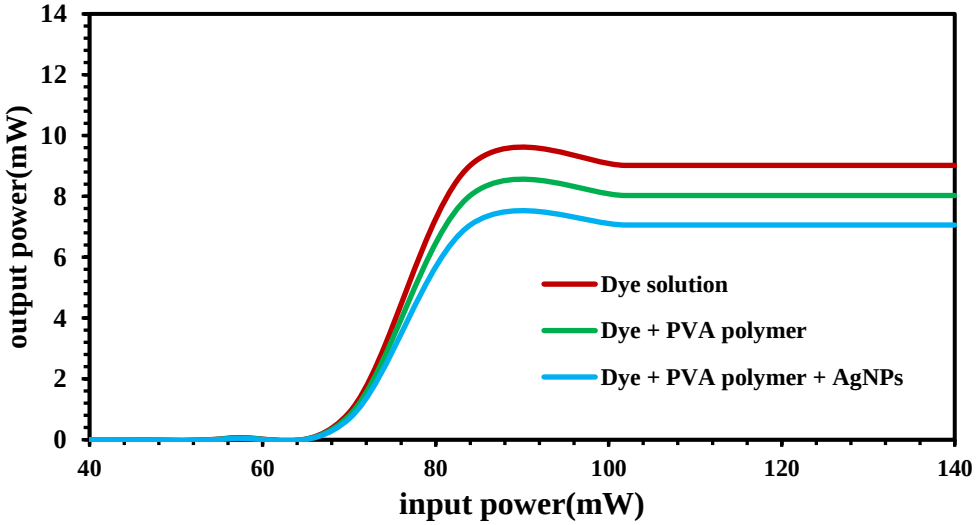

Figure(4.57) :The optical limiting response for all samples of Azure-B dye.

Table (4.6): The optical limiting response of (Acriflavine,Orcein and Azure-B) Dyes and their thin films doped with PVA polymer and Ag NPs .

Organic lased dyes	Samples	Limiting Threshold	Limiting Amplitude
Acriflavine	solution	78	4.54
	+PVA polymer	76	3.86
	PVA +AgNPs polymer	74	3.01
Orcein	solution	80	8.0
	+PVA polymer	78	6.4
	PVA +AgNPs polymer	77	5.8
Azure-B	solution	90	9.02
	+PVA polymer	88	8.13
	PVA polymer +AgNPs	86	6.50

4.8 Conclusions

The main conclusions that are obtained in this research:

1. The linear and nonlinear optical properties of all samples (solutions and thinfilms) of Acriflavine dye is larger than that of Orcen and Azure-B dyes.
2. The linear and non-linear optical properties of thinfilm each dye doped with (PVA) polymer and (AgNPs) is larger than thinfilm of the same dye doped with (PVA) polymer.
3. The flourecence quantum efficiency results indicated that the best dye to use as active laser medium was Acriflavine as solutions and thin films.
4. The nonlinearity of doped dyes is larger than those for pure dyes.
5. The nonlinear refractive index of all samples of (Acriflavine,Orcein and Azure-B) increases when increasing laser powers but the nonlinear absorption coefficient of all samples decreases when the increasing laser powers.
6. The results of the closed-aperture Z-Scan of all samples of Acriflavine dye is self-focusing phenomena while Orcen and Azure-B dyes are self-defocusing phenomena.
7. The results of the open-aperture Z-Scan of all samples of all dyes as solutions give two photon absorption phenomena ,while thin films of organic laser dyes give saturation absorbtion phenomena.
8. Acriflavine dye give linear and nonlinear optical parameters higher than that of other dyes.
9. The possibility of using all dyes (solutions and thin films) as good optical limiting, which have technological applications such as, optical-switching devices.
10. The properties of optical limiting for all samples (solutions and thin films) of Acriflavine dye are better than of the same samples of Orcen and Azure-B dyes.

11. The properties of optical limiting for thin films of all dyes are better than of dyes as solutions.

4.9 Future Works

In this context, a further investigation can be suggested as future works:

1. Studying the nonlinear optical properties of organic laser dyes using lasers with different wavelengths.
2. Studying the linear and nonlinear optical properties by Z-Scan technique for dyes doped with different polymers and different nanoparticles.
3. Studying the optical limiting behavior of different types of mixture of dyes.
4. Studying linear and nonlinear optical properties for thin film of different types of dyes prepared by other methods.

CHAPTER ONE

Introduction

CHAPTER TWO

Theoretical Part

CHAPTER THREE

Experimental work

CHAPTER FOUR

Results and Discussion

References

References

[1] R. Fork and Z. Kaplan, "***Thermal bleaching of rhodamine 6G in polymethyl methacrylate (PMMA)***", Appl. Phys. Lett.8 (1), 95–96, (1981).

[2] P. Brwee; "***Organic Chemistry***":2nd Ed, prentice Hall New Jeres, (1998).

[3] F. Schafer, "***Dye Laser***", Springer Verlag Berlin, Heidelberg New York, (1977).

[4] R. Mohamed," ***Nonlinear Optical Properties of PMMA Composite using Z-Scan Technique***", M.Sc. Thesis, University of Baghdad Institute of Laser for Postgraduate Studies, (2008).

[5] A. Abdul-Zahra Ali," ***Investigation of nonlinear optical properties for laser dyes-doped polymer thin film***", M.Sc. Thesis, University of Baghdad Institute of Laser for Postgraduate Studies, (2008).

[6] U. Brackmann, "***Lambda chrome Laser Dyes*** ", Lambda Physik, Gottingen, (1997).

[7] U.Gubler, C. Bosshard, and K. S. Lee. "***Polymers in Photonics Applications***." ,(2002).

[8] S. Singh, V.Kanetkar ,G.Sridhar, V. Muthuswamy, K. Raja," ***Solid-state polymeric dye lasers***", Journal of Luminescence, 1 , 285–291, (2003).

[9] D. Paul and L.Robeson," ***Polymer nanotechnology Nanocomposites***", journal polymer, 49, 3187–3204, (2008).

[10] A. Chatterjee and M. Islam, "***Fabrication and characterization of TiO_2–epoxy nanocomposite***", Materials Science and Engineering, 487, 574–585, (2008).

[11] S. Singha and M. J. Thomas," ***Permittivity and Tan Delta Characteristics of Epoxy Nanocomposites in the Frequency Range of 1 MHz–1 GHz***", IEEE Transaction on Dielectrics and Electrical Insulation ,15,1, 1070-9878, (2008).

[12] O.Abdollah, C. Simon, and A. Rostami. "***The effects of alumina nanoparticle on the properties of an epoxy resin system***." *Materials Chemistry and Physics* ,114.1, (2009).

[13] O. Shaker and Shafeeq, "***Nonlinear optical properties of polymer [PMMA] thin films doped with dye lasing compounds, Rhodamine 6G and Acriflavine in chloroform solvent by using dip coating method***.", *Iraqi Journal of Physics (IJP)* 15.35, 125-132, (2000).

[14] A.Furlani, R.D'Amato, M.Colapietro, G. Portalone, M.Casalboni, M.Falconieri, and M.Russo, , "***characterisation and optical properties of symmetrical and unsymmetrical Pt (II) and Pd (II) bis-acetylides***". *Journal of Organometallic Chemistry*, *627*(1), 13-22, (2001).

[15] S.Venugopal, "***Nonlinear Absorption and Excited State Dynamics in Rhodamine B Studied Using Z-Scan and Degenerate Four Wave Mixing Techniques*** " , Chemical physics Letters 361,5 ,439-445,(2002).

[16] R.Ganeev , "***Characterization of Nonlinear Optical Parameters of Polymethine Dyes*** " , Applied Physics B 76.6 , 683-686. (2003).

[17] K.Geetha, , M.Rajesh, V. Nampoori, C. Vallabhan, and P.Radhakrishnan, ***"Loss Characterization in Rhodamine 6G Doped Polymer Film Waveguide by Side Illumination Fluorescence***" ,Journal of Optics A: Pure and Applied Optics, 6, 379,(2004) .

[18] S.Chen, Z. Liu, W. Zang, J. Tian, W. Zhou, and F. Song," ***Sensitive Measurement of Optical Nonlinearities Using a Single Beam*** ", Materials Science and Engineering , 22, 9, 1911,(2005).

[19] D. Yan,"***effect of Ag Nano particles on optical properties of R6G doped PMMA films***", Chemical Physics Letters, 24, 4, 954 - 956, (2006).

[20] D. Obied "***Nonlinear optical properties of CdS thin film nanoparticles using z-Scan technique***.", *Iraqi* Journal. *Laser* Part A, (2007).

[21] A. Tawil. "***Study the Optical Properties of Fluorescein Sodium Dye Doped in Polymer Polyvinyl Alcohol***." (2008).

[22] Q. Mohammed, "***Nonlinear optical and optical limiting properties of Chicago sky blue 6B doped PVA film at 633 nm and 532 nm studied using a continuous wave laser***.", Modern Physics Letters *B* 22.16, 1589-1597, (2008).

[23] M. Zainab, ***''Improvement of Nonlinear Optical Properties for Mixture Laser Dyes Doped PMMA***", Iraqi Journal of laser, Part A, 9, 2,9-14, (2010).

[24] V. Sindhu and A. Ramalingam, ***"Third Order Optical Nonlinearities and Spectral Characteristics of Methylene Blue***", journal of Quantum formation Science,1,69-72, (2011).

[25] R. Manshad, and A. Hassa. "***Nonlinear characterization of orcein solution and dye doped polymer film for application in optical limiting***." Journal of Basrah Researches (Sciences), 38,4A, (2012).

[26] L. Hassan, F. Mahdi, and J. Abed Al-Zahra. "***Linear and Nonlinear Optical Properties of the Dye Laser (Acridine Dye***).", *Academic Research International*, 5,4, 135, (2014).

[27] F. Mata, ***'''Nonlinear Absorption and Photoluminescence Emission Behaviors of Rhodamine B Dye Chromophore***", Indian Journal of Applied Research, 5, ISS. 7, (2015).

[28] F.Tawil and K. Tahir," ***Study the optical properties of Fluorescein sodium dye doped in polymer Poly Polyvinyl alcohol for different thickness***". journal of Karbala university, *14*(1), 4-19, (2018).

[29] J. Tahir, and F. Tawil. "***Study the optical properties of Fluorescein sodium dye doped in polymer Poly Polyvinyl alcohol for different thickness***." Journal of Karbala university ,14.1, 4-19, (2018).

[30] R. Manshad, and M.Qusay "***Surface morphology and optical limiting properties of azure B doped PMMA film***.", Optical Materials ,92, 22-29, (2019).

[31] R. Muhammad, M. Krishnan, and G. Harun, "***Power-dependent nonlinear optical behaviors of ponceau BS chromophore at 532 nm via Z-scan technique***." Journal of Photochemistry and Photobiology A: Chemistry 397, 112574, (2020).

[32] A.Al Hussainey, and Ban A. Naser. "***Non-Linear Optical Properties of Organic Laser Dye***.", Annals of the Romanian Society for Cell Biology, 25.6 ,11556-11567, (2021).

[33] A. Ummu, M. Girisun, and S.Anandan, "***Nonlinear Optical Studies of Conjugated Organic Dyes for Optical Limiting Applications***." Journal of Molecular Structure, 1240, 130559, (2021).

[34] R. Menzel, ***"Photonics: Linear and Nonlinear Interactions of Laser Light and Matter"***, 2nd Edition, Springer, Berlin, ISBN: 978-3-662-04521-3, (2001).

[35] W. Silfvast, ***"Laser Fundamentals***", 2nd Edition, Cambridge University Press, (2004).

[36] R. Boyd, ***''Nonlinear Optics''***, 2nd Edition Academic press, London, (2003).

[37] B. Ulrich,***"Lambdachrome Laser Dyes",*** 3rd Edition, D-37079 Goettingen, Germany, (2000).

[38] V. Sindhu and A. Ramalingam,*" **Third Order Optical Nonlinearities and***

Spectral Characteristics of Methylene Blue", Journal of Quantum Information Science,1,69-72, (2011).

[39] F. Amal,*" Nonlinear Properties of Olive Oil Films Doped with Poly (Methyl Methacrylate), Polystyrene and Their Blend by Using Z-Scan Technique"*, International Journal of Advanced Technology in Engineering and Science,3,43-59, (2018).

[40] B.Bhowmik , P.angnly, " ***Photo physics of xanthene dyes in surfactant solution*** ", India, spectro chimic act part A 61,1997-2003,(2005).

[41] H. Lazem, ***"Spectroscopic Study of (E) benzylidene amino) Hydroxy Phenol Crystal and Study Nonlinear Optical Properties of It"***, Academic Research International, 5,5, 65- 72, (2014).

[42] H. Ali, *"**Non-linear Properties for Membranes of Rhodamine Tincture by Using Z-Scan Technique**"*, International Journal of Application or Innovation in Engineering and Management, 4, 9, 2319 – 4847, (2015).

[43] K. Wasan, *"**A Study of Linear and Nonlinear Optical Properties of Composite Poly Vinyl Cloride – B by Using Z-Scan Technique**"*, Journal of Babylon of pure and applied science, 23, 1, 368-377, (2015).

[44] I. Al-Deen and A. Al-Saidi, ***''Third - Order Nonlinear Optical Properties and Optical Limiting Behavior of Celestin Blue B Dye Doped Polymer Films''***, Journal of Photonic Materials and Technology, 4,1-7, (2019).

[45] H. Ali, A. Al-Hamdani,and A.Al-Khafaj,*" **Investigation of the Non-linear Properties of Hybrid Chlorophyll a doped TiO_2 Nano Particles** "*, International Journal of Computation and Applied Sciences, 2, 2399-4509, PP.27-32, (2017).

[46] Z. Xiaoqiang,C. Wang, and Y. Zeng, *"**Nonlinear Optical Properties of a Series of Azobenzene Liquid-Crystalline Materials**"*, Optik, 123, 26–29, (2012).

[47] C.Sung, C. W., S.Chen, and S.Sun, ***"Relationship Between the Photoluminescence and Conductivity of Undoped ZnO Thin Films Grown with Various Oxygen Pressures"***, Appl. Surf. Sci., (2009).

[48] J.Lehn and T. Kato, ***"Supramolecular Chemistry Concepts and Perspectives",*** Wiley-V CH, 295- 2414, (2002).

[49] H. Joakim***," Atomic Force and Scanning Tunneling Microscopy Studies of Single Walled Carbon Nanotubes",*** Ph.D., Thesis, Karlstad's university, (2006).

[50] Q. Hassan, "***Third-Order Nonlinearities and Optical Limiting Properties of Rose Bengal at 532 nm Wavelength*** ", Journal of Basrah Researches (Sciences) 33, 2, 76 - 82, (2007).

[51] Y. Ahmad, M. Palanichant, and P. Palanisamy, ***" Influence of Solvents Polarity on NLO Properties of Fluorone Dye"*** International Journal of Nonlinear Science, 7, 3, 290-300, (2009).

[52] V. Lenart," ***Nonlinear Optical Refraction of The Dye-Doped E7 Thermotropic Liquid Crystal at the Nematic-Isotropic Phase Transition***", cond. mat. soft, arxiv:1304.4537, 1-5, (2013).

[53] A.Mousa, Y.Kadhim, and B. Naser, ***" Non-Linear Optical Properties of Thin Films of Nematic Liquid Crystal Doped by Different Nanoparticles Materials"***, conference in university of Karbala, 6, 813 -832, (2017).

[54] E. Bahaa, ***" Fundamentals of Photonics "***, Ch.19, Wiley and Sons, 471-8396 5-5, (1991).

[55] A. Jawad and A. Lateef, "***Study of the Nonlinear Optical and Optical Limiting Properties of New Structures of Organic _Inorganic Materials for Photoinc Applications",*** University of Basrah, (2012).

[56] D.Paul1and L. Robesonb, ***''Polymer Nanotechnology Nanocomposites'',*** journal,49,3187-3204, (2008).

[57] W. Demtroder,*"Laser Spectroscopy Basic Concepts and Instrumentation "*, Springer Verlage, Berlin, New York, 5, (1981).

[58] R. Manshad and Q. Hassaen*," Optical Limiting Properties of Magenta Doped PMMA Under CW Laser Illumination"*, Pelagia Research Library,3,6, 3696-3702, (2012).

[59] J. Khawla, *" Nonlinear Optical Properties of $LiNbo_3$ Thin Film Using Z-Scan Technique"*, Journal of Kerbala University,12,3, 1-8, (2014).

[60] R. Boyd and G. Fischer, *''Nonlinear Optical Material'',* Encyclopedia of Materials: Since and Technology, 6237-6244, (2001).

[61] B. Bhushan *''Nanotechnology"*, Hand Book, Springer Heidelberg Dordrecht London New York, Nanoprobe Laboratory for Bio- and Nanotechnology and Biomimetics (NLB2) Ohio State University, ISBN: 978-3-642-02524-2, (2010).

[62] R. Boyd, *''Nonlinear Optics''*, 3rd. Edition, New York,USA, ISBN: 978-0-12-369470-6, (2008).

[63] B.Snavely and J. Betteley. "*Organic molecular photo physics "*,Vol. 2. Wiley-Interscience, (1973).

[64] J. Alda, "*Laser and Gaussian Beam Propagation and Transformation*", Marcel Dekker. Inc, 270, 999-1013, (2003).

[65] C. Ostela, *" Spectral-luminescent and lasing properties of laser active media based on distyrylbenzene derivatives in various media"*, journal of Applied physics ,80, 6, 3167-3173, (1996).

[66] N. Jawad*, " Non-linear Optical Studies of Liquid Crystal Materials Using Z-Scan Technique"*, M.Sc. Thesis, University of Babylon, (2018).

[67] K. Prasad, and S. Sudhir, "*Synthesis of Schiff Base Zinc Metal Complex $(MAPIMP)_2$ Zn and Development of HPLC Chromatographic Method for Its Analysis"*, Journal Chem. pharm, 2, 5 ,1 216-224, (2010).

[68] C. Annamalai, "***Current Trends in X-Ray Crystallography***", In Tech, Ch.7, pp.161-190, (2011).

[69] T. Theivasanthi, and M. Alagar, "***X-Ray Diffraction Studies of Coppe Nanopowder"***, Archives of physics research, 1, 2, 112-117, (2010).

[70] W. Silfvast, ***"Laser Fundamentals***", 2nd Edition, Cambridg University Press, (2004).

[71] G. Indebetouw,*"* ***Nonlinear Optical Studies of Dye-Doped Nematic Liquid Crystals"***, Ph.D. Thesis, Faculty of the Virginia Polytechnic Institute and State University, Blacksburg, Virginia, (2002).

[72] Y. Andy**,** Lin, H. C., Mo, T. S., & Chen, C. H., ***"Nonlinear Optical Property of Azo-Dye Doped Liquid Crystals Determined by Biphotonic Z-Sca Technique"***, Optics Express, 13,26,10634-10641, (2005)

[73] S. Patil, S. Rao, and S. Dharmaprakash, ***"Crystalline Perfection, Third-Order Nonlinear Optical Properties and Optical Limiting Studies Of 3,4-Dimethoxy-4-Methoxy Chalcone Single Crystal"***, Optics and Laser technology, 81, 70-76, (2016).

[74] L. Yong, and L. Dan, "***Fabrication and Application of 1-D Micro-Cavity Film Made by Cholesteric Liquid Crystal and Reactive Mesogen"***, *Optical* Materials Express 466, 6,2,691-696, (2016).

[75] V. Roman, M.Gamernyk, S.Malynych, and O. Zaichenko, *"* ***Spatial C2oherency of Light and Nonlinear Optical Properties of Colloidal Gold Studied by CW Z- ScanTechnique"***, Nano World Journal , 2,1,5-9, (2016).

[76] G.Saini, "***Spectroscopic studies of rhodamine 6G dispersed in polymethyl cyanoacrylate",*** Spectro chimica Acta Part A .61, 653–658, (2005).

[77] Z. Fryad and S. Patil,*"* ***Nonlinear Optical Properties and Optical Limiting Measurements of (1Z) (Dimethylamino) Phenyl] Methylene}4-Nitrobenzocarboxy***

Hydrazone Monohydrate under CW Laser Regime*", Photonics Journal*, 4,182-188, (2014).

[78] A. Ketamm and A. Hussain, "***The Study of the Nonlinear Optical Properties of Solutions under CW Laser Illumination***", Journal of Basrah Researches Sciences 38,4 ,73-79, (2012).

[79] F. Amal, *"**Optical Nonlinearity of Oxazine Dye Doped PMMA Films by Z-ScanTechniques**"*, Journal of Al-Nahrain University,15,2 ,106- 112, (2012).

[80] A. Hussain, Y. Alaa, and F. Mohammad, *"**Study of The Linear and Nonlinear Optical Properties of Neutral Red Doped Polyvinylpyrrolidone Film**"*, Journal of Basrah Researches (Sciences), 37,2 ,57-63, (2011).

[81] A.Javier, "***Laser and Gaussian beam propagation and transformation.***", Encyclopedia of optical engineering 999, (2003).

[82] H. Muncheryan, "***Principles and Practices of Laser Technology***", TAB Books Inc., USA, (1983).

[83] H. Nasser and O. D. Ali, "***Effect of molecular weight and illumination on optical constants of PMMA thin films***", Iranian Polymer Journal 19 (1) , 57-63, (2010).

[84] A. Maslyukov, S. Kaivola, M. Nyholm, and S. Popov, " ***Solid-state dye laser with modified poly (methyl methacrylate)-doped active elements***", Appl. Optics, 34(9), (1516-1518), (1995).

[85] C.Ladoulis, and T. Gill, "***Physical chemical studies on the specific interaction of an acriflavine-phosphotungstic acid complex with double-stranded nucleic acids***",The Journal of Cell Biology, 47(2), 500-511, (1970).

[86]M.Windholz, S.Budavari, L.Stroumtsos, and M. Fertig, "***The Merck index. An encyclopedia of chemicals and drugs "***,(No. 9th edition), (1976).

[87] R. Tripathi, M. Pudake, and N. Shrivastav, "***Antibacterial activity of poly (vinyl alcohol)-biogenic silver nanocomposite film for food packaging material***", Advances in Natural Sciences Nanoscience and Nanotechnology, 9, 1-5, (2018).

[88] E. Schuster, A. Ronald, and G.Bartolini. "***Direct proton magnetic resonance study of Co2. dag. complexes with imidazole, 4-methylpyridine, pyridine, pyrimidine, and purine in water-acetone mixtures***." Journal of the American Chemical Society ,92.8, 2304-2308, (1970).

[89] A. Tawil, "***Study of Linear and Nonlinear Optical Properties of Fluorescein Sodium Dye***", M.Sc. Thesis, University of Karbala, (2017).

[90] C.Winter, C. Manning, R. Oliver, and C. Hill, "***Measurement of the large optical nonlinearity of nickel dithiolene doped polymers***." Optics communications, 90,1-3, 139-143, (1992).

[91] L. Gómez, S. Cuppo, and N. Figueiredo," ***Nonlinear Optical Properties of Liquid Crystals Probed by Z-Scan Technique "*** Braz. Journal Phys, 33, 4, 813- 820, (2003).

[92] A. Nathera and Z. NooR," ***Energy Transfer Process Between Two Laser Compounds Coumarin 334 and Rhodamine 590***", Iraqi Journal of Physics,14,31, (2016).

[93] D. Seth, D. Chakraborty and N.Sarkar, "***Study of energy transfer from 7-amino coumarin donors to rhodamine 6G acceptor in non-aqueous reverse micelles***", Chemical Physics Letters, 401, (2005).

[94] C.Clementi, C.Miliani, and G. Favaro, " ***A powerful non-invasive diagnostic technique for natural dyes used in artefacts***": Part I. Spectral characterization of orcein in solution, on silk and wool laboratory-standards and a fragment of Renaissance tapestry." Spectrochemical Acta Part A: Molecular and Biomolecular Spectroscopy 64.4, 906-912, (2006).

[95] H. Izharul, and A. Raj. "***Biodegradation of Azure-B dye by Serratia liquefaciens and its validation by phytotoxicity, genotoxicity and cytotoxicity studies***." Chemosphere 196, (2018).

[96] C. Kaplan, G. Karakus, and N. Tuzcu, "***Synthesis, characterization and in vitro antibacterial assessments of a novel modified poly [maleic anhydride-alt-acrylic acid]/acriflavine conjugate***." ,71.11,2903-2921, (2014).

[97] C.Clementi, ,C.Miliani, A.Romani, and G. Favaro, , "***In situ fluorimetry: A powerful non-invasive diagnostic technique for natural dyes used in artefacts: Part I. Spectral characterization of orcein in solution, on silk and wool laboratory-standards and a fragment of Renaissance tapestry***." Spectrochemical Acta Part A: Molecular and Biomolecular Spectroscopy ,64.4, 906-912, (2006).

[98] M. Sheik-Bahae, A. Said, T. Wel, D. Hagan and E.Van,"***Sensitive Measurement of Optical Nonlinearities Using a single Beam***", IEEE Journal of Quantum Electronic, 26,4, 760-769, (1990).

[99] S. Tikhomirova, V.Bryukhanov, V. V., N. S., & Slezhkin, V. A., "***Fluorescence of Acriflavine Molecules on Surface of Mesoporous Silica Gel in The Presence of The Silver Nanoparticles***.", Education & Science Without Borders 5.9, (2014).

[100] B.Herman, " ***Basic Concepts in Fluorescence***" , Microscopy Resource Center , (2012).

[101] O.Abdulazeez, , H. Yassin, and A. Ban. "***Nonlinear Optical Properties of Pure and Dye Doped Nematic Liquid Crystals***." International journal chemical Science 4, 2601-2610, (2016).

[102] Q.Ali " ***Photobleaching Spectroscopic Studies and lifetime Measurements of Fluorescent Organic Dyes*** ", a Thesis, University of Baghdad, College of Science, (2013).

[103] A. Ketamm and A. Hussain, "***The Study of the Nonlinear Optical Properties of Solutions under CW Laser Illumination***", Journal of Basrah Researches Sciences 38,4 ,73-79, (2012).